

**M.Tech.  
Thesis**

**SMART POWER FLOW REGULATION IN  
EV CHARGING SYSTEM WITH  
BIDIRECTIONAL ENERGY TRANSFER**

**KAUMUDI KUMARI**

**MAY  
2025**

# **SMART POWER FLOW REGULATION IN EV CHARGING SYSTEM WITH BIDIRECTIONAL ENERGY TRANSFER**

**Thesis Submitted  
in Partial Fulfilment of the Requirements for the  
Degree of**

**MASTER OF TECHNOLOGY  
in**

**POWER ELECTRONICS & SYSTEMS**

**by**

**KAUMUDI KUMARI**

**(2k23/PES/10)**

**Under the Supervision of  
Prof. MUKHTIAR SINGH  
(Professor, EED, DTU)**



**To the**

**DEPARTMENT OF ELECTRICAL ENGINEERING  
DELHI TECHNOLOGICAL UNIVERSITY**

**(Formerly Delhi College of Engineering)**

**Shahbad Daulatpur, Main Bawana Road, Delhi-110042, India**

**MAY, 2025**

## **CANDIDATE’S DECLARATION**

I **Kaumudi Kumari** Roll No. 2k23/PES/10 student of M.Tech (Power Electronics & System), hereby certify that the work which is being presented in the thesis entitled in partial fulfilment of the requirements for the award of the Degree of Master of technology submitted in the Department of electrical Engg., Delhi Technological University is an authentic record of my own work carried out during the period from 2023 to 2025 under the supervision of **Prof. Mukhtiar** sir The matter presented in the thesis has not been submitted by me for award of any other degree of this or any other institute.

**Candidate’s signature**

This is to certify that the student has incorporated all the corrections suggested by examiner in the thesis and the statement made by the candidate is correct to the best of our knowledge.

**Signature of Supervisor (s)**

**Signature of External Examiner**

## **CERTIFICATE BY THE SUPERVISOR(s)**

Certified that **Kaumudi Kumari** (2k23/PES/10) has carried out their search work presented in this thesis entitled “**Smart Power Flow Regulation in EV Charging System with Bidirectional Energy Transfer**” for the award of Master of Technology from Department of Electrical Engineering, Delhi Technological University, Delhi, under my/our supervision. The thesis embodies results of original work, and studies are carried out by the student herself and the contents of the thesis do not form the basis for the award of any other degree to the candidate or to anybody else from this or any other University /Institute.

**Signature**

**Prof. MUKHTIAR SINGH**

**Date**

DEPARTMENT OF ELECTRICAL ENGINEERING  
DELHI TECHNOLOGICAL UNIVERSITY  
(Formerly Delhi College of Engineering)  
Bawana Road, Delhi -110042

**CERTIFICATE**

This is certified that the thesis entitled “**SMART POWER FLOW REGULATION IN EV CHARGING SYSTEM WITH BIDIRECTIONAL ENERGY TRANSFER**” being submitted by Miss “**KAUMUDI KUMARI**”, Roll No. 2k23/PES/10, in partial fulfilment of the requirement for the award of degree of Master of Technology of Power Electronics and System in the Department of Electrical Engineering, Delhi Technological University.

*Date:\_\_\_/\_\_\_/*

**Prof. Mukhtiar Singh**

Department of Electrical Engineering

Delhi Technological University,

Delhi Shahbad Daulatpur, Delhi-110042

India

**Kaumudi Kumari**

**(2K23/PES/10)**

## ABSTRACT

Using a model predictive control technique based on finite control sets for the second-stage OBC (On-Board Charger) to direct the power flow from the main grid to an EV battery is the main goal of the proposed study. Traditional methods like proportional integral control and direct power control can be used to regulate power converters. Even while these traditional methods function satisfactorily in steady state, they suffer greatly in dynamic operating environments. In order to adjust the switching states to the dynamic operating conditions, a model predictive control (MPC) has been incorporated in the suggested work. The design and performance analysis of MPC have been thoroughly simulated and displayed using the MATLAB/Simulink environment. The outcomes of the simulation have been widely shared. The necessity for intelligent and effective EV chargers linked into smart home systems has been highlighted by the quick uptake of electric vehicles (EVs). This work describes the use of finite controller-based model predictive control (FC-MPC) to create a robust control strategy for an EV charger in a smart home. To obtain excellent performance under dynamic load conditions, the suggested method combines the predictive optimization of MPC with the adaptive decision-making power of finite logic. While retaining strong performance against disruptions such changes in renewable energy and grid uncertainty, the control system guarantees optimal charging, grid stability, and low energy costs. The efficiency of the suggested FC-MPC system in providing dependable, adaptable, and efficient EV charging options for smart homes is confirmed by simulation results. It focuses on a single-phase rectifier that has two power conversion stages: DC/DC and AC/DC. In order to convert direct current (DC) to alternating current (AC) for the inverter DC bus, a buck boost converter needs grid power and a voltage source with a passive filter. Bidirectional power transfer is made possible by these converters, however the high frequency switching action puts a great deal of strain on the switches in terms of voltage and current, which could result in physical damage. Two control levels are used by the inverter: secondary control and power management. Power management transfers the power reference to the secondary control level after modifying it based on the battery's status. With the use of MATLAB simulations, this paper investigates a bidirectional buck-boost DC-DC converter that is FC-MPC controlled for battery charging and discharging applications.

## ACKNOWLEDGEMENT

I want to sincerely thank everyone who helped with this thesis and helped me along the way over the course of this incredible research adventure.

First and foremost, I want to sincerely thank Prof. Mukhtiar Singh, my research guide, for his unwavering support throughout my M.Tech journey and associated studies. I've found inspiration and direction in his perseverance, drive, and vast knowledge. Throughout the research and thesis writing process, his advice was invaluable. His unending assistance on my personal front is also very appreciated; without it, I could not have completed my task.

Besides my supervisor, I would like to thank **Phd. Scholar Mr. Gaurav Yadav sir** for supporting me when needed and giving me constant encouragement while I conducted my research.

***Date:*** / \_\_\_\_ /

**Signature**

**Kaumudi Kumari**

**(2K23/PES/10)**

## TABLE OF CONTENTS

CANDIDATE'S DECLARATION	ii
SUPERVISOR'S DECLARATION	iii
CERTIFICATE	iv
ABSTRACT	v
ACKNOWLEDGEMENTS	vi
TABLE OF CONTENTS	vii
<b>CHAPTER 1. INTRODUCTION</b>	
1.1 Why Electric Vehicle?	1
1.2 Electric Vehicle Topology	4
1.3 Battery Charging Profile	8
1.4 Electric Vehicle (EV) Charger Topology	10
1.5 Electric Vehicle Charging Standards	13
1.6 Motivation	14
1.7 Objective	15
1.8 Outline of Thesis	15
<b>CHAPTER 2. OPTIMAL DESIGN AND PERFORMANCE ANALYSIS OF MODEL PREDICTIVE CONTROL FOR EV CHARGING APPLICATION</b>	
2.1 Electric Vehicle Charging Operating Modes	17
2.2 System Description	17
2.3 DC-DC Converter	18
2.4 Results and Simulation	21
2.5 Conclusion	25
<b>CHAPTER 3. OPTIMAL DESIGN AND PERFORMANCE ANALYSIS OF MODEL PREDICTIVE CONTROL FOR EV DISCHARGING APPLICATION</b>	
3.1 Electric Vehicle Discharging Operating Mode	26
3.2 Controller Design	27
3.3 Result and Simulation	31

3.4 Conclusion	34
<b>CHAPTER 4. Comparison of Charging and Discharging Operation of Electric Vehicle through MPC</b>	
4.1 Introduction	35
4.2 Controller Design	36
4.3 Result and Simulation	38
4.4 Conclusion	43
<b>CHAPTER 5. Implementation of Robust Control for Smart Home EV Charger through FC -MPC</b>	
5.1 Introduction	44
5.2 Controller Design	45
5.3 Results and Simulation	47
5.4 Conclusion	52
<b>CHAPTER 6. Simulation and Experimental Results</b>	
6.1 Modelling of EV Charger	53
6.2 AC-DC Converter Modelling(single-Phase)	54
6.3 DC-DC Converter Modelling(single-Phase)	55
6.4 Simulation Result	57
6.5 Experimental Results	63
<b>CHAPTER 7. Conclusion and future Scope of Research Work</b>	
7.1 Research Work Conclusion	70
7.2 Future Scope of Research	71
List of Publication	72
References	73



## List of Tables

S NO	Table Name	Page no.
1	Table 1.1: Type of Charger.	8
2	Table 1.2: Comparison of On-Board Charger and Off-Board Charger	12
3	Table 1.3: Charger Operating Modes	13
4	Table 1.4: IEC Charging Standards	13
5	Table 2.1: System Parameters for Charging	21
6	Table3.1 Comparison of MPC and PI	28
7	Table 4.1 Comparison of Charging and Discharging Operation of Electric Vehicle through MPC	38
8	Table 4.2 THD during different working Condition.	42
9	Table5.1 Step change in $I_{bat}$	47
10	Table6.1 Parameters of Bidirectional Charging System	53

## **LIST OF FIGURES**

<b>S No.</b>	<b>Figure Name</b>	<b>Page no.</b>
1	Fig.1.1 Electric Vehicle	3
2	Fig.1.2 Types of Electric Vehicle	4
3	Fig.1.3 Typical EV architecture	7
4	Fig.1.4 Battery Charging Profile	9
5	Fig.1.5 EV Charger	10
6	Fig.1.6 General structure of EV charger.	11
7	Fig.1.7 EV charger with ON/OFF Board	12
8	Fig. 2.1 Circuit topology of an AC/DC converter that is linked to a battery through a DC/DC converter.	18
9	Fig. 2.2 MPC with reference design	18
10	Fig. 2.3 Flowchart of MPC	20
11	Fig.2.4 Comparison of PI and MPC controller with reference current.	20
12	Fig.2.5 Reference change operating condition	22
13	Fig.2.6 THD under reference change operating conditions.	22
14	Fig.2.7 Nonideal Source operating condition	23
15	Fig.2.8 THD under nonideal operating conditions	23
16	Fig.2.9 Load change operating conditions	24
17	Fig.2.10 THD under Load change operating conditions	24
18	Fig.3.1Circuit topology of an AC/DC converter that is linked to a battery through a DC/DC converter.	27
19	Fig.3.2 AMPC Controller Design for EV Charger	28
20	Fig.3.3 Reference change operating conditions in discharging state.	31
21	Fig.3.4 Reference change THD under discharging state.	32

22	Fig.3.5 Nonideal operating conditions under discharging conditions.	32
23	Fig.3.6 Nonideal source change THD under discharging state	33
24	Fig.3.7 Load change operating conditions under discharging conditions	33
25	Fig.3.8 THD under Load change operating conditions in discharging state	34
26	Fig.4.1 MPC Controller	36
27	Fig.4.2 Reference change operating condition showing both charging and discharging.	39
28	Fig.4.3 Reference change THD under charging	39
29	Fig.4.4 Reference change THD under discharging state.	39
30	Fig.4.5 Nonideal Source operating condition under charging state and discharging state.	40
31	Fig.4.6 Nonideal source change THD under charging state	41
32	Fig.4.7 Nonideal source change THD under discharging state	41
33	Fig.4.8 Load change operating condition under charging state and discharging state	41
34	Fig.4.9 THD under load change operating conditions in charging state.	42
35	Fig.4.10 THD under load change operating conditions in discharging state.	42
36	Fig.5.1 Circuit topology of an AC/DC converter that is linked to a battery through a DC/DC converter.	46
37	Fig.5.2 Controller	46
38	Fig.5.3 Reference change operating condition showing both charging and discharging.	48

39	Fig.5.4 Step change in $I_{bat}$ during charging condition	49
40	Fig.5.5 Step change in $I_{bat}$ during discharging condition	50
41	Fig.5.6 Step change in $V_{DC}$ during charging condition.	50
42	Fig.5.7 Step change in $V_{DC}$ during discharging condition.	51
43	Fig.6.1 Switching Model of single-phase.	54
44	Fig.6.2 AC-DC converter switching model	54
45	Fig.6.3 DC-DC converter topology	55
46	Fig.6.4 DC-DC buck operation ON state	56
47	Fig.6.5 DC-DC buck operation OFF state	57
48	Fig.6.6 Current and Voltage relation of Unidirectional charger	58
49	Fig.6.7 Current and voltage relation during a) in phase b) Out-of-Phase	58
50	Fig.6.8 Comparison of PI and MPC controller with reference current.	58
51	Fig.6.9 Reference change operating condition showing charging State	58
52	Fig.6.10 THD under reference change operating conditions	58
53	Fig.6.11 Nonideal Source operating condition under charging state	59
54	Fig.6.12 THD under nonideal operating conditions	59
55	Fig.6.13 Load change operating condition under charging state.	59
56	Fig.6.14 THD under Load change operating conditions	59
57	Fig.6.15 Reference change operating condition showing discharging state.	60
58	Fig.6.16 THD under reference change discharging operating conditions.	60

59	Fig.6.17 Nonideal Source operating condition under	60
	discharging state.	
60	Fig.6.18 THD under nonideal discharging operating	60
	conditions	
61	Fig.6.19 Load change operating condition under	61
	discharging state	
62	Fig.6.20 THD under Load change discharging operating	61
	conditions.	
63	Fig.6.21 Reference change operating condition showing	61
	both charging and discharging.	
64	Fig.6.22 Nonideal source operating condition under	61
	charging state and discharging state.	
65	Fig.6.23 Load change operating condition under charging	62
	state and discharging state.	
66	Fig.6.24 Reference change operating condition showing	62
	both charging and discharging.	
67	Fig.6.25 Step change in $I_{bat}$ during charging condition	62
68	Fig.6.26 Step change in $I_{bat}$ during discharging condition	62
69	Fig.6.27 Step change in $V_{DC}$ during charging condition	63
70	Fig.6.28 Step change in $V_{DC}$ during discharging condition	63
71	Fig.6.29 Bidirectional DC-DC converter	63
72	Fig.6.30 Microcontroller launchpad	64
73	Fig.6.31 Gate driver circuit	64
74	Fig.6.32 Bidirectional Converter with gate driver circuit	65
75	Fig.6.33 Switch Stress	65
76	Fig.6.34 Capacitor Voltage	66
77	Fig.6.35 Inductor Current	66
78	Fig.6.36 8IRFP260N MOSFET	67
79	Fig.6.37 9MUR860 Diode	67

80	Fig.6.38 Electrolytic Capacitor	67
81	Fig.6.39 TLP350	67
82	Fig.6.40 Hi-Link	67
83	Fig.6.41 Terminal Connectors	67
84	Fig.6.42 Ferrite Core Inductor	68
85	Fig.6.43 Dimension of Core	68
86	Fig.6.44 Voltage Sensor	68
87	Fig.6.45 Power Supply for Sensor	68
88	Fig.6.46 Step Down transformer	68
89	Fig.6.47 Schematic of power supply	68
90	Fig.6.48 PCB Design of power supply	69
91	Fig.6.49 Heat Sink	69
92	Fig.6.50 DC Fan for cooling	69
93	Fig.6.51 Launchpad F28379D	69

## **List of Symbols, Abbreviation and Nomenclature**

<b>S No</b>	<b>Abbreviation Name</b>	<b>Full Name</b>
1	EV	Electric vehicle
2	CDC	DC-link capacitance
3	IC	Internal Combustion Engines
4	CNG	Compressed Natural Gas
5	FCEV	Fuel Cell Electric Vehicle
6	VDC	DC-link voltage
7	I <sub>bat</sub>	Battery current
8	HEV	Hybrid Electric Vehicle
9	AEV	All- Electric Vehicle
10	BEV	Battery Electric Vehicle
11	D	Duty ratio

12	AC	Alternating Current
13	DC	Direct Current
14	V2G	Vehicle to Grid
15	G2V	Grid to Vehicle
16	PWM	Pulse Width Modulation
17	PI	Proportional Integral
18	MPC	Model Predictive Control
19	SOC	State of Charge
20	IGBT	Insulated Gate Bipolar Transistor
21	DG	Distribution Grid
22	DSP	Digital Signal Processor
23	THD	Total Harmonics Distortion
24	Cf	DC-DC converter filter capacitance



25	RC	Repetitive Controller
26	IEEE	Institute of Electric and Electronics Engineers
27	IEC	International Electrotechnical Commission
28	DER	Distributed Energy Resources
29	DCFC	DC Fast Charging
30	AISC	Automotive Industry Standards Committee
31	IS	Indian Standard

32	ISO	International Organization for Standardization
33	OBC	On-board Battery Chargers
34	CCS	Constant Current Control
35	CCS	Combined Charging System
36	FD	Fractional Delay
37	CAN	Controlled Area Network
38	SAE	Society of automotive engineers
39	BEVC-AC001	Bharat EV charger-AC001 Technical Standard Committee
40	TSC	
41	SMC	Sliding Mode Control
42	OCPP	Open Charge Point Protocol
43	CAN	Controlled Area Network

44	AIS	Automotive Industry Standard
45	ARAI	Automotive Research Association of India
46	V2G	Grid to vehicle
47	V2V	Vehicle to Grid
48	FD	Fractional Delay
49	FC	Finite controller
50	FORC	Fractional Order Repetitive Controller
51	IMP	Internal Model Principal
52	PR	Proportional Resonant
53	HB	Hysteresis Band
54	BEVC-DC001	Bharat EV charger- DC001
55	Vbat	Battery voltage
56	L <sub>s</sub>	Grid side inductor
57	PCC	Point of common coupling

# CHAPTER -1

## INTRODUCTION

### 1.1 Why Electric Vehicle?

Electric vehicles (EVs) are widely used in a variety of industries, including public transportation, private automobiles and commercial trades. The efficiency and cleanliness of electric vehicles (EVs) make them a significant part of the transportation system of the near future [1]. EV batteries act as a vital component of electric mobility, assist the main grid by using OBC to charge active power to or from the grid [2]. Installing EV charging stations in residential and commercial spaces is necessary to accommodate this demand [3]. A single-phase onboard EV charger is the subject of research in order to address current harmonics in smart homes and supply reactive power to the main grid. Various techniques have been employed to regulate power flow in EV chargers, which includes: direct power control (DPC), proportional integral control (PI), and voltage-oriented control (VOC). PI control technique is oldest control technique which is having good steady state response, however tuning of PI parameters is time consuming task. In VOC, the PI controllers are necessary to produce the reference values. In DPC control technique, to determine the ideal switching state, a planned switching table is employed [4]. The DPC does not require modulators, internal current loops, or phase-locked loops (PLL), in contrast to the PI controller. However, the high-power waves produced by this technique significantly change grid currents. For the control of power electronics, a model predictive control (MPC) with a finite control set has recently surfaced [5]. In contrast to pure PI control, VOC, and DPC techniques, the MPC strategy eliminates the need for additional voltage/current loops, modulators, or PLLs. The primary benefit of MPC is that system constraints may be introduced directly to the cost function, negating the need for modulation and synchronization [6]. It is the best option for advanced control applications due to its resilience, excellent performance, and predictive capability [7]. Because of its ability to handle multivariable systems, explicitly consider constraints, and optimize control performance over a future horizon, it is particularly appealing for a wide range of applications, from advanced driver-assistance systems in automotive engineering to process control in the chemical industries [8]. In order to predict future states and outputs, MPC solves an optimization problem at each control interval using a dynamic model of the system [9]. Because of its predictive character, the controller may proactively modify control inputs, foresee and mitigate future disruptions, and guarantee that operational limitations are met [10].

A paradigm shift from fossil fuel vehicles to electric vehicles (EVs), which are more efficient, sustainable, and emit zero emissions, is required due to the depletion of oil reserves. Over the past 20 years, interest in EV research has grown dramatically as a means of discouraging the use of fossil fuels in an effort to reduce pollution and greenhouse gas

emissions. The low driving range of these vehicles is impeding their ability to overtake the automobile sector, as consumers still choose conventional fuel-based vehicles, despite the fact that the business is expanding rapidly. As a result, HEVs, or hybrid electric cars, are becoming more and more popular. At least two energy sources, including electrical energy, are present in these kinds of vehicles. Both a traditional gasoline engine and an electric motor are carried by them. Therefore, a HEV is very dependent on petrol but offers a long driving range. Compared to gasoline and electric vehicles, which only have one powertrain, hybrid vehicles are far more complicated, have two powertrains, are more costly, and require more maintenance. But since they don't require liquid fuel, EVs offer a clean alternative for the environment. Compared to other gasoline-based vehicles, they may save more on fuel and maintenance, have a high torque, and are very responsive.

The importance of electric Vehicles (EVs) in addressing environmental issues, encouraging sustainable mobility, and providing possible financial advantages makes them a hot topic. Since EVs are thought to be a way to cut down on tailpipe emissions, enhance air quality, and lessen dependency on fossil fuels, they are a major topic of study in fields like energy, transportation, and sustainability. For the Battery inverter current control, this work proposes an advanced model predictive control (AMPC) to bring high-quality electricity into the network. The inverter has two control levels: the first is a simple hysteretic power management level that shifts the power reference to the second level based on the battery's state of charge (SoC) value, The second level is an advanced MPC controller that drives the inverter to inject the right quantity of high-quality current in line with the reference without requiring a module. With the selected control strategies, a simulation of our hybrid system will be accomplished. A new control method for power electronic converters is called advanced model predictive control, or AMPC. The benefits of AMPC include its capacity to manage intricate, nonlinear systems and accomplish many control goals while abiding by a number of restrictions. By skipping the repetitive computations of the cost functions and states forecasts, AMPC provides a much lower computing overhead. However, AMPC heavily depends on the power converter's dynamic model. They are therefore more prone to ambiguities and interruptions. This paper presents a novel approach to increase the robustness and reliability of the AMPC for electric vehicle chargers by treating the dynamic model of the converter as a black box. Next, a recursive least squares algorithm-based adaptive estimating technique is suggested for online dynamic.

Improved performance, computation speed, resilience, or adaptability in dynamic systems are the goals of Advanced Model Predictive Control (MPC), which is a more advanced version of the basic MPC framework. In domains where real-time operation is crucial and system dynamics might be complex, such as power electronics, drives, and energy systems, these upgraded versions are especially pertinent.

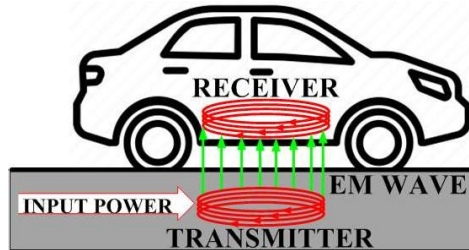


**Fig.1.1 Electric Vehicle**

The car runs solely on battery power when in electric only mode, as seen in Fig. 1.1. The DC-DC and AC-DC converters are used in this process to transfer electrical energy. In this mode, the vehicle is powered solely by the electrical energy of the battery pack and no fuel is used. As a result, this mode is highly appropriate for environmental perspectives.

➤ **Advantages for the Environment**

Zero tailpipe emissions: Since EVs don't emit CO<sub>2</sub> or NO<sub>x</sub>, they help to clean up the air.  
 Reduced greenhouse gas emissions: EVs frequently have a lower carbon footprint than internal combustion engine (ICE) vehicles, even when power generation is taken into consideration.

➤ **Efficiency in Energy Use**

Compared to gasoline engines, which convert about 20–30% of electrical energy from the grid to power at the wheels, electric vehicles (EVs) convert approximately 85–90%.

➤ **Lower Operating Expenses**

Reduced fuel costs: Compared to gasoline and diesel, electricity is typically less expensive.

Reduced maintenance: EVs require no oil changes, have fewer moving parts, and have regenerative braking, which reduces brake wear.

➤ **Advantages of Performance**

Instant torque: Offers rapid and seamless acceleration.

Quiet operation: EVs produce less noise pollution since they operate more silently than ICE cars.

➤ **The Independence of Energy**

uses power generated domestically, especially from renewable energy sources, to lessen dependency on imported fossil fuels.

## 1.2 Electric Vehicle Topology:

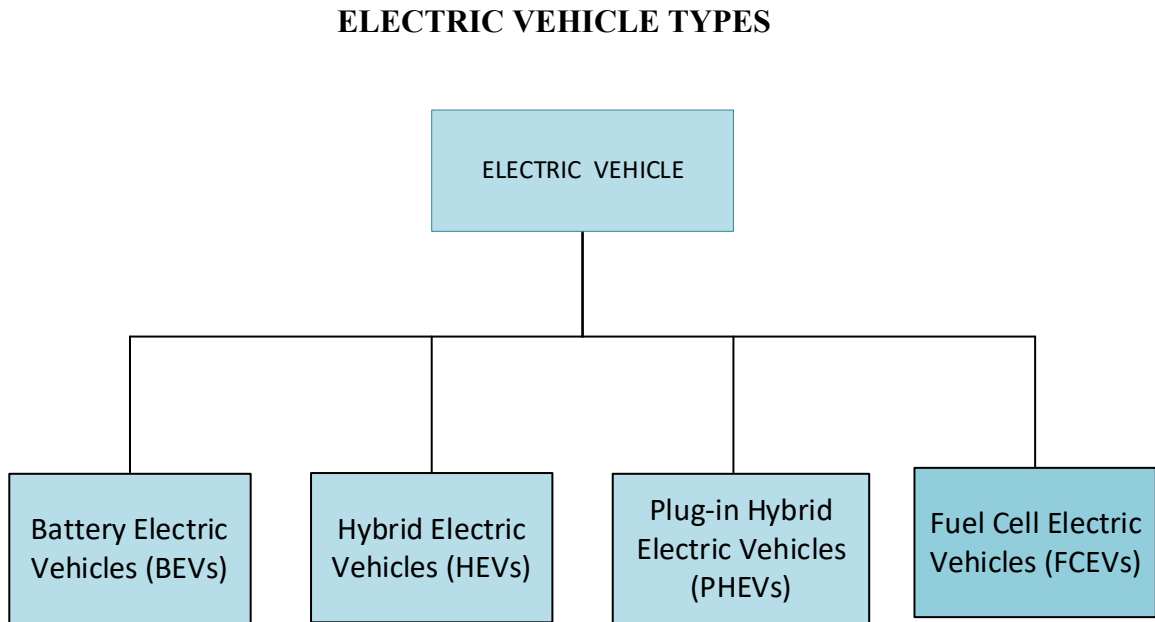


**Fig.1.2 Types of Electric Vehicle**

### 1. Battery Electric Vehicles (BEVs):

- **Definition:** Battery electric vehicles are fully electric cars that power themselves exclusively using electricity stored in rechargeable battery packs. They don't utilize fossil fuels or internal combustion engines (ICEs). Rather, BEVs are propelled by electric motors, and external electricity sources, such as public or home chargers, are used to recharge their batteries.
- **Charging:** They are recharged by plugging them into a power outlet.
- **Example:** Tesla Model 3, Nissan Leaf.

### 2. Hybrid Electric Vehicles (HEVs):

- **Definition:** A hybrid electric vehicle is an internal combustion engine (ICE) that is combined with an electric motor and battery to improve fuel efficiency and reduce emissions. In contrast to Battery Electric Vehicles (BEVs), HEVs rely on regenerative braking and the combustion engine (ICE) to charge their batteries. The electric motor boosts overall efficiency by helping the engine when it accelerates, idles, or drives at low speeds.
- **Charging:** The battery is charged primarily through regenerative braking

**and the gasoline engine.**

- **Example: Toyota Prius.**

### **3. Plug-in Hybrid Electric Vehicles (PHEVs):**

- **Definition:**  
Plug-in hybrid electric cars combine a gasoline engine and electric motor, and their batteries are larger than those of traditional hybrids. Connecting the car to an external power source will recharge this bigger battery. For a limited time, PHEVs can run exclusively on electricity. After that, they can transition to hybrid mode, which offers more flexibility and lower fuel usage by utilizing the gasoline engine to help or take over.
- **Charging: They can be recharged from an external power source, similar to BEVs.**
- **Example: Ford Fusion Energi, Hyundai Ioniq Plug-In.**

### **4. Fuel Cell Electric Vehicles (FCEVs):**

- **Definition:** Fuel Cell Electric Vehicles: A hydrogen fuel cell uses an electrochemical reaction between hydrogen and oxygen to produce power. The car is driven by an electric motor that is powered by this electricity. FCEVs are a zero-emission substitute since they only produce water vapor as a byproduct. Because they are charged with hydrogen gas instead of electricity, they can be refuelled more quickly than BEVs.
- **Charging: They are refuelled with hydrogen, similar to gasoline vehicles.**
- **Example: Toyota Mirai.**

### **Battery Electric Vehicle (BEV):**

EVs with a single energy source, such as a battery, are referred to as BEVs. The BEV is solely reliant on the battery pack's electricity. Therefore, the BEV's range is directly correlated with its battery pack capacity. Usually, these cars can go 100–250 km on a single charge, although larger battery-bank cars can go 300–500 km. Nevertheless, these ranges could change based on driving circumstances and style. Additionally, BEVs are good for the environment and far less cost of operation.

### **Hybrid Electric Vehicle (HEV):**

The fuel and battery pack are the two energy sources for these EV models. Both of them have engines that run on internal combustion (IC).and the electrical drivetrain. The electrical energy source is suitable for usage in urban settings, at modest speeds, and when low power is needed. In situations where traffic is



congested, it can aid in lowering fuel use. These vehicles switch to internal combustion engines when high speed is needed. Additionally, combining the two drivetrains can improve the vehicle's performance. However, the cost of HEVs is higher than that of BEVs because of the two energy sources.

### **Plug-in Hybrid Electric Vehicle (PHEV):**

PHEVs have two powertrains (an electric motor and a gasoline engine), but their primary means of propulsion is electric. Although the gasoline engine increases driving range or charges the battery supply, it necessitates a larger battery pack than a HEV.

### **FCEVs, or fuel cell electric vehicles:**

EVs that use a fuel cell to power their powertrain are referred to as FCEVs. The benefit of this type of vehicle is that it requires the same amount of time to refuel as a conventional vehicle and produces power using fuel cells, which generate no carbon. Yet, FCEVs are not very popular because of their drawbacks, which include expensive fuel cell costs, hydrogen storage, transportation, and manufacture, as well as the fuel cell's life cycle.

The three main electric components of an EV are the electric motor with gear box, energy storage system (battery), and power electronics converter for motor driving and battery charging (Fig. 1.3). The installation of quick EV chargers is essential to addressing the issue of EVs' limited driving range. Both ON board and OFF board charging are the two charging methods used by the system. Outdoor chargers are the term for off-board chargers, while on-board chargers are mounted on the car. Two-stage or single-stage EV chargers are both possible. A single power conversion stage, or AC to DC, makes up a single stage charger. where the car battery pack is connected to the DC side and the grid is connected to the AC side. A dual-stage EV charger, on the other hand, consists of two interconnected power conversion stages, such as DC-DC and AC-DC converters, positioned back-to-back.

In addition to providing galvanic isolation between the grid and the battery pack, the second stage DC-DC converter also reduces ripple on the battery side. The battery life can be increased by using a DC-DC stage between the battery and the AC-DC conversion stage. Using a DC-DC stage, however, will result in higher hardware costs, worse efficiency, and more components. Additionally, single-stage chargers require a higher voltage at the DC link than the amplitude of the AC side voltage, despite having comparatively less control complexity than two-stage chargers. Nevertheless, the EV charger uses a two-stage dialogue in accordance with battery specifications to achieve the necessary voltage level.

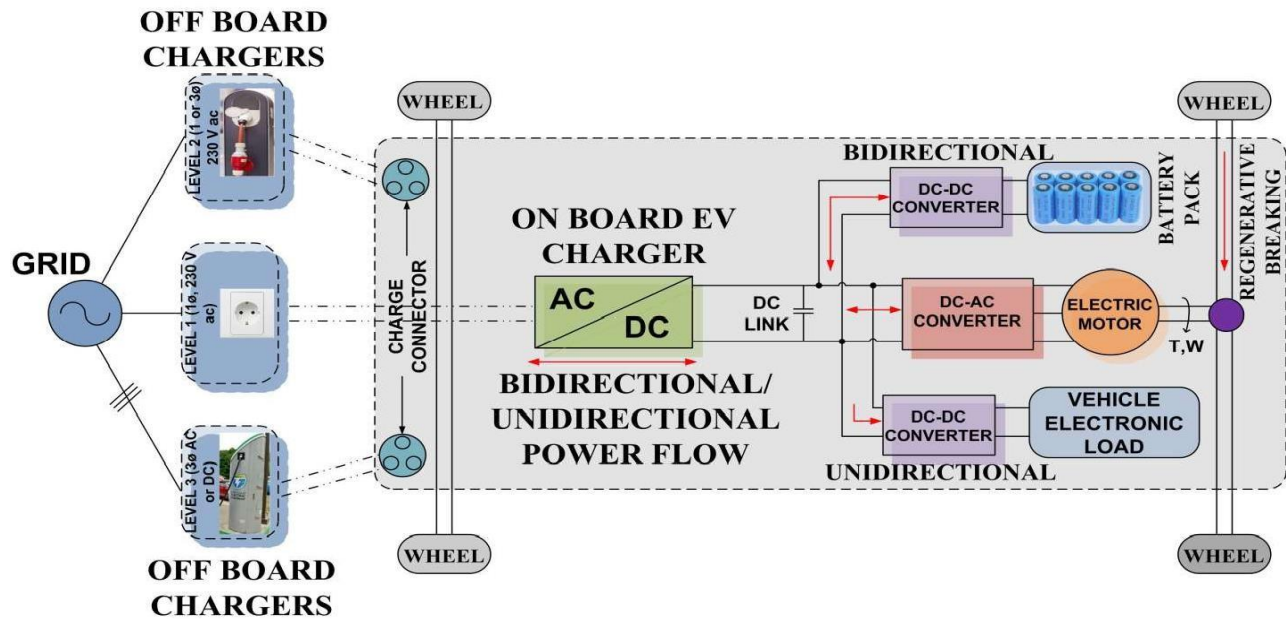


**Fig.1.3 Typical EV architecture**

However, the primary obstacles that have impeded EVs' general success are their high cost, low driving range, battery life, energy storage capacity, charging challenges, and lack of infrastructure for charging.

Both onboard and offboard chargers are used to charge electric vehicle (EV) batteries by converting AC power to DC power; however, their locations and charging speeds vary. Because they are built into the car, onboard chargers enable flexible charging from regular AC outlets, but at a slower rate. External to the car, offboard chargers are usually located at specific charging stations and offer better charging speeds, especially for DC fast charging.

The demand for quick and effective charging stations is rising as electric vehicles become more and more popular. The best way to reduce the charging time is with DC off-board chargers. The size of the battery determines how long it takes to charge, but many cars can be charged to 80% capacity in less than an hour with standard DC fast chargers. Instead of plugging in overnight for a full charge, drivers may now refuel throughout the day or during a brief stop thanks to the shorter charging time. The output of DC chargers has been increasing steadily, with some models presently reaching 350 kW

### 1.3 Battery charging profile:

#### EV charger

An electric vehicle (EV) charger is a device that recharges an EV's battery by drawing electricity from the power grid. It transforms AC or DC power from the grid into the appropriate voltage and current level that the EV battery needs. AC chargers, which use the vehicle's onboard charger, and DC fast chargers, which charge the battery directly, are two of the different types and power levels of EV chargers. Some systems can also offer bidirectional charging for vehicle-to-grid (V2G) applications.

Constant voltage (CV) and constant current (CC) charging profiles are the two types typically utilized for battery charging. When starting up, a fixed amount of electricity is sent to the battery through the use of CC charging. Once a specific voltage level is reached, the charging method is switched to CV charging. In the course of this, There is relatively little charging current flowing in the battery, and a steady voltage is controlled across the battery terminal. When using CC charging, the battery is charged to 80% SOC, with CV charging covering the remaining 20%. The remaining 75% of the whole charging time is spent on CV charging, with CC charging taking about 25% of that time. The charging period for a lithium-ion battery with a maximum voltage of 4.2 V is approximately 50 minutes for CC charging and 2 hours 40 minutes for CV charging. Thus, the battery listed above will take about three hours and thirty minutes to fully charge.

**Table 1.1: Charger Types**

Type of Charger	Active Power Transfer	Reactive Power Operation
Unidirectional	Charging just or grid to vehicle (G2V) only.	NO
Bidirectional	Vehicle to grid (V2G)/discharge and grid to vehicle (G2V)/charge	Inductive and capacitive both

#### Charging Rate (C-rate):

Each battery has its own C-rate, or rated charging current rate. C stands for the charging current needed to fully charge a battery in an hour.  $n \times C$ , or  $n$  times the designated charging rate, is the battery charging current.  $n$  may be greater than or less than one.

An example would be a battery with  $n = 0.5$  that takes two hours to fully charge at half its rated current, and a battery with  $n = 2$  that charges at twice its rate.

### Charging Profile:

The two charging profile types that are commonly used for battery charging are constant voltage (CV) and constant current (CC). When the battery is first starting up, a fixed amount of electricity is delivered to it via CC charging. Once a specific voltage level is reached, the charging method is switched to CV charging. A steady voltage across the battery terminal is maintained throughout this time, and the battery experiences very little charging current flow.

The battery is charged to 80% SOC while using CC charging, and the remaining 20% is charged using CV charging. About 25% of the whole charging time is spent with CC charging, while the remaining 75% is spent with CV charging. As shown in Fig. 1.4, the charging time for a lithium-ion battery with a maximum voltage of 4.2 V is approximately 50 minutes for CC charging and 2 hours 40 minutes for CV charging. Consequently, the aforementioned battery will take about three hours and thirty minutes to fully charge.

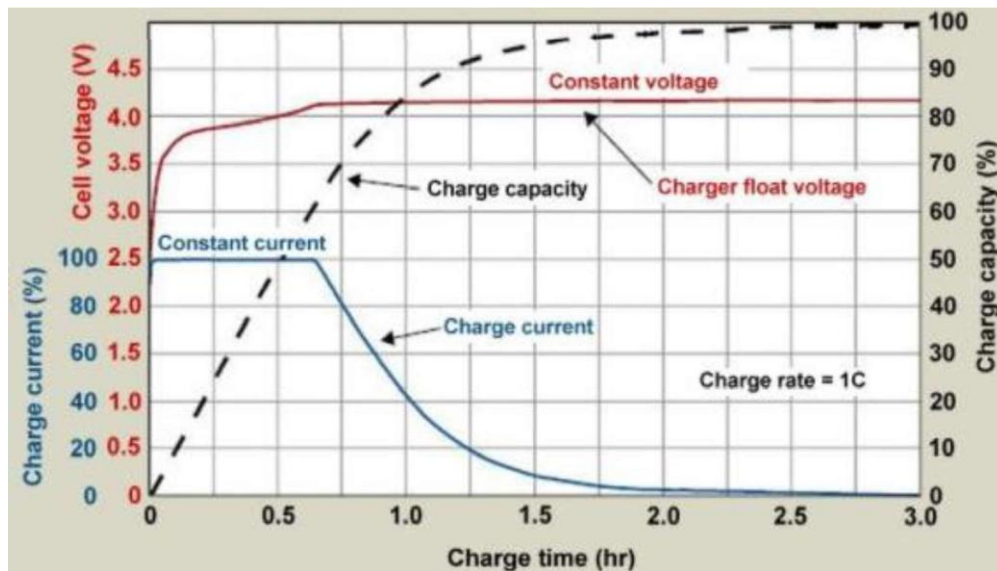


Fig.1.4 Battery Charging Profile

### Battery Capacity:

The battery capacity is determined by the amount of free charge that the active material generates at the negative electrode and consumes at the positive electrode. Stated differently, it refers to the entire amount of energy that a battery can hold. The units of measurement are watt-hour (Wh) or ampere-hour (Ah), where 1 Ah is equivalent to 3600 coulomb (C).

## 1.4 Electric Vehicle (EV) Charger Topologies:

Based on their location (onboard/offboard) and power level (AC/DC), EV chargers can be widely classified. The internal power conversion architecture, or topology, transforms grid power into appropriate power for vehicle battery charging. Fig 1.5 show the EV charger.

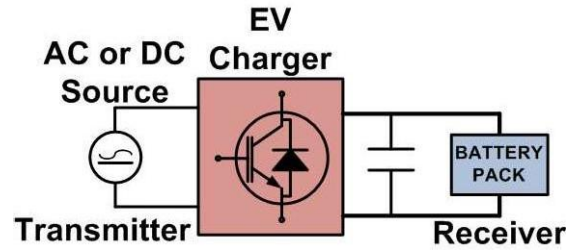


Fig.1.5 EV Charger

### Types of EV Chargers:

#### 1. AC chargers (onboard chargers)

Inside the car, an onboard charger (OBC) transforms power from AC to DC. charge that is usually slower (Level 1 or 2).

#### 2. Offboard chargers, or DC chargers

The battery receives power that has been externally converted to DC. permits Level 3 fast or ultra-rapid charging.

### Typical Topologies for EV Charging:

#### A. Onboard Topology for AC Charger

##### 1. PFC Stage AC-DC Converter Boost PFC Converter

Interleaved PFC Boost

Totem-Pole PFC (efficient, modern)

##### 2. DC-DC Converter (Control and Isolation)

Full-Bridge Conversion

Because of its high efficiency, LLC Resonant Converter is well-liked.

PSFB, or phase-shifted full bridge

#### B. Offboard DC Fast Charger Topology

## 1. Grid Interface (AC-DC Front-End)

- Power Factor Correction (PFC) 3-Phase Rectifier
- Unidirectional Vienna Rectifier
- Three-Phase Bidirectional Active Front-End (AFE) Inverter

## 2. Battery Interface (DC-DC Converter)

- Separate converters:
  - Bridge with Dual Active (DAB).
  - Full Bridge Phase-Shifted (PSFB).
  - LLC Converters or Series Resonant Converters.

Bidirectional Chargers (V2G – Vehicle-to-Grid) Required for Grid-to-Vehicle (G2V) and Vehicle-to-Grid (V2G) operations.

Uses bidirectional DC-DC and AC-DC stages:

- Bidirectional AFE (inverter/rectifier)
- Bidirectional DAB or PSFB converters

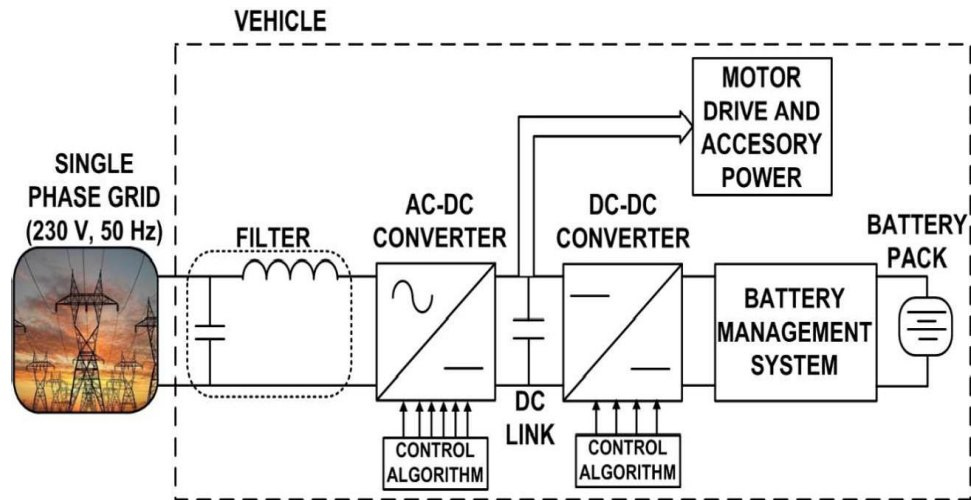


**Fig.1.6 General structure of EV charger.**

An electric motor with gearbox, a battery-powered energy storage system, and a power electronics converter for motor driving and battery charging make up the EV's three primary electric components. The installation of rapid EV chargers is essential to addressing the issue of EVs' limited driving range. The system employs two charging techniques: ON board charging and OFF board charging. On-board chargers are installed on the vehicle, whereas off-board chargers are known as outdoor chargers. The general layout of an EV charger is shown in Figure 1.6.

A power electronic circuit installed inside an EV called an On-Board Charger (OBC) transforms grid-supplied AC into regulated DC in order to charge the battery.

An off-board charger is a big, external charger that converts AC to DC and delivers DC straight to the car battery. These chargers are usually found at charging stations.

**Table1.2: Comparison of On-Board Charger and Off-Board Charger**

Charger Type	Location	AC/DC Conversion	Power Level	Use Case
On-Board Charger	Inside the vehicle	Inside the vehicle	Low to medium (up to ~22 kW)	Home and public AC charging
Off-Board Charger	Outside the vehicle (station)	In the charging station	Medium to high (up to 350+ kW)	Fast public DC charging

Fig. 1.7 illustrates how EV chargers can be used to enhance grid power quality. In order to support the utility reactively as well, the EV user can permit the on-board charger to communicate with the grid. The local load's reactive current can be supplied by the charger. By doing this, transmission line efficiency will increase and distribution transformer overloading will be reduced.

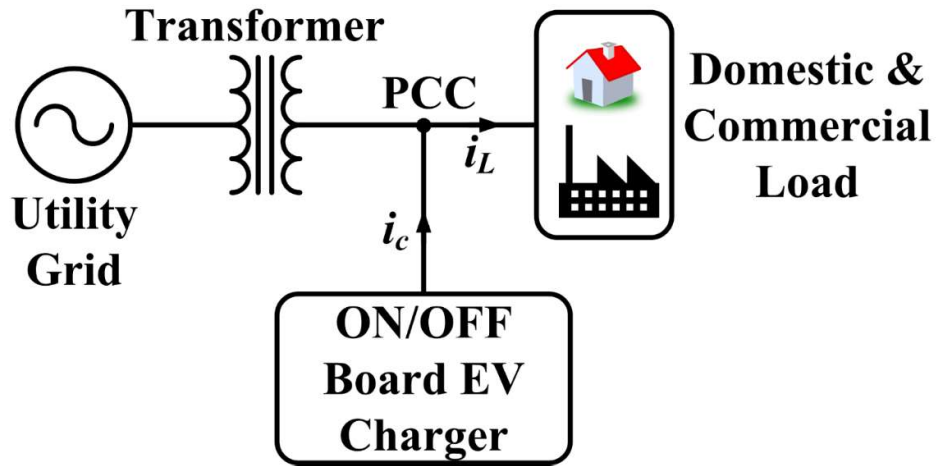


**Fig.1.7 EV charger with ON/OFF Board**

note that only eight modes of operation listed in Table 1.3 are feasible in four quadrant operation with active and reactive power exchange.

**Table 1.3: Charger Operating Modes**

<b>Active power (W)</b>	<b>Reactive power (VAR)</b>	<b>Operation</b>	<b>Power Factor</b>
Positive	Zero	Charging	1
Negative	Zero	Discharging	-1
Zero	Positive	Inductive	0
Zero	Negative	Capacitive	0
Positive	Positive	Inductive-Charging	Lagging
Positive	Negative	Capacitive-Charging	Leading
Negative	Positive	Inductive-Discharging	Lagging
Negative	Negative	Capacitive-Discharging	Leading

### 1.5 Electric Vehicle Charging Standards:

International standards are developed by the International Electrotechnical Commission (IEC). For all associated electrical and electronic technologies, it develops the international standards. The IEC standards encompass a broad range of technologies, including semiconductors, batteries, solar energy, power grid, nanotechnology, and many more. Numerous standards that address various facets of EV charging have also been produced by the IEC. For example, IEC 61851 addressed the general requirements for EV chargers, while IEC 62196 deals with connections, plugs, socket outlets, and vehicle inlets. However, IEC 61980 addressed EV wireless charging systems.

**Table 1.4: IEC charging standards.**

<b>Charging Method</b>	<b>Voltage level(V)</b>	<b>Supply system</b>	<b>Maximum Current (Amp)</b>	<b>Maximum Power (KW)</b>
AC Level 1	240	AC Single -phase	16	3.3
AC Level 2	240	AC Single -phase	32	7.6
AC Level 3	415	AC Three -phase	250	120
DC Fast Charging	600	DC	400	240



## 1.6 MOTIVATION:

The transportation industry's future lies with EVs. In terms of electric vehicles, India is a developing nation. By 2030, it is predicted that 80% of two- and three-wheelers, 30% of private automobiles, 70% of commercial vehicles, and 40% of buses will be electric. Compared to cars with internal combustion engines, electric vehicles are far more efficient. They require less upkeep, are simpler in design, produce less noise, and do not harm the environment. Since the number of EVs is growing daily, it is anticipated that many EVs will be linked to the grid at one point in time. In terms of stability, this can be quite beneficial to utility. The EV has the ability to both actively and reactively support the grid.

It can simultaneously correct reactive power and provide active power to the grid in an emergency. Furthermore, if an EV is run with inadequate control, it may pollute the grid. Because of this, a suitable charging regulation is essential for both grid quality and battery life. In addition to providing reactive power (either inductive or capacitive), the EV charger's reactive power correction also filters current harmonics and regulates voltage to a certain degree. By supplementing reactive power with EVs, reactive power compensators, such as static synchronous compensators, static VAR compensators, and capacitor banks, can be installed and maintained at lower prices.

Furthermore, the possibility of voltage fluctuation is further decreased by the regulated exchange of reactive power. This keeps the grid steady and compliant with the rules. However, because of undesired ripple current, reactive power correction via EV charger may cause significant stress on the battery and shorten its life cycle.

A key component of EV charger design is control theory. Closed-loop control guarantees steady operation, precise regulation of current and voltage, and compliance with battery charging profiles (e.g., CC-CV, constant current/constant voltage). By predicting system behaviour and optimizing control operations, more advanced controllers—like Model Predictive Control (MPC)—allow proactive regulation.

The development of EV chargers is essentially driven by the need to solve the problems of reliable control, intelligent communication, efficient power conversion, and smooth integration with the developing smart grid. These problems present a wealth of opportunities for investigation and creativity, with important ramifications for future mobility and energy sustainability.

## 1.7 OBJECTIVE:

The design of an EV charger controller is suggested by this research project. In this context, a laboratory-designed EV charger prototype has been created using the dSPACE 11004. This work focuses on reducing second-order ripple in a single-stage off-board EV charger and designing the control architecture for an off-board EV charger. To reduce the inherent tendency of creating second order ripple on the DC side, a new control architecture for a single stage off-board EV charger has been developed. A single-phase AC-DC converter is used for this in order to charge. Additionally, the control system was created with off-board EV charging in mind. These EV chargers have two stages of conversion: DC-DC and AC-DC. Proportional integral (PI), proportional resonant (PR), plant integrated proportional integrated (PIPI), and model predictive controller (MPC) are the foundations of the independent controllers for both converters. Thus, the primary goal of the proposed study is to create a reliable control system for an EV charger that can work in a variety of G2V and V2G modes while keeping the DC side's ripple content within an acceptable range. In the event that a battery charges more slowly, the EV charger can compensate reactive power (either inductive or capacitive) and provide active power to the grid if necessary. In that scenario, the charger's remaining rating is used to compensate for reactive power in order to maximize charger rating use. Additionally, the EV charger can enhance the power quality by acting as an active power filter when the battery is not attached to it. All EV charger controller performance has been evaluated in eight distinct modes, including adjusting linear/non-linear reactive power and charging/discharging.

The MATLAB/Simulink environment has been used to simulate and validate the performance of all proposed control approaches, with a hardware prototype being used for real-time validation.

## 1.8 OUTLINE OF THESIS:

**Chapter -1:** The introduction and fundamental characteristics of EVs and their varieties are covered in this chapter. Standards for EV chargers and different battery types while charging have also been covered.

**Chapter -2:** The modes of operation of EV chargers are presented in this chapter, including the Optimal Design and Performance Analysis of Model Predictive Control for EV Charging Application of electric vehicles with experimental validation.

**Chapter -3:** The Optimal Design and Performance Analysis of Model Predictive Control for EV Discharging Application of electric vehicles with experimental validation is one of the modes of operation of EV chargers explained in this chapter.

**Chapter -4:** This chapter describes the comparison of electric vehicle charging and discharging operations using MPC, along with the necessary results and validation.

**Chapter-5:** Implementation of Robust Control for Smart Home EV Charger through FC -MPC is described in this chapter with valid simulation results and parameter mentioned in the figure.

**Chapter-6:** This chapter describes EV charger modeling, simulation, and experimental results. All results are shown with name and data.

**Chapter-7:** This chapter provides a description of the conclusion and future scope.

## CHAPTER-2

### OPTIMAL DESIGN AND PERFORMANCE ANALYSIS OF MODEL PREDICTIVE CONTROL FOR EV CHARGING APPLICATION

#### 2.1 Electric Vehicle Charger Operating Modes:

The primary benefit of MPC is that system constraints may be introduced directly to the cost function, negating the need for modulation and synchronization. It is the best option for advanced control applications due to its resilience, excellent performance, and predictive capability. It is especially appealing for a wide range of applications, from advanced driver-assistance systems in automotive engineering to process control in the chemical industries, due to its capacity to handle multivariable systems, explicitly consider constraints, and optimize control performance over a future horizon. In order to predict future states and outputs, MPC solves an optimization problem at each control interval using a dynamic model of the system. Because of its predictive character, the controller may proactively modify control inputs, foresee and mitigate future disruptions, and guarantee that operational limitations are met. It is a type of classical control that is not suited for complicated systems with many inputs and outputs, time delays, and nonlinearities. This work proposes and experimentally verifies a finite Model Predictive Control (MPC) approach for bidirectional power flow in electric vehicle (EV) chargers. An efficient two-level on-board electric vehicle charger can function according to the suggested technique. This technique allows for the decoupled regulation of reactive and active power. The finite MPC technique chooses the best voltage vector among potential voltage vectors for a two-level single-phase converter. An ideal switching state is chosen and applied to the charger based on the position of the intended error vector. Compared to the traditional MPC approach, this enhancement lessens the ripples in active and reactive power and improves the steady-state performance of the grid currents. Concerning multivariable systems, limitations, and optimal performance, MPC is typically more effective than other controllers.

#### 2.2 SYSTEM DESCRIPTION:

Fig.2.1 displays an onboard charger with a two-level, single-phase construction. Four insulated gate bipolar transistor (IGBT) switches ( $S_1, S_2, S_3$ , and  $S_4$ ) in a bridge form comprise the initial stage which is AC/DC converter. This AC/DC converter comprises of resistance (R) and input line inductors (L) connect the single-phase rectifier to a balanced power supply ( $v_g$ ). Under the given controlled configuration, the first stage AC/DC converter functions as a regulated rectifier. A DC/DC converter comprising two IGBT switches makes up the second step. Furthermore, a constant current (CC) charging

technique is utilized to charge the lithium-ion battery. Henceforth, a DC/DC converter runs in buck mode when charging a battery. Two IGBT-diode switches ( $G_1$  and  $G_2$ ) make up the DC/DC rear-end converter's second stage. An output inductor ( $L_{DC}$ ) is utilized to interface the DC/DC converter with the EV battery. The EV battery is linked in parallel with a filter capacitor ( $C_b$ ).

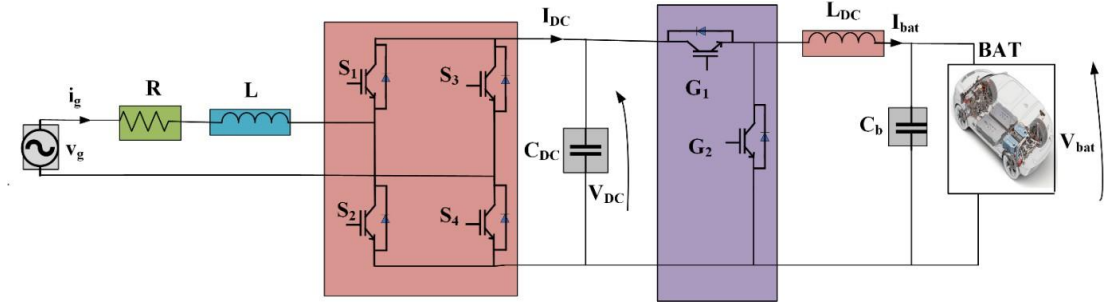


**Fig.2.1 Circuit topology of an AC/DC converter that is linked to a battery through a DC/DC converter.**

### 2.3 DC-DC CONVERTER:

As shown in Figure 2.2. on the DC side, a filter capacitor ( $C_b$ ) is provided to filter the DC voltage ( $V_{DC}$ ). The different chargers are capable of meeting different charging demands. When charging the battery via the main grid, the DC/DC converter functions as a buck-type converter is used, In order to effectively step down and regulate the voltage, improve power management, and guarantee lower power dissipation, a buck converter is frequently employed after the rectifier stage.

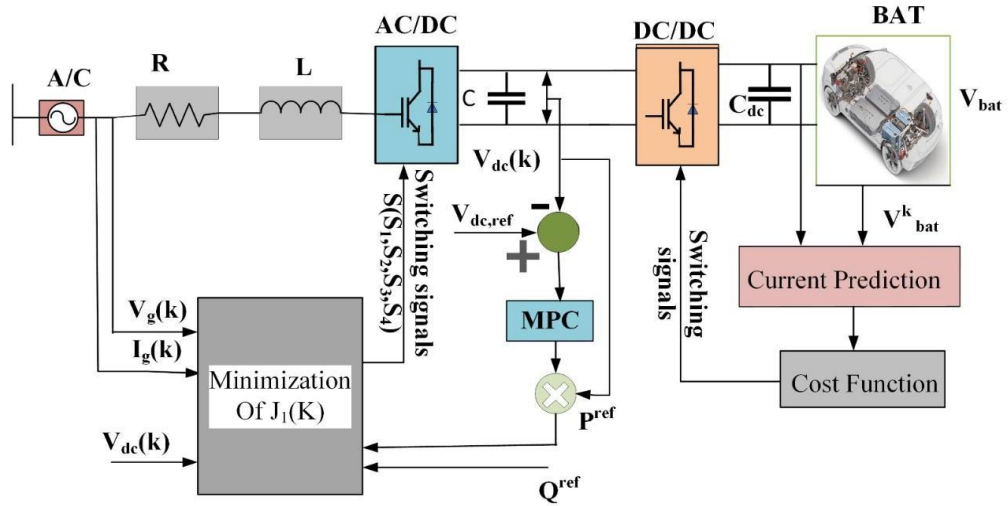


**Fig.2.2 MPC with reference design**

The DC/DC converter mathematical model can be represented by the following equations:

$$G(k)V_{DC}(k) = L_{DC} \frac{dI_{bat}(k)}{dt} + V_{bat}(k) \quad (1)$$

where  $G(k)$  represents the present switching state,  $L_{DC}$  is the filter inductor on battery side. The switching state  $G(k)$  is defined as 1 when the lower switch  $G_2$  is off and the upper switch  $G_1$  is on. Otherwise, when  $G_1$  is on and  $G_2$  is off, it is set to zero, meaning that in the switching state,  $G$  equals 1. In the absence of such,  $G(k)$  is defined as 0. Additionally,  $V_{bat}(k)$  and  $I_{bat}(k)$  represent the instantaneous voltage and current of the EV battery, respectively,  $V_{DC}(k)$  is the voltage of the DC capacitor. One can compute the anticipated battery current for the subsequent sample period by following the equation.

$$I_{bat}(k+1) = I_{bat}(k) + \frac{T_s}{L_{DC}} (G(k)V_{DC}(k) - V_{bat}(k)) \quad (2)$$

$$J(k) = \frac{k_i}{I_{bat}^{rated}} (I_{bat}^{ref}(k+1) - I_{bat}(k+1))^2 = J_2 \quad (3)$$

Where  $T_s$  is the sample interval,  $I_{bat}^{rated}$  and  $I_{bat}^{ref}$  stand for the rated and reference value of battery current respectively and  $I_{bat}(k+1)$  is the future value of the battery current. The DC/DC converter's job is to keep an eye on the battery current so that the electric vehicle battery can be charged. Thus, the DC-link voltage ( $V_{DC}$ ), the grid voltage ( $v_g$ ), the grid current ( $i_g$ ), and the battery current ( $I_{bat}$ ) are the four targets for this MPC technique. The switching states  $S(k)$  and  $G(k)$  that can minimize this cost function are chosen by creating a cost function  $J$  to accomplish this multi-objective control. The goal of selecting a switching state  $G(k)$  for the DC/DC converter is to minimize the cost function ( $J_2$ ).

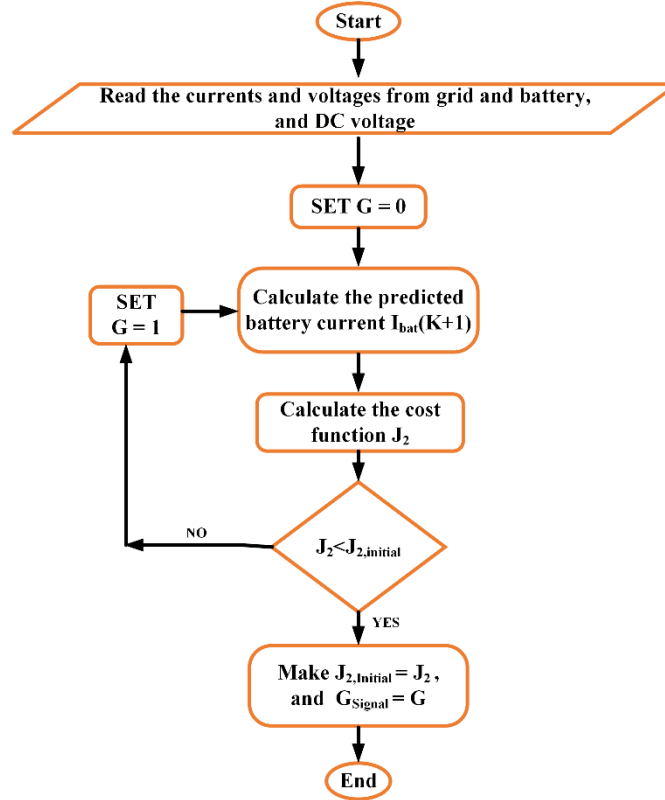


**Fig.2.3 Flowchart of MPC**

The suggested approach and the traditional MPC scheme are contrasted in a flowchart Fig.2.3, which also illustrates the decision-making process and procedural phases in the control algorithm, which would normally show the processing of inputs, the generation of control signals by the MPC technique, and the transitions between various operational modes of the system.

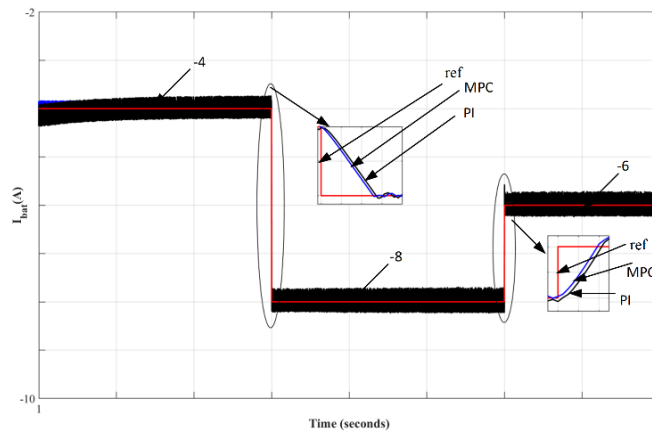


**Fig2.4 Comparison of PI and MPC controller with reference current**

Fig.2.4 Show the comparison of two controller i.e MPC and PI with reference current, here battery current of MPC acquire the steady state earlier while battery current of PI will take little longer time for stability, this is shown in the transition point. Hence we can say that MPC is better than PI controller. This Fig. shows the change in current at the transition point of both  $I_{ref}$  and  $I_{bat}$ . Henceforth it can be concluded that the proposed control of DC/DC converter in charging mode satisfies the condition.

## 2.4. RESULTS AND SIMULATION:

To illustrate the functionality of both the suggested and traditional controllers, this section provides some simulation results. Model as the EV charger in MATLAB/Simulink, the single-phase converter shown in Fig.2.1. The output of the MATLAB/Simulink simulation is displayed in scope to demonstrate the system's resilience. The purpose of this simulation is to evaluate the system's functionality.

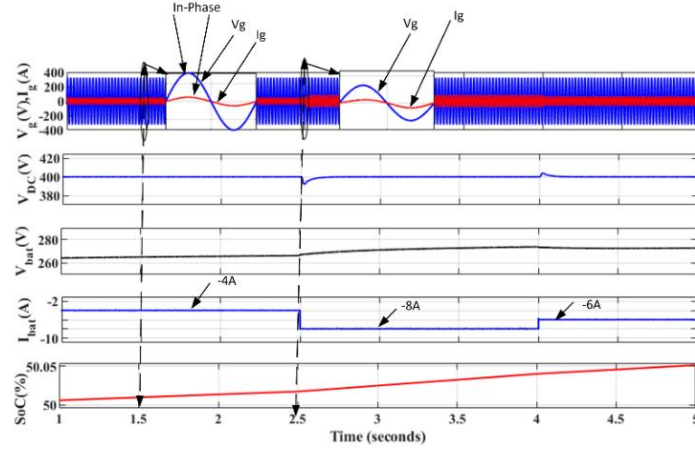
**Table 2.1: System Parameter for Bidirectional Charger**

Symbol	Quantity	Value
$(v_g)$	Grid voltage	325V(rms)
$k_p$	Active power Factor	1
$k_q$	Reactive Power Factor	1
$(V_{DC}),$	DC voltage	400 V
$T_s$	Sampling Time	12e-9sec
L	Inductance	4e-3mH
frequency	Sampling frequency	50khz
$I_{ref}$	Reference current	-5A
$V_{bat}$	Battery voltage	260 V
$i_{bat}$	Battery current	5A

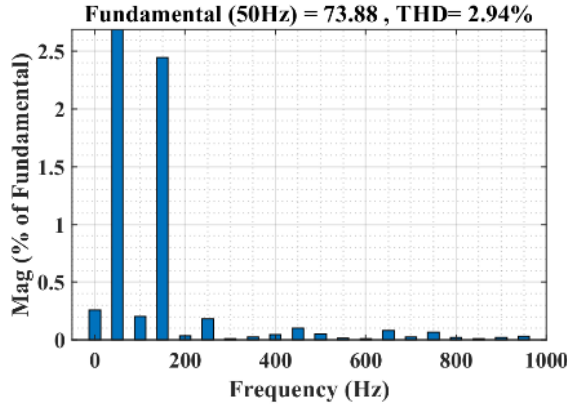
The charger's responsiveness is demonstrated under a range of grid voltage fluctuations. The simulation also examines the behaviour of the system in standard grid settings and in the combination of several scenarios. The waveforms show how the battery charges by comparing changes in battery current, non-ideal source conditions, and load changes in the source. Fig.2.5 show reference change operating condition means we are changing the reference current at different value to show the system is robust and result is shown accordingly. These waveforms show  $v_g$  and  $I_g$  are in phase, and have unity power factor, the constant DC link voltage,  $V_{DC}$ , which changes at reference point, further attest to  $i_{bat}$ ,  $V_{bat}$  and SoC. Where  $i_{bat}$  changes -4A, -8A and -6A.  $V_{bat}$  changes at reference point i.e 2.5sec and 4sec at time scale.



Fig.2.6 show the THD under reference change operating conditions and its value is 2.94% Which is almost correct for this condition.

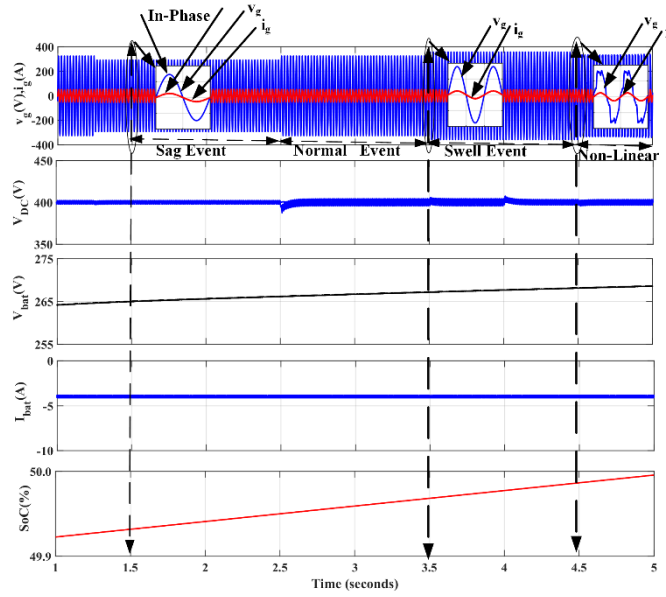


**Fig.2.5 Reference change operating condition**



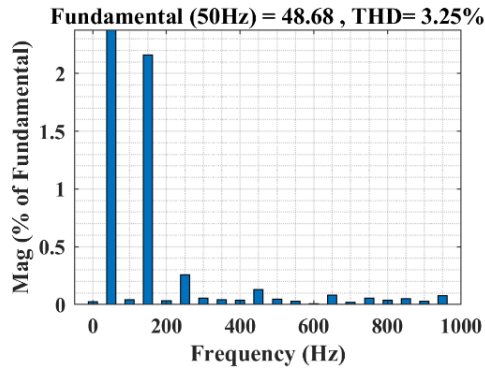
**Fig.2.6 THD under reference change operating conditions.**

Fig.2.7 show the non-ideal operating condition means we are changing source from ideal to non-ideal to check the system robustness whether it works on non-ideal condition or not but it's perfectly working on non-ideal condition as shown .These waveforms show in-phase  $v_g$  and  $I_g$ , and sag event and swell events, normal event and non-linear event so on, in the constant DC link voltage,  $V_{DC}$ , further attest to  $i_{bat}$ ,  $V_{bat}$  and SoC. The built-in charger further demonstrates how well  $i_{bat}$  regulated charging current controls the charging process.



**Fig.2.7 Nonideal Source operating condition**

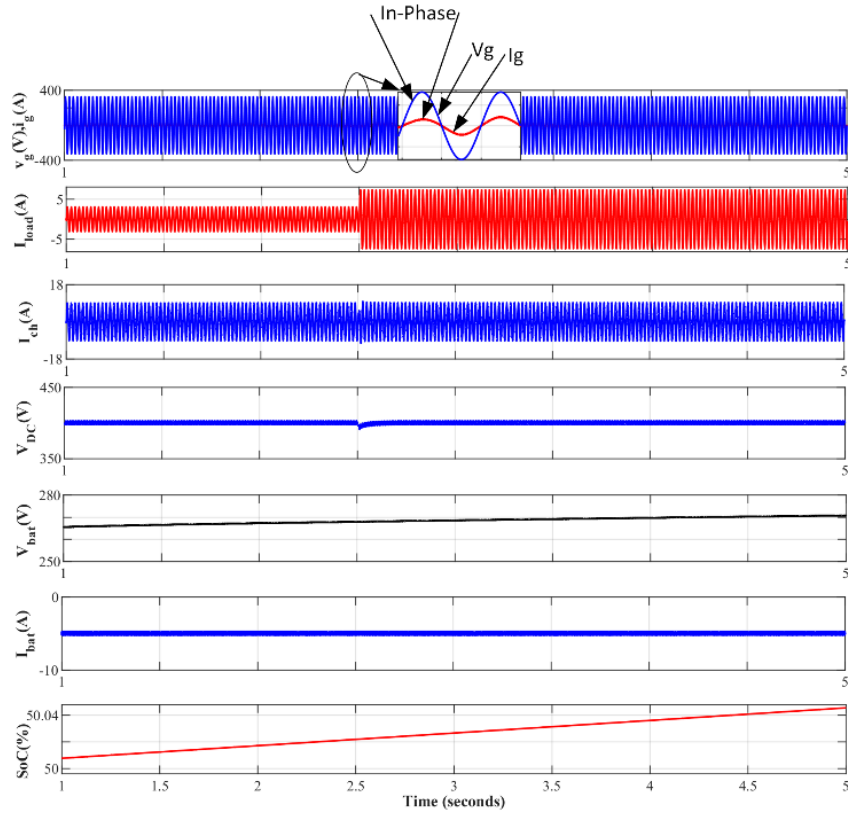
Fig.2.8 shows The THD under non-ideal operating condition which means when source is not ideal the value of THD is calculated and its value is 3.25% which is perfectly correct.



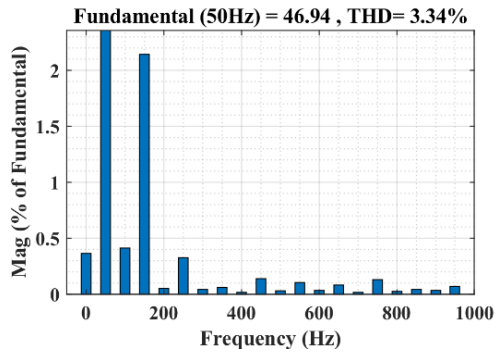
**Fig.2.8 THD under nonideal operating conditions**

Fig.2.9 show load changes operating condition which means if we vary load in the system how the system response it is shown in the Fig. These waveforms show in-phase  $v_g$  and  $I_g$ , and  $I_{load}$  and  $I_{ch}$  changes of current in the constant DC link voltage,  $V_{DC}$ , further attest to  $i_{bat}$ ,  $V_{bat}$  and SoC.

Fig.2.10 shows The THD under load change operating condition which means when load is changed, the value of THD is calculated and its value is 3.34% which is perfectly correct.



**Fig.2.9 Load change operating conditions**



**Fig.2.10 THD under Load change operating conditions**

Also MPC is faster than PI. MPC uses a model of the system to predict future behavior over a defined time horizon. It solves an optimization problem at each control step to minimize a cost function (e.g., tracking error, control effort). MPC can explicitly handle constraints on inputs, outputs, and states. The controller makes decisions based on predicted future states, not just current errors. PI controllers use a simple feedback mechanism to correct errors between a setpoint and the measured process variable. PI control does not require a mathematical model of the system. PI controllers typically do

not handle constraints explicitly; they are generally designed for linear systems without hard constraints.

The control action is based on the current and past errors, without future prediction. MPC requires solving an optimization problem online, which can be computationally intensive depending on the system's complexity. More challenging to implement due to the need for a dynamic model and real-time optimization algorithms. Simple to implement with straightforward tuning methods (e.g., Ziegler-Nichols). Requires minimal computational resources, making it suitable for systems with limited processing power. MPC often provides better performance, especially in systems with multiple inputs and outputs (MIMO) or systems with significant delays. The controller can achieve near-optimal performance by considering future behavior and constraints. PI controllers perform well in Single Input Single Output (SISO) systems and where the system dynamics are simple. In more complex systems, especially those with delays or nonlinearities, PI controllers may not achieve optimal performance. MPC can handle model uncertainties to some extent, but performance may degrade if the model is inaccurate.

MPC can be extended to adapt to changing conditions by updating the model online. PI controllers are generally robust and can perform well even with some level of model uncertainty or disturbances, though not as well as MPC in complex scenarios. PI controllers usually do not adapt to changing conditions unless combined with adaptive mechanisms. Commonly used in complex, multi-variable systems such as chemical process control, power systems, autonomous vehicles, and aerospace. Widely used in industries where performance, safety, and constraint handling are critical. Widely used in simpler industrial control systems such as temperature control, motor drives, and other SISO control problems. Preferred in applications where simplicity and ease of use are more critical than optimal performance. Involves tuning the weights in the cost function and setting the prediction and control horizons. Requires expertise and system-specific knowledge. Typically involves tuning two parameters (proportional gain and integral time constant), with several heuristic and analytical methods available.

## **2.5 CONCLUSION:**

This work provides a model predictive control (MPC) for electric vehicle (EV) chargers using a finite control set. In the traditional MPC method, the DC voltage reference is used to provide an active power reference using a PI controller which has single fixed set of coefficients. This work proposes to replace the PI control loop with a customized reference-based MPC method. The suggested plan may accomplish multi objective control, which includes separately regulating the DC voltage, and battery charging current. Amazingly, the recommended method prevents the DC voltage from overshooting or undershooting. It is feasible to design separate battery current, reactive power, and DC voltage controllers.

## **CHAPTER- 3**

### **OPTIMAL DESIGN AND PERFORMANCE ANALYSIS OF MODEL PREDICTIVE CONTROL FOR EV DISCHARGING APPLICATION**

#### **3.1 Electric Vehicle Discharger Operating Modes:**

Electric vehicle has evolved to seem more advanced, fuel-efficient, low-maintenance, and ecologically beneficial in recent decades. The power electronic converter is the main component that supports the battery and the source [1]. Because fossil fuels are more readily available, there are more and more electric vehicle on the road every day. An electric vehicle's battery is typically charged by the grid, which frequently adds more strain to the system. Because of this, the grid's load is supported and decreased when the battery is able to release its stored power during periods of high load demand, according to the notion of grid to load. Owners of electric vehicles can use the energy stored in their batteries to generate a certain amount of revenue.

Several benefits are offered. Because it plays a critical role in decision-making and helps to mitigate grid-related instabilities, the smart grid offers significant hope. The idea under discussion is called vehicle-to-grid (V2G) [2]. The main goal of this project is to construct an isolated, bidirectional, fast-response, current-controlled DC-DC converter that can simulate an electric vehicle battery's on-road current in a laboratory or manufacturing setting [3]. The two bidirectional phases of the suggested converter are seen in Fig.3.1. A single-phase full-bridge AC-DC converter powers the front end and is in the process of charging. It becomes a DC-AC converter to recover energy discharged from battery to grid [4]. The second stage controls the charging and discharging current of the battery using a different DC-DC converter.

For the Battery inverter current control, this work proposes an advanced model predictive control (AMPC) to bring high-quality electricity into the network [5]. The inverter has two control levels: the first is a simple hysteretic power management level that shifts the power reference to the second level based on the battery's state of charge (SoC) value, The second level is an advanced MPC controller that drives the inverter to inject the right quantity of high-quality current in line with the reference without requiring a module [6]. With the selected control strategies, a simulation of our hybrid system will be accomplished.

A new control method for power electronic converters is called advanced model predictive control, or AMPC. The benefits of AMPC include its capacity to manage intricate, nonlinear systems and accomplish many control goals while abiding by a number of restrictions. By skipping the repetitive computations of the cost functions and states

forecasts, AMPC provides a much lower computing overhead. However, AMPC heavily depends on the power converter's dynamic model. They are therefore more prone to ambiguities and interruptions. This paper presents a novel approach to increase the robustness and reliability of the AMPC for electric vehicle chargers by treating the dynamic model of the converter as a black box. Next, a recursive least squares algorithm-based adaptive estimating technique is suggested for online dynamic. Improved performance, computation speed, resilience, or adaptability in dynamic systems are the goals of Advanced Model Predictive Control (MPC), which is a more advanced version of the basic MPC framework. In domains where real-time operation is crucial and system dynamics might be complex, such as power electronics, drives, and energy systems, these upgraded versions are especially pertinent.

This research proposes and experimentally verifies an advanced MPC approach with extended voltage for bidirectional power flow EV chargers. The rest of the paper is structured as follows. The two-way EV charger system's controller design is displayed in Section II. In this part, the AMPC scheme concept for this two-stage charger is also thoroughly discussed. Part III contains the outcomes of tests and simulations related to the charging and discharging states. Section IV presents the concluding findings.

### 3.2 CONTROLLER DESIGN:

Advanced Model Predictive Control (AMPC) is a sophisticated control technique that solves a dynamic optimization problem at each time step to forecast and optimize a system's future behaviour. In order to forecast future outputs over a finite prediction horizon while taking input, state, and output restrictions into account, AMPC employs a mathematical model of the system. It determines the best control measures to accomplish the intended goals, such performance, stability, or efficiency, based on these forecasts. Fig.3.2. AMPC controller design for EV charger.

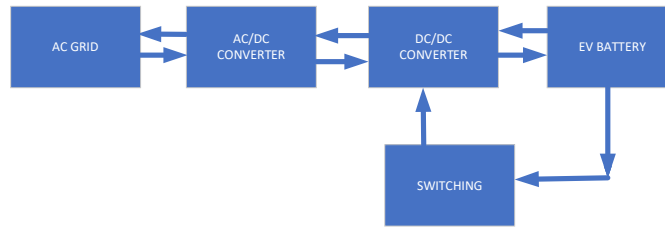


**Fig.3.1 Circuit topology of an AC/DC converter that is linked to a battery through a DC/DC converter.**

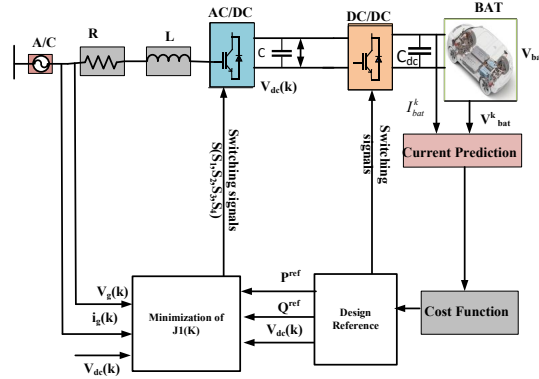


**Fig.3.2 AMPC controller design for EV charger.**

The continuous control inputs in advanced MPC can have any value as long as it stays within the specified bounds. This makes it possible to regulate system variables more precisely and with smoother control actions. Advanced MPC can reach more optimal solutions through continuous optimization, especially in complex systems with considerable unpredictability. The control inputs in Finite Set MPC are chosen from a predetermined, distinct set of potential control actions. This restricts the control resolution, which could result in less seamless transitions and, under some circumstances, less-than-ideal performance.

At every stage, Advanced MPC uses increasingly complex solvers capable of minimizing a continuous cost function across a prediction horizon to solve a continuous optimization issue. This makes it possible to adjust several performance criteria (such as power quality and energy efficiency) and can enhance performance for complicated, nonlinear systems.

**Table3.1: Comparison of MPC and PI**

Aspect	Model Predictive Control (MPC)	Proportional-Integral (PI) Control
Control Strategy	Based on optimization, it forecasts future behaviour using a system model.	Feedback-based, depending on mistakes from the past and present.
Prediction Capability	forecasts future conditions over a given time frame.	No ability to forecast
Response to Constraints	specifically manages a number of limitations (voltage, current, SOC, etc.)	does not naturally manage limitations.

Dynamic Performance	Better dynamic reaction, particularly in systems with several variables.	Ideal for single-variable, linear systems with minimal dynamics.
---------------------	--	--

Systems with complicated dynamics and many control objectives, like nonlinear systems or systems with multiple constraints, are better suited. Advanced MPC can manage more complex control objectives, such as balancing thermal restrictions, optimizing battery life, and minimizing energy loss.

Explicit limitations on inputs, outputs, and states can be handled continuously by Advanced MPC. This is especially crucial in applications with stringent power, voltage, and temperature restrictions, such as electric automobiles.

It demands additional processing power because of the model's complexity and ongoing optimization. However, even for complicated systems, real-time implementation is becoming more and more possible due to advancements in algorithms and processing capacity. Advanced MPC can lower switching losses and component stress, such as that of power transistors, because it uses continuous control inputs. This results in a longer system lifespan and higher efficiency, particularly in high-frequency switching applications like DC-DC converters, makes it possible to more precisely adjust performance parameters like response time, stability, and power quality by allowing for more flexibility of the cost function and prediction model. Smoother and more accurate control actions are the result of continuous control inputs. Improved performance in intricate, nonlinear systems as a result of more advanced optimization algorithms. Managing limitations explicitly for better system efficiency and safety. It decreased switching losses, improved system performance, and decreased component wear. More adaptability while managing various performance measures and adjusting control objectives.

The DC/DC converter mathematical model can be represented by the following equation:

$$i_L^{ref}(k+1) = -G(k+1)i_{bat}^{ref}(k+1) \quad (1)$$

where  $G(k+1)$  represents the next switching state. The switching state  $G(k+1)$  is defined as 1 when the lower switch  $G_2$  is off and the upper switch  $G_1$  is on. Otherwise, when  $G_1$  is on and  $G_2$  is off, it is set to zero, meaning that in the switching state,  $G(k+1)$  equals 1. In the absence of such,  $G(k+1)$  is defined as 0.

Where  $T_s$  is the sample interval,  $i_L^{ref}(k+1)$  is load current reference and  $i_{bat}^{ref}(k+1)$  stand for battery current reference.

$$i_{dc}^{ref}(k+1) = i_L^{ref}(k+1) - i_c^{ref}(k+1) \quad (2)$$



$i_c^{ref}(k+1)$  is capacitor current reference, the switching states  $S(k)$  and  $G(k)$  that can minimize this cost function are chosen by creating a cost function  $J$  to accomplish this multi-objective control. Minimizing the cost function ( $J$ ) is the aim of choosing a switching state  $G(k)$  for the DC/DC converter.  $i_{dc}^{ref}(k+1)$  is the expected DC-link current and can be obtained through  $i_c^{ref}(k+1)$  and  $i_L^{ref}(k+1)$ . The expected DC-link current  $i_{DC}^{ref}(k+1)$  can be calculated from  $i_L^{ref}(k+1)$  (load current reference) and  $i_c^{ref}(k+1)$  (capacitor current reference) as shown in equation (2).

$$i_c^{ref}(k+1) = \frac{C}{MT_s} [V_{DC}^{ref}(k) - V_{DC}(k)] \quad (3)$$

$V_{DC}^{ref}$  is the given battery voltage reference,  $V_{DC}^{\sim ref}$  is DC-link filtered voltage reference,  $V_{DC}(k)$  is the measured system state voltage. Knowing that the capacitor current reference  $i_c^{ref}(k+1)$  is only controlled by the DC-link filtered voltage reference,  $V_{DC}^{\sim ref}$  and can be calculated by equation (3) and equation (4).

$$i_c^{ref}(k+1) = C \frac{d(V_{DC}(k+1))}{T_s} \quad (4)$$

$$V_{DC}^{\sim ref}(k+1) = V_{DC}(k) + \frac{1}{M} (V_{DC}^{ref}(k) - V_{DC}(k)) \quad (5)$$

The filtered reference signal  $V_{DC}^{\sim ref}$  is obtained by introducing a reference prediction horizon  $M$ . Next, equation (5) yields the filtered reference signal,  $V_{DC}^{\sim ref}$ .

$$i_c^{ref} = \frac{C}{T_s} (V_{DC}^{\sim ref}(k+1) - V_{DC}(k)) \quad (6)$$

The modified  $i_c^{ref}(k+1)$  can be obtained from equation (6).

$$i_{dc}^{ref}(k+1) = G(k+1)i_{bat}^{ref}(k+1) + \frac{C}{MT_s} (V_{DC}^{ref}(k) - V_{DC}(k)) \quad (7)$$

$$J(k) = \frac{k_i}{I_{bat}^{rated}} (I_{bat}^{ref}(k+1) - I_{bat}(k+1))^2 = J_2 \quad (8)$$

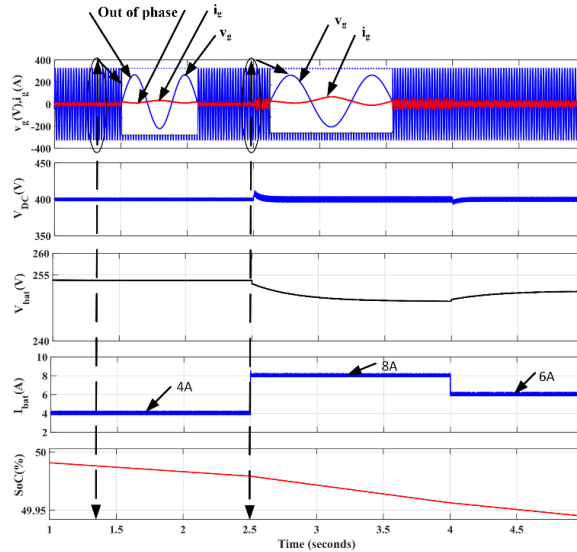
Therefore, the expected DC-link current  $i_{dc}^{ref}(k+1)$  can be calculated from equation (7).

A cost function  $J$  is established in order to accomplish this multi-objective control, and the switching states  $S(k)$  and  $G(k)$  that are able to minimize this cost function are chosen. The DC/DC converter's switching state  $G(k)$  is selected in order to minimize the cost function ( $J_2$ ). Equation (8) defines  $J_2$ .

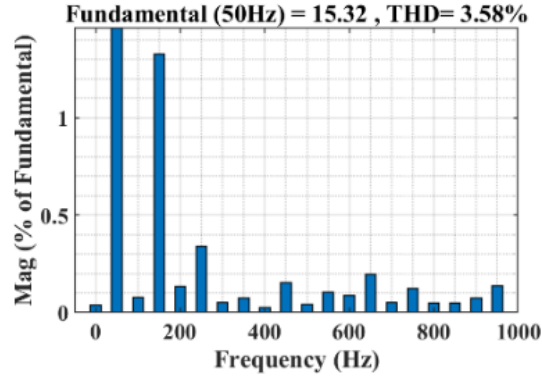
### 3.3 RESULT AND SIMULATION:

To illustrate how the recommended and sophisticated controllers work, a few simulation results are presented in this section. Make an EV charger model of the single-phase converter with MATLAB/Simulink. The output of the simulation is displayed in scope to demonstrate the system's resilience. The purpose of this simulation is to evaluate the system's performance.

In this section we show how sensitive the converter is to various variations in grid voltage. The behaviours of the system in both normal grid settings and when multiple scenarios are combined is also examined by the simulation. In order to illustrate how the battery charges, the waveforms compare variations in battery current, non-ideal source conditions, and source load variations. Figure 3.3 illustrates the reference change operating state under discharging condition, which is achieved by varying the reference current at various values to demonstrate the robustness of the system and the corresponding results. The constant DC link voltage  $V_{DC}$ , which varies at the reference point, further attests to  $I_{bat}$ ,  $V_{bat}$ , and SoC. These waveforms also demonstrate that  $v_g$  and  $i_g$  are out of phase. Whereas  $I_{bat}$  alterations 4A, 8A, and 6A.  $V_{bat}$  varies at the point of reference, i.e. Fig.3.4 show the THD under reference change operating conditions in discharging state and it's value is 3.58% Which is almost correct for this condition.

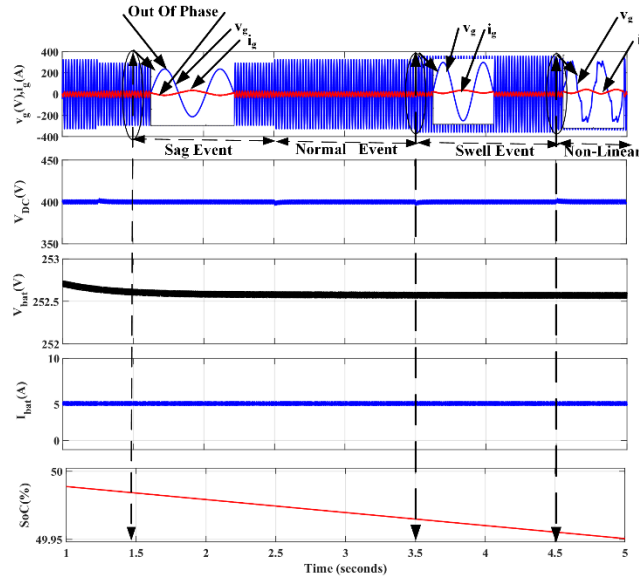


**Fig.3.3 Reference change operating conditions in discharging state.**



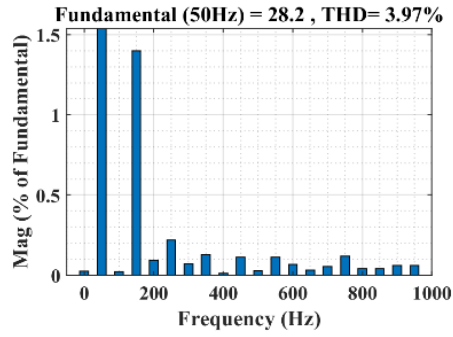
**Fig.3.4 Reference change THD under discharging state.**

Fig.3.5 show the non-ideal operating condition in discharging state means we are changing source from ideal to non-ideal to check the system robustness whether it works on non-ideal condition or not but it's perfectly working on non-ideal condition as shown. These waveforms show out-of-phase  $v_g$  and  $i_g$ , and sag event, normal event swell events and non-linear event so on, in the constant DC link voltage,  $V_{DC}$ , further attest to  $I_{bat}$ ,  $V_{bat}$  and SoC. The built-in charger further demonstrates how well  $I_{bat}$  regulated discharging current controls the discharging process.



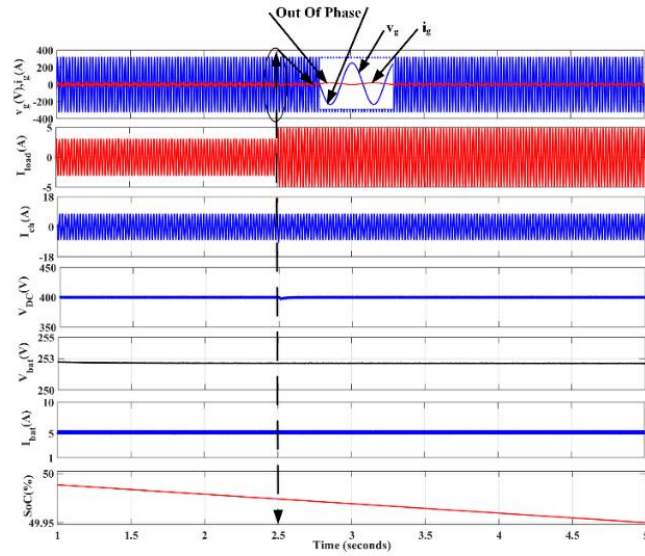
**Fig.3.5 Nonideal operating conditions under discharging conditions.**

Fig.3.6 shows The THD under non-ideal operating condition in discharging mode which means when source is not ideal the value of THD is calculated and it's value is 3.97% which is perfectly correct.



**Fig. 3.6 Nonideal source change THD under discharging state**

Fig.3.7 show load change operating condition in discharging mode which means if we vary load in the system how the system response it is shown in the Fig. These waveforms show out-of-phase  $v_g$  and  $i_g$ . In addition,  $i_{load}$  and  $i_{ch}$  is shown, in the constant DC link voltage,  $V_{DC}$ , further attest to  $I_{bat}$ ,  $V_{bat}$  and SoC. Fig.3.8 shows The THD under load change operating condition in discharging condition, which means when load is changed, the value of THD is calculated and its value is 4.57% which is perfectly correct.



**Fig.3.7 Load change operating conditions under discharging condition.**

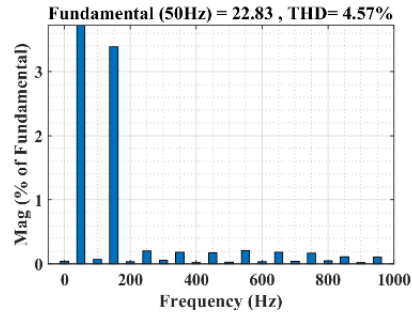


**Fig.3.8 THD under Load change operating conditions in discharging state**

### 3.4 CONCLUSION:

In this work, an Advanced Model Predictive Control (AMPC) technique for electric vehicle (EV) applications has been successfully developed and designed. Important issues including dynamic performance, energy efficiency, and system restrictions are successfully addressed by the suggested control framework. Through the utilization of MPC's predictive capabilities, the method optimizes power distribution, guaranteeing seamless operation and improved vehicle performance. The success of the suggested AMPC strategy is confirmed by simulation and experimental findings, which show better tracking accuracy, lower energy usage, and more comfortable driving when compared to traditional control techniques. Furthermore, AMPC is a viable option for contemporary EV powertrain control because to its real-time handling of multi-variable restrictions.

## CHAPTER-4

### Comparison of Charging and Discharging Operation of Electric Vehicle through MPC

#### 4.1 INTRODUCTION:

In recent decades, electric vehicles have become increasingly sophisticated, fuel-efficient, low-maintenance, and environmentally friendly. The primary part supporting the source and battery is the power electronic converter [1]-[5]. The number of electric vehicles on the road is increasing daily due to the easier access to fossil fuels. The grid usually charges the battery of an electric car, which often puts additional load on the infrastructure. According to the concept of grid to load, this means that when the battery can release its stored power during times of high load demand, the grid's load is supported and reduced. Electric car owners can make a specific amount of money by using the energy that is stored in their batteries. The suggested strategy has a number of advantages. Future energy management has a lot of promise because to the smart grid, which is essential for making decisions and reducing grid-related instability. The idea of Vehicle-to-Grid (V2G), in which electric cars (EVs) communicate with the electrical grid to improve efficiency and stability, is examined in this study [6]-[10]. The main goal is to create a current-controlled, isolated, bidirectional, fast response DC-DC converter that can simulate the on-road current of an EV battery in a manufacturing or laboratory setting [11]. As shown in Fig.1, the suggested converter has two bidirectional stages. The front-end stage functions as a DC-AC converter to return discharged energy to the grid and uses a single-phase full-bridge AC-DC converter for charging [12]. A specialized DC-DC converter is incorporated into the second stage to efficiently control the battery's charging and discharging currents. In order to guarantee high-quality power injection into the grid, this work presents a Model Predictive regulation (MPC) technique for battery inverter current regulation [13]. There are two control levels for the inverter: Power Management Level: Depending on the battery's State of Charge (SoC), a basic hysteretic controller modifies the power reference. MPC Level: Without the need for further modules, the MPC controller accurately controls the inverter's output current to match the reference signal [14]-[17]. Model predictive control, or MPC, is a novel approach to power electronic converter control. Among MPC's advantages are its ability to handle complex, nonlinear systems and achieve numerous control objectives while adhering to several constraints [18]-[20]. MPC offers a significantly reduced computer overhead by avoiding the tedious calculations of the cost functions and states projections. But for MPC, the power converter Buck and Boost dynamic model is essential. As a result, they are more vulnerable to misunderstandings and disruptions. By considering the converter's dynamic model as a "black box," this research offers a novel method for enhancing the MPC's robustness and dependability for electric vehicle chargers. Next, an adaptive estimation method based on

the recursive least squares algorithm is proposed for online dynamic. Model Predictive Control (MPC) is a more sophisticated variant of the fundamental MPC framework that aims to improve system performance, computation speed, robustness, or adaptability in dynamic systems. Such improved versions are particularly relevant in fields like power electronics, drives, and energy systems, where real-time operation is essential and system dynamics may be complex. This research proposes and experimentally verifies an advanced MPC approach with extended voltage for bidirectional power flow EV chargers. The rest of the paper is structured as follows. The two-way EV charger system's controller design is displayed in Section II. In this part, the MPC scheme concept for this two-stage charger is also thoroughly discussed. Part III contains the outcomes of tests and simulations related to the charging and discharging states. Section IV presents the concluding findings. In order to minimize a cost function at each control interval, MPC solves an optimization issue, usually striking a balance between control effort and performance (tracking reference).

## 4.2 CONTROLLER DESIGN:

Model Predictive Control (MPC) is an advanced control method that forecasts and optimizes the future behaviour of a system by solving a dynamic optimization problem at each time step. MPC uses a mathematical model of the system to anticipate future outputs over a finite prediction horizon while accounting for input, state, and output constraints. Based on these projections, it chooses the most effective control strategies to achieve the desired outcomes, such as efficiency, performance, or stability.

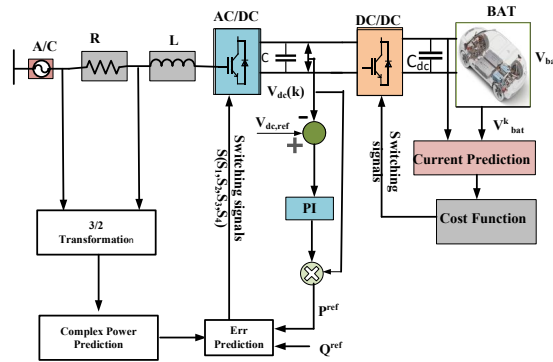


**Fig.4.1 MPC Controller**

As long as it remains within the designated parameters, the continuous control inputs in advanced MPC can have any value. This enables smoother control actions and more accurate regulation of system variables. Through ongoing optimization, advanced MPC can arrive at more optimal solutions, particularly in complex systems with significant

unpredictability. In MPC, the control inputs are selected from a predefined, discrete set of possible control actions. This limits the control resolution, which may lead to less smooth transitions and, in certain cases, subpar performance. In order to tackle a continuous optimization problem, MPC employs progressively more sophisticated solvers that can minimize a continuous cost function over a prediction horizon. This can improve performance for complex, nonlinear systems and allows for the adjustment of many performance criteria (such power quality and energy efficiency). It is more appropriate for systems with complex dynamics and numerous control objectives, such as nonlinear systems or systems with numerous restrictions. More complicated control goals, like limiting energy loss, maximizing battery life, and balancing temperature constraints, can be handled by advanced MPC. MPC can continuously manage explicit constraints on inputs, outputs, and states. This is particularly important for applications like electric cars that have rigorous power, voltage, and temperature requirements. The intricacy of the model and continuous optimization make it require more computing power. But thanks to improvements in processing power and algorithms, real-time implementation is becoming increasingly feasible, even for complex systems. Because advanced MPC employs continuous control inputs, it can reduce switching losses and component stress, including that of power transistors. determines the reference power by using the battery's State of Charge (SoC). alternates between charging and discharging phases using a hysteretic control technique. keeps the system's voltage and current within safe bounds This leads to increased efficiency and a longer system lifespan, especially in high-frequency switching applications like DC-DC converters. allows for greater flexibility, which enables more accurate adjustment of performance characteristics including response time, stability, and power quality. Fig. 4.1 show the MPC Controller for the system.

**Table 4.1: Comparison of Charging and Discharging Operation of Electric Vehicle through MPC.**

<b>Aspect</b>	<b>Charging Operation</b>	<b>Discharging Operation</b>
Objective	Charge the EV battery effectively using the ideal current and voltage levels.	Maintain SOC limitations while supplying the grid or load with electricity from the EV battery.
Direction of Power Flow	From EV battery to grid/charger.	V2G (EV battery to grid) or V2L (EV battery to load)
Control Variables	Battery voltage and charging current	output voltage and discharge current



Constraints		Maximum current, thermal restrictions, and SOC upper limit	Power quality, current restrictions, and SOC lower limit
Optimization (MPC)	Goals	Reduce charging time and losses while preserving battery health.	Increase energy economy while preserving voltage stability.

### 4.3 RESULT AND SIMULATION:

To illustrate how the recommended and sophisticated controllers work, a few simulation results are presented in this section. Make an EV charger model of the single-phase converter with MATLAB/Simulink. The output of the simulation is displayed in scope to demonstrate the system's resilience. The purpose of this simulation is to evaluate the system's performance.

In this section we show how sensitive the converter is to various variations in grid voltage. The behaviors of the system in both normal grid settings and when multiple scenarios are combined is also examined by the simulation. In order to illustrate how the battery charges, the waveforms compare variations in battery current, non-ideal source conditions, and source load variations. Figure 4.2 illustrates the reference change operating state under charging and discharging condition, which is achieved by varying the reference current at various values to demonstrate the robustness of the system and the corresponding results. The constant DC link voltage  $V_{DC}$ , which varies at the reference point, further attests to  $I_{bat}$ ,  $V_{bat}$ , and SoC. These waveforms also demonstrate that  $v_g$  and  $i_g$  are in phase and have unity power factor when charging and out of phase when discharging. Whereas  $I_{bat}$  alterations -4A, -8A, and -6A.  $V_{bat}$  varies at the point of reference, i.e. Fig.4.3 show the THD under reference change operating conditions in charging state and its value is 2.94% Which is almost correct for this condition because it is less than 5% and Fig.4.4 show the THD under reference change operating conditions in discharging state and its value is 3.58% Which is almost correct for this condition.

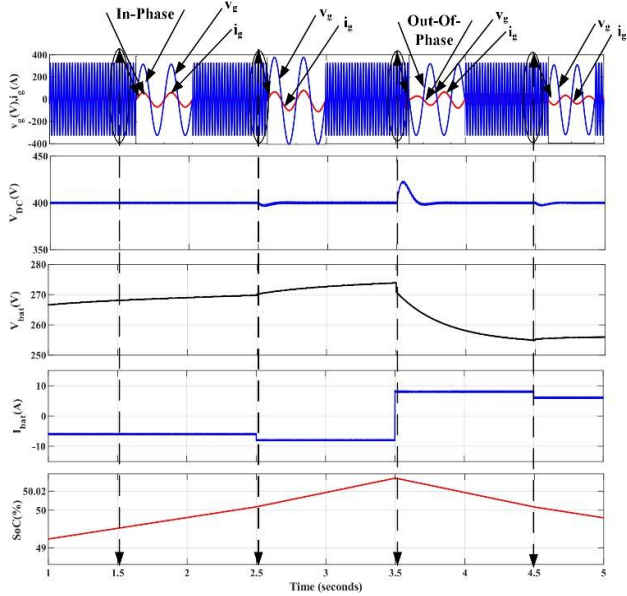


**Fig.4.2 Reference change operating condition showing both charging and discharging.**

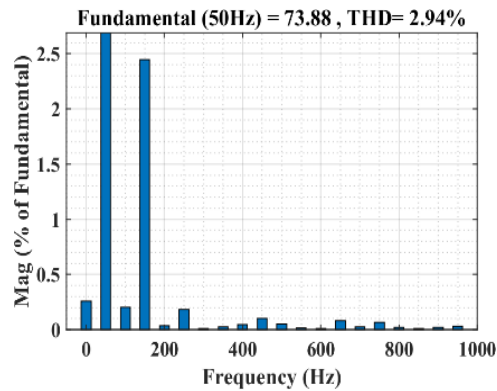


**Fig.4.3 Reference change THD under charging**

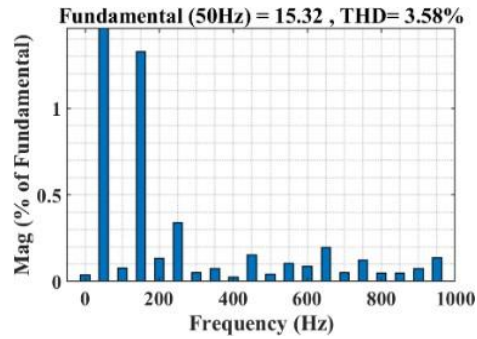


**Fig.4.4 Reference change THD under discharging state.**

Due to the fact that it is likewise less than 5%. Fig.4.5 show the non-ideal operating condition in charging and discharging state means we are changing source from ideal to non-ideal to check the system robustness whether it works on non-ideal condition or not but it's perfectly working on non-ideal condition as shown .These waveforms show in-phase  $v_g$  and  $i_g$  and out of phase in  $v_g$  and  $i_g$  , and sag event, normal event ,swell events and non-linear event so on, in the constant DC link voltage,  $V_{DC}$ , further attest to  $I_{bat}$ ,  $V_{bat}$  and SoC. The built-in charger further demonstrates how well  $I_{bat}$  regulated charging current controls the charging and discharging process. Fig.4.6 shows The THD under non-ideal operating condition in charging mode which means when source is not ideal the value of THD is calculated and it's value is 3.34% which is perfectly correct. due to the fact that it is likewise less than 5%. Fig.4.7 shows The THD under non-ideal operating condition in discharging mode which means when source is not ideal the value of THD is calculated and it's value is 3.97% which is perfectly correct. Fig.4.8 show load change operating condition in charging and discharging state which means if we vary load in the system how the system response it is shown in the Fig. These waveforms show in-phase and out of phase of  $v_g$  and  $i_g$ , in addition,  $i_{load}$  and  $i_{ch}$  is shown, in the constant DC link voltage  $V_{DC}$  further attest to  $I_{bat}$ ,  $V_{bat}$  and SoC.

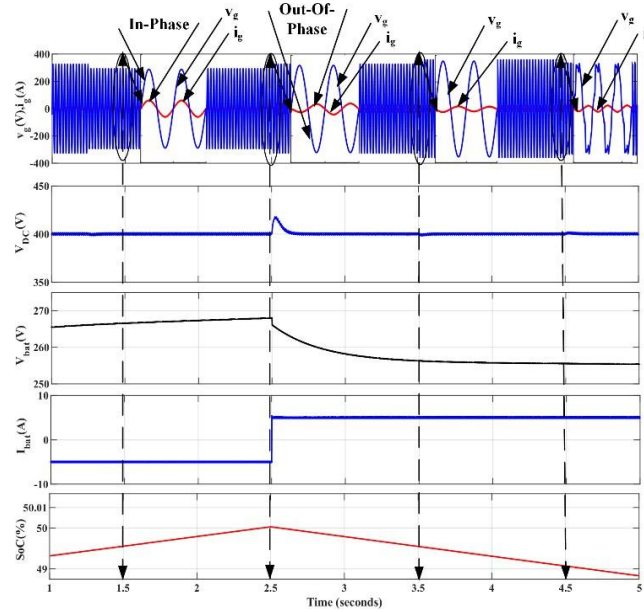


**Fig.4.5 Nonideal Source operating condition under charging state and discharging state.**

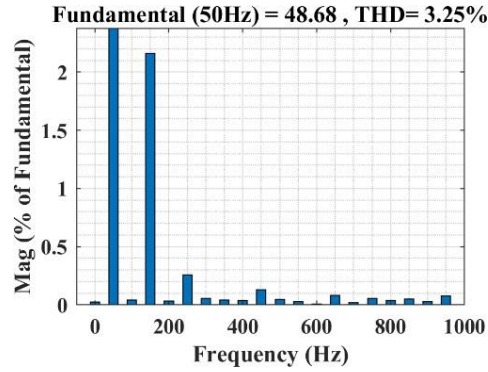


**Fig.4.6 Nonideal source change THD under charging state.**

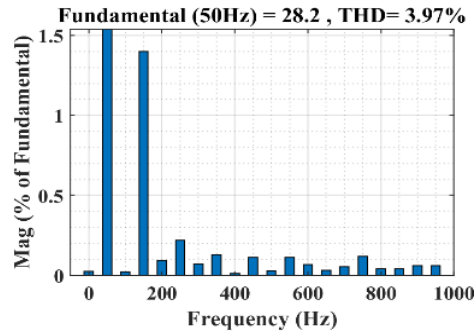


**Fig.4.7 Nonideal source change THD under discharging state.**

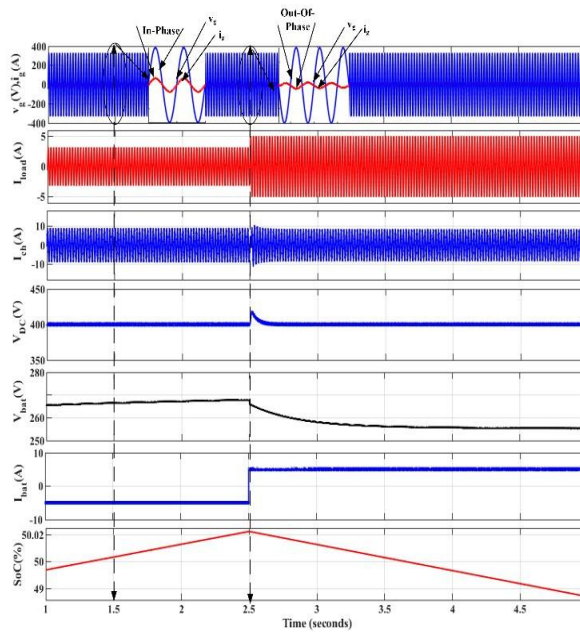


**Fig.4.8 Load change operating condition under charging state and discharging state.**

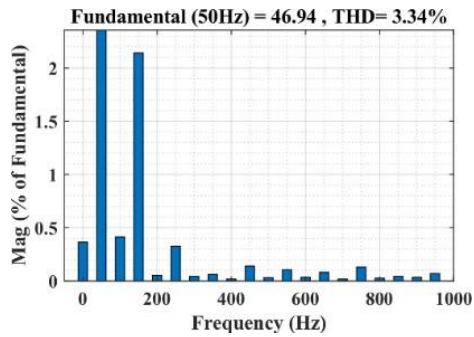


**Fig.4.9 THD under Load change operating conditions in charging state.**

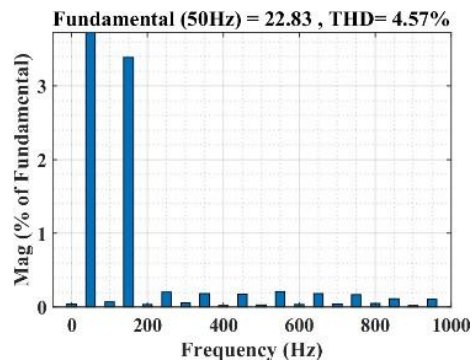


**Fig.4.10 THD under Load change operating conditions in discharging state.**

Fig.4.10 THD under Load change operating conditions in discharging state. Fig.4.9 shows The THD under non-ideal operating condition in charging mode which means when source is not ideal the value of THD is calculated and it's value is 3.34% which is perfectly correct. due to the fact that it is likewise less than 5%.

**Table 4.2 : THD during different working Condition.**

<b>Charging</b>	<b>THD (%)</b>	<b>Discharging</b>	<b>THD (%)</b>
Reference Change Operating Condition	2.94%	Reference Change Operating Condition	3.58%
Non-Ideal Operating Condition	3.25%	Non-Ideal Operating Condition	3.97%
Load-Change Operating Condition	3.34%	Load-Change Operating Condition	4.57%

Fig.4.9 shows The THD under non-ideal operating condition in charging mode which means when source is not ideal the value of THD is calculated and it's value is 3.34% which is perfectly correct. due to the fact that it is likewise less than 5%. Fig.4.10 shows The THD under non- ideal operating condition in discharging mode which means when source is not ideal the value of THD is calculated and it's value is 4.57% which is perfectly correct. due to the fact that it is likewise less than 5%.

#### **4.4 CONCLUSION:**

In order to lessen the burden on the electrical grid, the project's main goal is to create a functional, bidirectional EV battery charger that can also provide electricity to it. The electrical system is under additional strain due to the electric vehicle industry's explosive growth. Bidirectional systems optimize benefits for both V2G and G2V systems by allowing power to flow both ways. Therefore, the DC/DC converter performs buck-boost converter tasks. Through V2G, energy generated by local EV owners can be used and fed back into the power grid. This is accomplished via assigning supervision. In order to facilitate effective power flow management between the battery and the grid, this study proposed a real-time Model Predictive Control (MPC) technique for bidirectional electric vehicle (EV) charging and discharging. The suggested method combines a two-stage power conversion system, which consists of a bidirectional DC-DC converter and a single-phase full-bridge AC-DC converter, with MPC controller. The control method ensures high-quality power injection into the grid while efficiently regulating the charging and discharging currents.

## CHAPTER-5

### Implementation of Robust Control for Smart Home EV Charger through FC-MPC

#### 5.1 INTRODUCTION:

Electric vehicle (EV) adoption has increased demand for intelligent, dependable, and efficient charging infrastructure. An essential part of this ecosystem are smart home EV chargers, which allow for user convenience, grid-friendly operation, and efficient charging schedules. Uncertainties like shifting grid voltage, fluctuating EV battery conditions, and changes in load demand, however, make it difficult to guarantee steady and effective charger operation. In order to overcome these obstacles, this study investigates the use of Finite-Control Set Model Predictive Control (FC-MPC) to build robust control techniques for a smart home EV charger. Model Predictive Control (MPC) is a popular option for dynamic charging applications because of its multi-variable control, predictive capabilities, and capacity to manage system restrictions. Because FC-MPC, a discrete form of MPC, manipulates the switching states directly and does not require a separate modulation stage, it is especially well suited for power electronic converters [1]. Because fossil fuels are more readily available, there are more and more electric vehicle on the road every day. An electric vehicle's battery is typically charged by the grid, which frequently adds more strain to the system. Because of this, the grid's load is supported and decreased when the battery is able to release its stored power during periods of high load demand, according to the notion of grid to load. Owners of electric vehicles can use the energy stored in their batteries to generate a certain amount of revenue. Several benefits are offered. Because it plays a critical role in decision-making and helps to mitigate grid-related instabilities, the smart grid offers significant hope. The idea under discussion is called vehicle-to-grid (V2G) [2]. The main goal of this project is to construct an isolated, bidirectional, fast-response, current-controlled DC-DC converter that can simulate an electric vehicle battery's on road current in a laboratory or manufacturing setting [3]. The two bidirectional phases of the suggested converter are seen in Fig. 5.1. A single-phase full-bridge AC-DC converter powers the front end and is in the process of charging. It becomes a DC-AC converter to recover energy discharged from battery to grid [4]. The second stage controls the charging and discharging current of the battery using a different DC-DC converter. For the Battery inverter current control, this work proposes a model predictive control (MPC) to bring high-quality electricity into the network [5]. The inverter has two control levels: the first is a simple hysteretic power management level that shifts the power reference to the second level based on the battery's state of charge (SoC) value, The second level is MPC controller that drives the inverter to inject the right quantity of high-quality current in line with the reference without requiring a module [6]. With the selected control strategies, a simulation of our hybrid system will be accomplished. A

new control method for power electronic converters is called model predictive control, or MPC. The benefits of MPC include its capacity to manage intricate, nonlinear systems and accomplish many control goals while abiding by a number of restrictions [7]. By skipping the repetitive computations of the cost functions and states forecasts, MPC provides a much lower computing overhead. However, MPC heavily depends on the power converter's dynamic model. They are therefore more prone to ambiguities and interruptions. This paper presents a novel approach to increase the robustness and reliability of the MPC for electric vehicle chargers by treating the dynamic model of the converter as a black box. Next, a recursive least squares algorithm-based adaptive estimating technique is suggested for online dynamic. Effective and reliable control mechanisms for EV chargers in smart homes are required due to the substantial pressure that the growing popularity of electric vehicles (EVs) has placed on residential power networks. Grid stability, energy efficiency, cost optimization, and smooth integration with renewable energy sources are some of the issues that a well designed charger must handle. Advanced control techniques have become an essential solution to meet these objectives. Because it can manage multi-objective optimization in real time, Finite Control Set Model Predictive Control (FCS MPC) is a potential method for tackling these issues. By minimizing a predetermined cost function, FCS-MPC chooses the best course of action for control and forecasts the system's future behaviour over a finite time horizon. Because of this feature, it is perfect for dynamic systems like smart home EV chargers, which function, The suggested control strategy ensures optimal energy use and power quality while strengthening the charger's resilience to load fluctuations, grid disruptions, and model uncertainties. The study assesses the FC-MPC-based controller's performance in relation to traditional control schemes, highlighting its benefits in terms of quicker response times, lower harmonic distortion, and increased efficiency. The rest of the paper is structured as follows. The two-way EV charger system's controller design is displayed in Section II. In this part, the MPC scheme concept for this two-stage charger is also thoroughly discussed. Part III contains the outcomes of tests and simulations related to the charging and discharging states. Section IV presents the concluding findings.

## **5.2 CONTROLLER DESIGN:**

Model Predictive Control (MPC) is a sophisticated control technique that solves a dynamic optimization problem at each time step to forecast and optimize a system's future behaviour. In order to forecast future outputs over a finite prediction horizon while taking input, state, and output restrictions into account, MPC employs a mathematical model of the system. It determines the best control measures to accomplish the intended goals, such performance, stability, or efficiency, based on these forecasts.



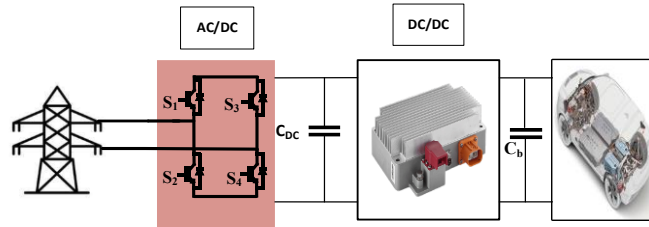


**Fig.5.1 Circuit topology of an AC/DC converter that is linked to a battery through a DC/DC converter.**

Reduce voltage/current tracking error. To guarantee seamless charging, penalize large control movements. Limits on battery current, grid voltage, and maximum/minimum charging power. Calculate the difference between the expected and actual behaviour of the system. To make up for model discrepancies, modify the control input appropriately. The continuous control inputs in MPC can have any value as long as it stays within the specified bounds. This makes it possible to regulate system variables more precisely and with smoother control actions. MPC can reach more optimal solutions through continuous optimization, especially in complex systems with considerable unpredictability. The control inputs in FS-MPC are chosen from a predetermined, distinct set of potential control actions. This restricts the control resolution, which could result in less seamless transitions and, under some circumstances, less-than-ideal performance.

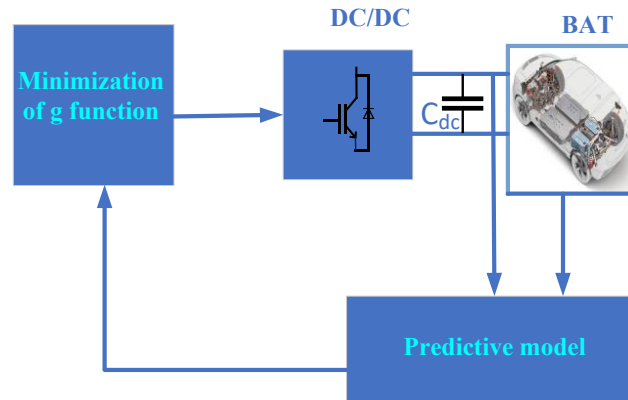


**Fig.5.2 MPC Controller for DC/DC**

At every stage, MPC uses increasingly complex solvers capable of minimizing a continuous cost function across a prediction horizon to solve a continuous optimization issue. This makes it possible to adjust several performance criteria (such as power quality and energy efficiency) and can enhance performance for complicated, nonlinear systems. Systems with complicated dynamics and many control objectives, like nonlinear systems or systems with multiple constraints, are better suited. MPC can manage more complex control objectives, such as balancing thermal restrictions, optimizing battery life, and minimizing energy loss. Explicit limitations on inputs, outputs, and states can be handled continuously by MPC. This is especially crucial in

applications with stringent power, voltage, and temperature restrictions, such as electric automobiles. It demands additional processing power because of the model's complexity and ongoing optimization. However, even for complicated systems, real-time implementation is becoming more and more possible due to advancements in algorithms and processing capacity. MPC can lower switching losses and component stress, such as that of power transistors, because it uses continuous control inputs. This results in a longer system lifespan and higher efficiency, particularly in high-frequency switching applications like DC-DC converters. makes it possible to more precisely adjust performance parameters like response time, stability, and power quality by allowing for more flexibility of the cost function and prediction model. Smoother and more accurate control actions are the result of continuous control inputs. Improved performance in intricate, nonlinear systems as a result of more advanced optimization algorithms. Managing limitations explicitly for better system efficiency and safety. It decreased switching losses, improved system performance, and decreased component wear. More adaptability while managing various performance measures and adjusting control objectives.

**Table 5.1: Step change in  $I_{bat}$**

Step change in $I_{bat}$	Value
Charging	-8A to -6A
Discharging	8A to 6A

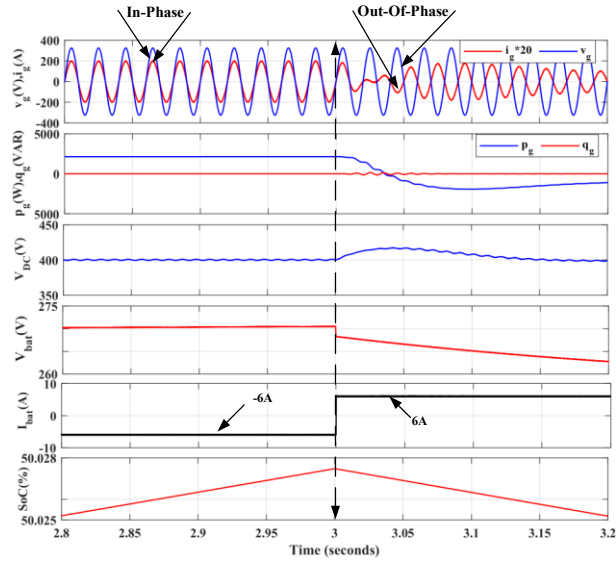
### 5.3 RESULT AND SIMULATION:

To illustrate how the recommended and sophisticated controllers work, a few simulation results are presented in this section. Make an EV charger model of the single-phase converter with MATLAB/Simulink. The output of the simulation is displayed in scope to demonstrate the system's resilience. The purpose of this simulation is to evaluate the system's performance.

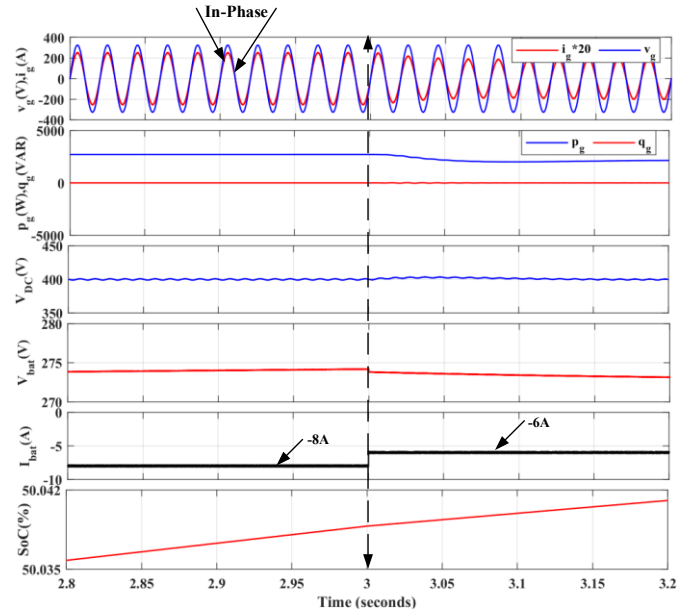
In this section we show how sensitive the converter is to various variations in grid voltage. The behaviours of the system in both normal grid settings and when multiple scenarios are combined is also examined by the simulation. In order to illustrate how the battery charges, the waveforms compare variations in battery current, non-ideal source conditions, and source load variations. Figure 5.3 illustrates the reference change operating state under charging and discharging condition, which is achieved by varying the reference current at various values to demonstrate the robustness of the system and the corresponding results. The constant DC link voltage  $V_{DC}$ , which varies at the reference point, further attests to  $I_{bat}$ ,  $V_{bat}$ , and SoC. These waveforms also demonstrate that  $v_g$  and  $i_g$  are in phase and have unity power factor when charging and out of phase when discharging. Whereas  $I_{bat}$  alterations -8A, and -6A.  $V_{bat}$  varies at the point of reference.

Figure 5.4 show  $I_{bat}$  step change operating condition in charging state means we are changing battery current from -8A to -6A to check the system robustness whether it works on step change of  $I_{bat}$  but it's perfectly working on step change condition as shown .These waveforms show in-phase  $v_g$  and  $i_g$  and out of phase in  $v_g$  and  $i_g$  , in the constant DC link voltage,  $V_{DC}$ , further attest to  $I_{bat}$ ,  $V_{bat}$  and SoC. The built-in charger further demonstrates how well  $I_{bat}$  regulated charging current controls the charging and discharging process.

FC-MPC's significance in smart home EV chargers in contrast to conventional PI controllers, FC-MPC has the ability to anticipate and address disruptions before they have an impact on system performance. (a)Quick Dynamic Response: Makes it possible to quickly adjust to variations in EV charging requirements and power availability (b)Integration with Renewable Energy: Makes smart homes more environmentally friendly by guaranteeing steady operation when charging EVs using solar or wind energy. Scalability: Adaptable to microgrid applications, enabling many EV chargers to manage energy in unison.



**Fig.5.3 Reference change operating condition showing both charging and discharging.**



**Fig.5.4 Step change in  $I_{bat}$  during charging condition**

Figure 5.5 show  $I_{bat}$  step change operating condition in discharging state means we are changing battery current from 8A to 6A to check the system robustness whether it works on step change of  $I_{bat}$  but it's perfectly working on step change condition as shown. These waveforms show in-phase  $v_g$  and  $i_g$  and out of phase in  $v_g$  and  $i_g$ , in the constant DC link voltage,  $V_{DC}$ , further attest to  $I_{bat}$ ,  $V_{bat}$  and SoC. The built-in charger further demonstrates how well  $I_{bat}$  regulated charging current controls the charging and discharging process.

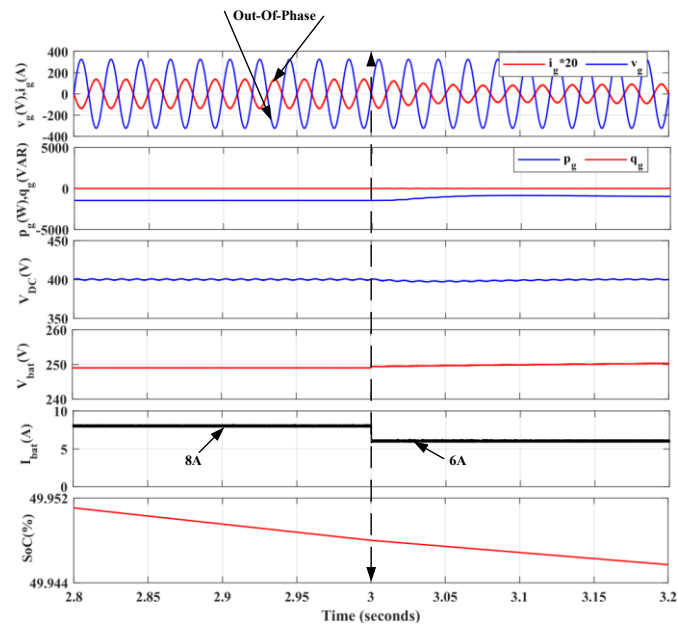


**Fig.5.5 Step change in  $I_{bat}$  during discharging condition**

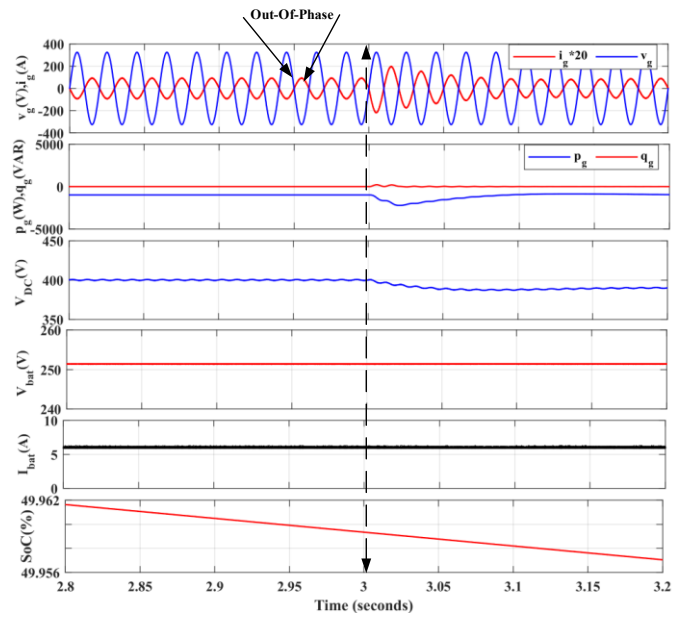


**Fig.5.6 Step change in  $V_{DC}$  during charging condition.**

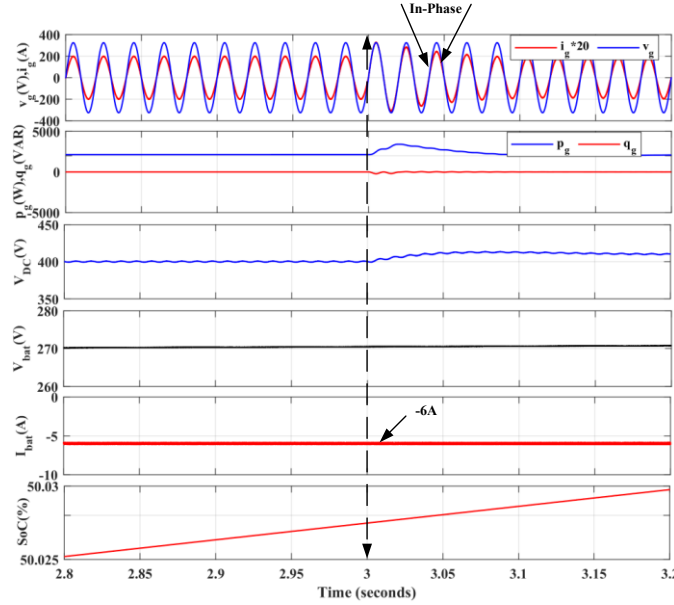


**Fig.5.7 Step change in  $V_{DC}$  during discharging condition.**

Fig.5.6 shows the Step change in  $V_{DC}$  during charging operating condition which means,  $V_{DC}$  is changing from 400 to 430 to check the system robustness whether it works on step change of  $V_{DC}$  but it's perfectly working on step change condition as shown. These waveforms show in-phase  $v_g$  and  $i_g$  and out of phase in  $v_g$  and  $i_g$  which is perfectly correct, in the constant battery current,  $I_{bat}$ , further attest to  $I_{bat}$ ,  $V_{bat}$  and SoC. The built-in charger further demonstrates how well  $V_{DC}$  regulated charging voltage controls the charging and discharging process. Fig.5.7 shows the Step change in  $V_{DC}$  during discharging operating condition which means,  $V_{DC}$  is changing from 400 to 430 to check the system robustness whether it works on step change of  $V_{DC}$  but it's perfectly working on step change condition as shown. These waveforms show in-phase  $v_g$  and  $i_g$  and out of phase in  $v_g$  and  $i_g$  which is perfectly correct, in the constant battery current,  $I_{bat}$ , further attest to  $I_{bat}$ ,  $V_{bat}$  and SoC. The built-in charger further demonstrates how well  $V_{DC}$  regulated charging voltage controls the charging and discharging process.

EV Charger Benefits of FC-MPC are High Efficiency: Losses are minimized via strategic switching. Flexibility: Adjusts to load and grid circumstances as they vary. Battery Protection: To increase battery life, safe charging patterns are maintained. Grid Support: Facilitates operations such as voltage regulation and reactive power adjustment.

Model for Prediction, make predictions about the charger's future behaviour for every potential switching state using the state-space representation. Add restrictions such grid code requirements, charging profiles, and limits on current and voltage. The

Design of the Cost Function create a cost function using the following components: (a)Performance Monitoring: Reduce the discrepancy between the intended and actual charging voltage and current. (b)Reducing switching losses and extending converter life can be achieved by minimizing switching transitions. (c)Grid Interaction: Make sure grid standards are followed and lessen the effects of disruptions. Battery health: Put restrictions in place to keep the EV battery from overcharging or overheating. (d)Improvement Assess every potential switching condition at every sampling interval. Choose the switching state that minimizes the cost function after computing it for each state. Put the charger in the best possible switching state. (e)Strengthening of Robustness To manage prediction model uncertainties, include adaptive techniques or disturbance observers. To adapt the model dynamically to system conditions, use real-time parameter identification.

## **5.4 CONCLUSION:**

The project's primary objective is to develop an effective, bidirectional EV battery charger that can also supply power to the electrical grid in order to reduce the strain on it. The rapid expansion of the electric vehicle sector is putting further demand on the electrical system. Power can move in both ways in a bidirectional system, which maximizes benefits for both V2G and G2V systems. Thus, buck-boost converter functions are carried out by the DC/DC converter. Energy produced by nearby EV owners can be utilized via V2G and returned to the power system. Assigning supervision is how this is done.

## CHAPTER -6

### MODELLING, SIMULATION AND EXPERIMENTAL RESULTS OF EV CHARGER

#### 6.1 MODELLING OF EV CHARGER:

This chapter show the implementation and control architecture of a two-stage off-board EV charger. Because the dq frame is challenging, the inner control in this chapter is carried out in the AC domain, where the signals are periodic. The Model Predictive Controller (MPC), Model Predictive Control (MPC) is a sophisticated control technique that forecasts and optimizes future control actions using a dynamic model of the system. At every sampling instant, it solves an optimization problem online while taking goals, constraints, and future behaviour into account. which has been successfully built and implemented for the suggested job, is found to be highly helpful of fixed frequency in case of single-phase systems.

**Table 6.1: Parameter Values of Bidirectional Charging Systems**

Symbol	Quantity	Value
$(v_g)$	Grid voltage	325V(rms)
$k_p$	Active power Factor	1
$k_q$	Reactive Power Factor	1
$(V_{DC}),$	DC voltage	400 V
$T_s$	Sampling Time	12e-9sec
L	Inductance	4e-3mH
frequency	Sampling frequency	50khz
$I_{ref}$	Reference current	-5A
$V_{bat}$	Battery voltage	260 V
$i_{bat}$	Battery current	5A



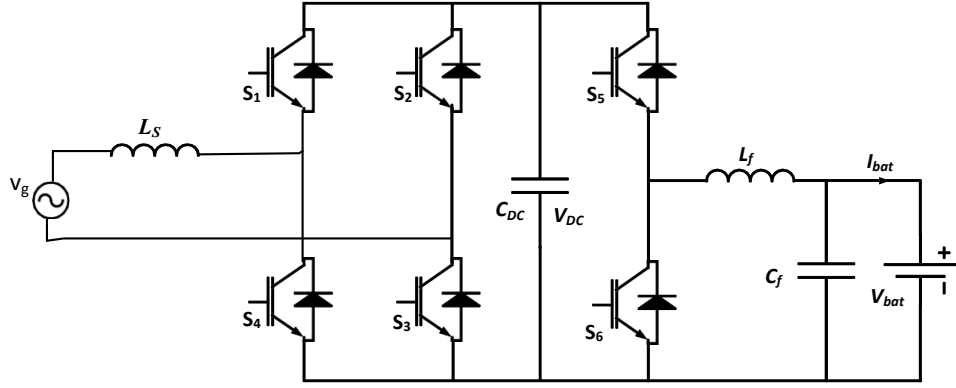


**Fig.6.1 Switching model of single-phase**

## 6.2 AC-DC Converter Modelling (Single-Phase):

Mathematical modelling of simple AC-DC converter has been done in this section. A switching model of AC-DC converter has been shown in fig 6.2

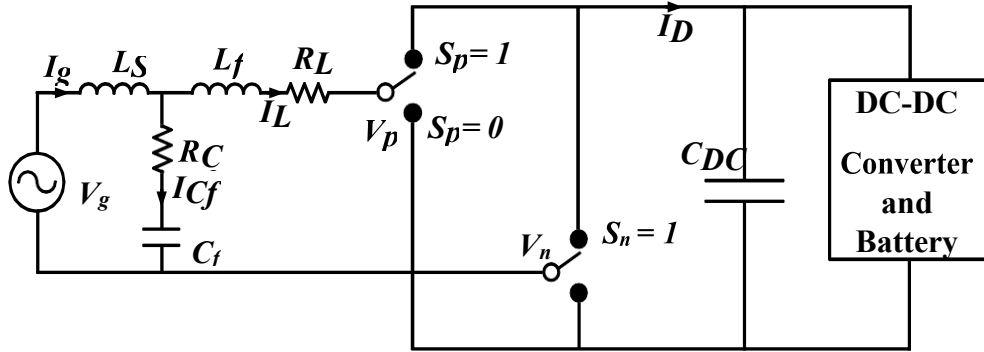


**Fig.6.2 AC-DC converter switching model**

The grid voltage is represented by  $V_g$ ,  $L_s$  is grid side inductor,  $L_f$  and  $C_f$  is AC side filter inductance and capacitance respectively and  $R_{Lf}$  and  $R_{Cf}$  are equivalent series resistance (ESR) of filter inductance and capacitance respectively. The representation of ON state of switch  $S_1$  and  $S_3$  are represented by  $S_p = 1$  and  $S_p = 0$  respectively. Where,  $S_n = 1$  and  $S_n = 0$  are the representation of ON state of switch  $S_2$  and  $S_4$  respectively. Therefore, when switch  $S_1$  and  $S_4$  are on and  $S_3$  and  $S_2$  are off then the grid current  $I_g$  is equal to DC side current  $I_{DC}$  and  $V_{pn}$  equals to  $V_{DC}$ . The ON state of switch  $S_1$  and  $S_4$  is expressed as follow.

$$V_{pn} = V_p - V_n \quad (1)$$

$$S_p * V_{DC} - S_n * V_{DC} = (S_p - S_n) * V_{DC} \quad (2)$$

$$= S_{pn} * V_{DC} \quad (3)$$

$$S_{pn} = S_p - S_n \quad (4)$$

$$I_{DC} = (S_p - S_n)I_{Lf} = S_{pn} * I_{Lf} \quad (5)$$

Now Apply Kirchoff's voltage law (KVL)in outer loop and neglecting capacitor

$$V_g = V_{Ls} + V_{Cf} \quad (6)$$

$$\frac{dI_g}{dt} = \frac{V_g}{L_s} - \frac{V_{Cf}}{L_s} \quad (7)$$

Applying KVL, in the inner loop, we get

$$V_{Cf} = V_{Lf} + I_{Lf} * R_{Lf} + V_{pn} \quad (8)$$

$$\frac{dI_{Lf}}{dt} = \frac{V_{Cf}}{L_f} - \frac{I_{Lf} * R_{Lf}}{L_f} - \frac{V_{pn}}{L_f} \quad (9)$$

At junction, Applying KCL, we get

$$I_g = I_{Lf} + I_{Cf} \quad (10)$$

$$\frac{dV_{Cf}}{dt} = \frac{I_g}{C_f} - \frac{I_{Lf}}{C_f} \quad (11)$$

### 6.3 DC-DC Converter Modelling:

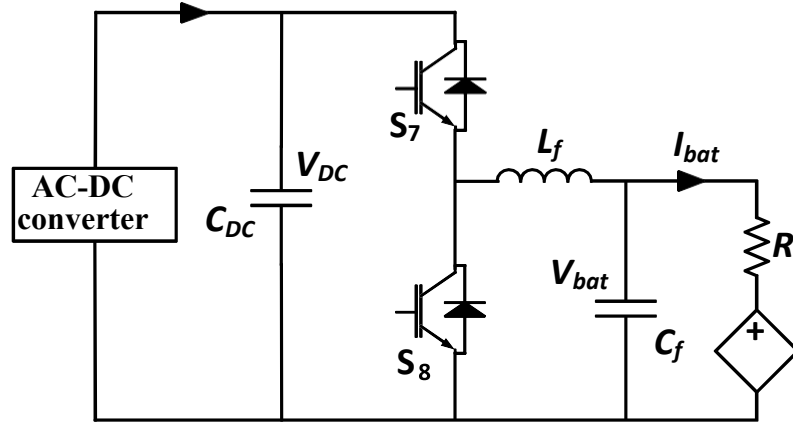


**Fig.6.3 DC-DC converter topology.**

The topology of the second stage DC-DC converter is displayed in Fig. 6.3. It is made up of two IGBT switches and is bidirectional. When the battery is charging, it operates in buck mode; when the active power is being sent to the grid, it operates in boost mode.

#### Switch S7 is on and S8 is off

Below is a discussion of the average modelling of the DC-DC converter when switch S7 is turned on. The current flow direction when switch S7 is in the on state and when switch S8 is in the off state is seen in Fig. 6.4.

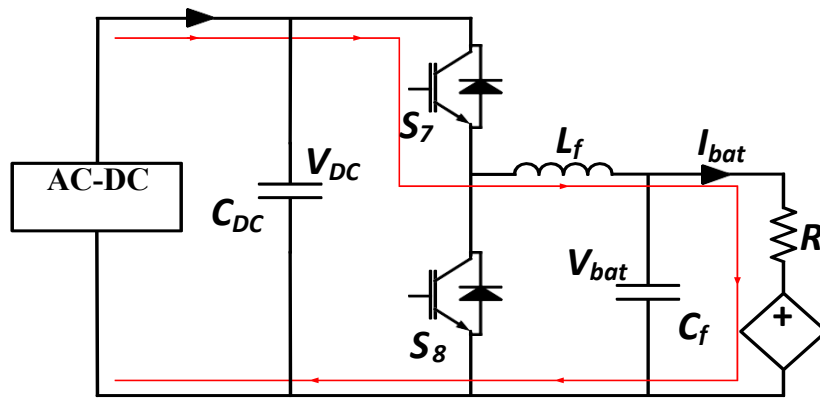


**Fig.6.4 DC-DC buck operation ON state.**

KVL in outer loop gives,

$$V_{DC} = V_{Lf} + V_{bat} \quad (1)$$

$$\frac{dI_{Lf}}{dt} = \frac{V_{DC}}{L_f} - \frac{V_{bat}}{L_f} \quad (2)$$

The current across the inductor is denoted by  $I_{Lf}$ , while the voltage across the filter inductance  $L_f$  and capacitance  $C_f$  are represented by  $V_{Lf}$  and  $V_{bat}$  respectively. At the battery side, KCL now gives

$$I_{Lf} = I_{Cf} + I_{bat} \quad (3)$$

$$\frac{dV_{bat}}{dt} = \frac{I_{Lf}}{C_f} - \frac{I_{bat}}{C_f} \quad (4)$$

Here, current through capacitor  $C_f$  is  $I_{Cf}$ . Now apply KCL at DC-link capacitor gives,

$$I_{DC} = I_{CDC} + I_{Lf} \quad (5)$$

$$\frac{dV_{DC}}{dt} = \frac{I_{DC}}{C_{DC}} - \frac{I_{Lf}}{C_{DC}} \quad (6)$$

**Switch S7 OFF and S8 ON**

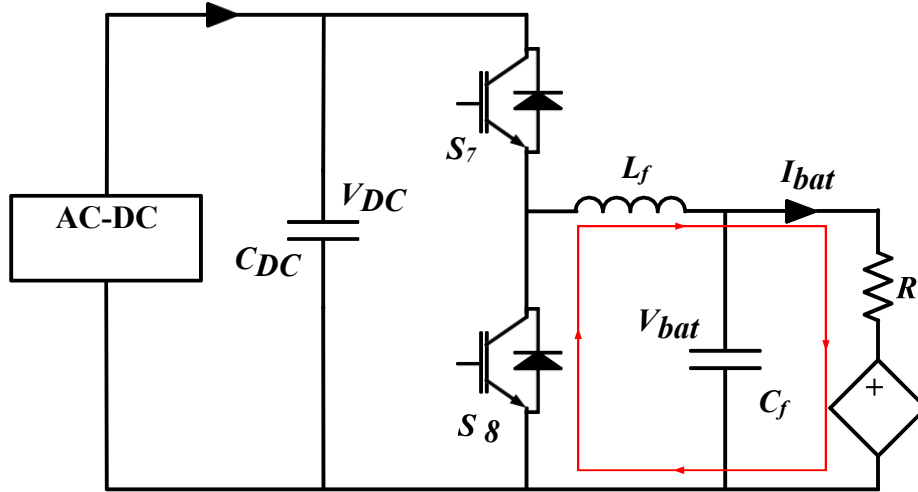


**Fig.6.5 DC-DC buck operation OFF state**

Apply KVL in the Battery loop,

$$0 = V_{L_f} + V_{bat} \quad (1)$$

$$\frac{dI_{L_f}}{dt} = -\frac{V_{bat}}{L_f} \quad (2)$$

At battery side, apply KCL

$$I_{L_f} = I_{C_f} + I_{bat} \quad (3)$$

$$\frac{dV_{bat}}{dt} = \frac{I_{L_f}}{C_f} - \frac{I_{bat}}{C_f} \quad (4)$$

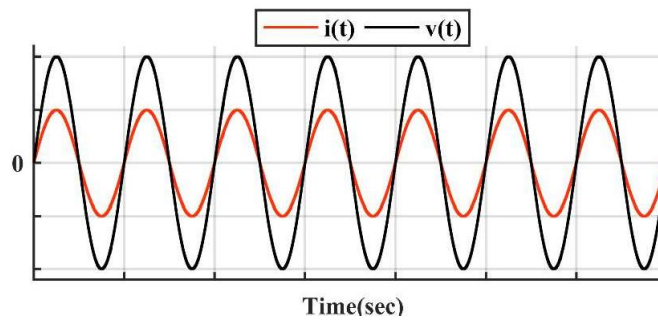
Now, DC-Link capacitor side, apply KCL

$$I_{DC} = I_{CDC} \quad (5)$$

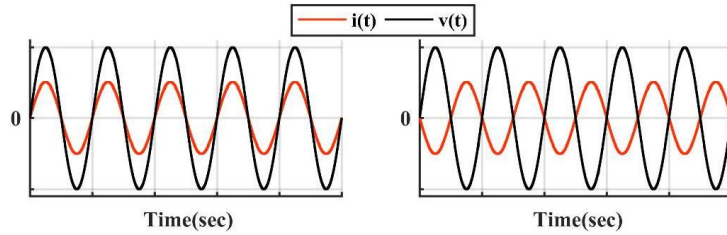
$$\frac{dV_{DC}}{dt} = \frac{I_{DC}}{C_{DC}} \quad (6)$$

Fig 6.2 show two IGBT that operate in both directions. It operates in buck mode when a battery is present and boost mode when active power is sent to the grid.

#### 6.4 Simulation Result:



**Fig.6.6 Current and voltage relation of unidirectional charger .**



**Fig.6.7: Current and voltage relation during (a) in phase (b) Out-of-Phase**

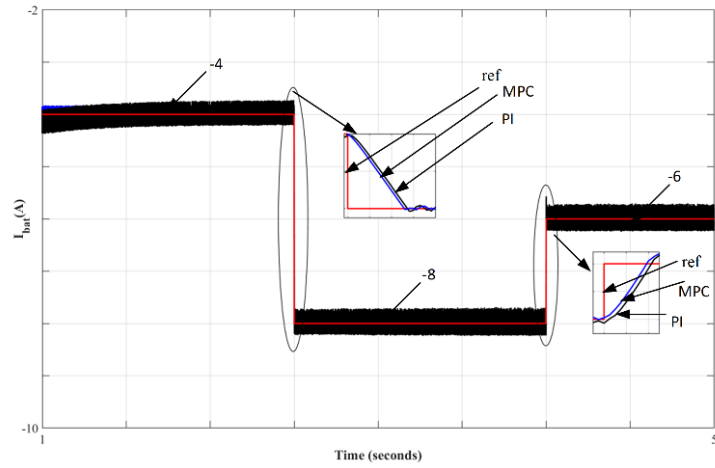


**Fig.6.8 Comparison of PI and MPC controller with reference current**

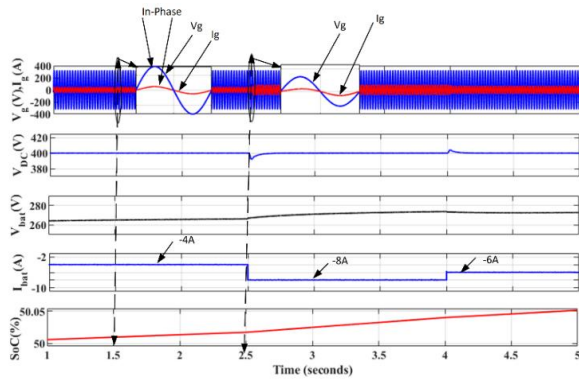


**Fig.6.9 Reference change operating condition showing charging State**

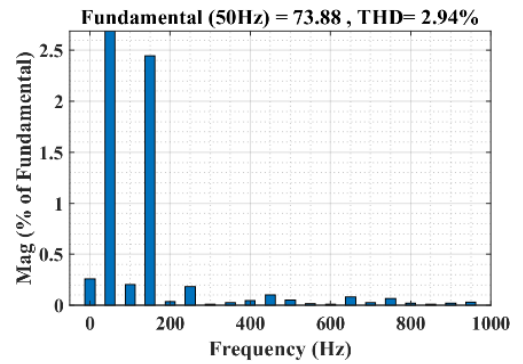


**Fig.6.10 THD under reference change operating conditions.**

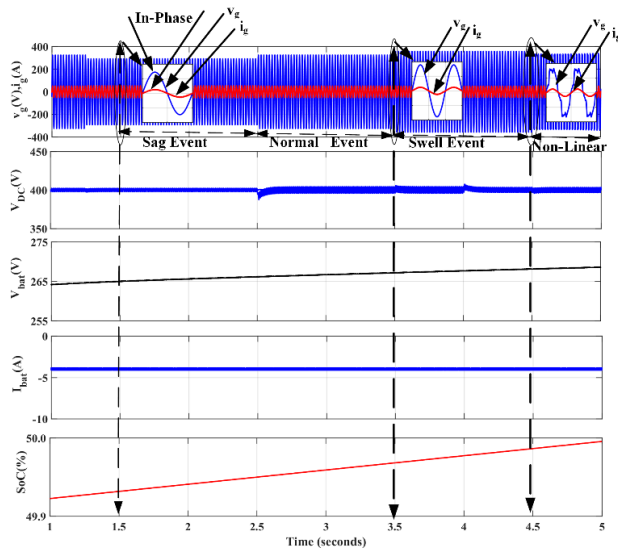


**Fig.6.11 Nonideal Source operating condition under charging state .**

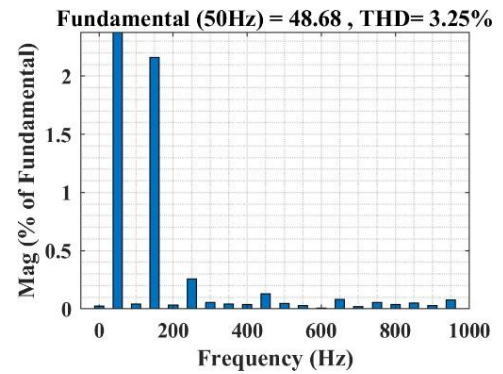


**Fig.6.12 THD under nonideal operating conditions.**

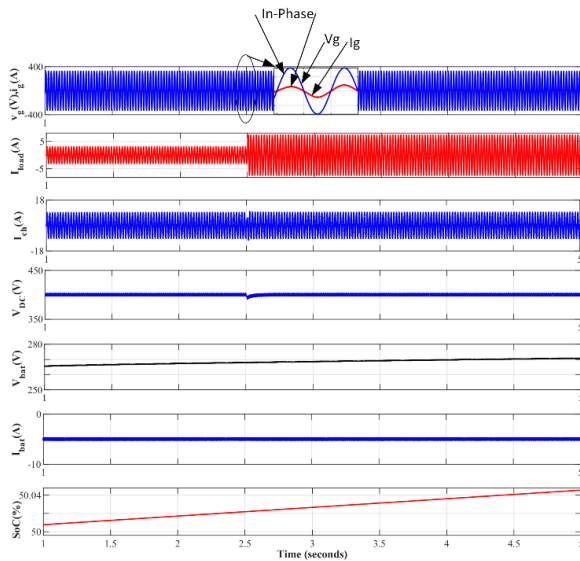


**Fig.6.13 Load change operating condition under charging state.**

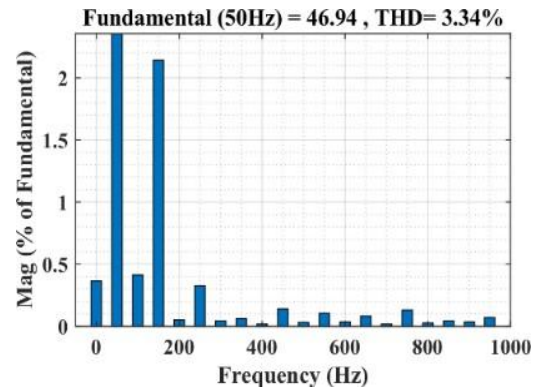


**Fig.6.14 THD under Load change operating conditions.**



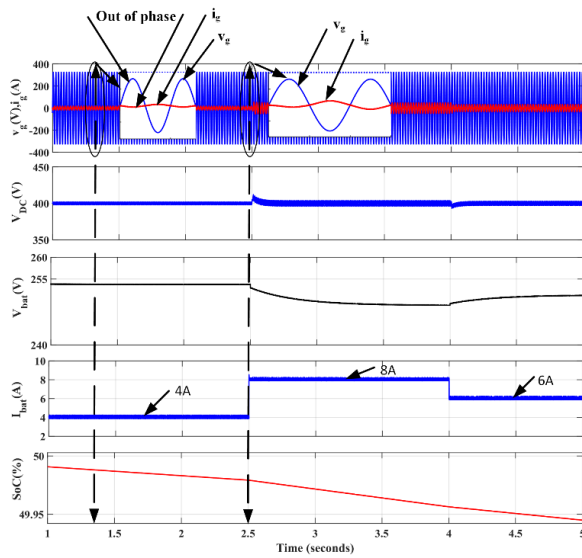


**Fig.6.15 Reference change operating condition showing discharging state.**

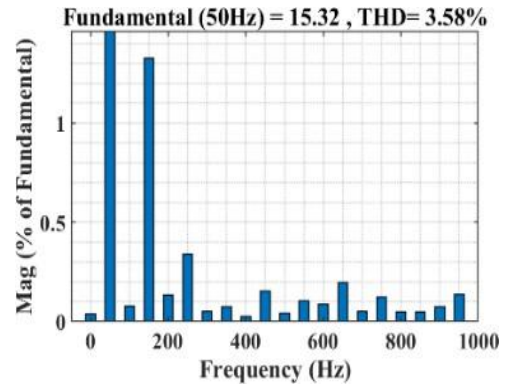


**Fig.6.16 THD under reference change discharging operating conditions.**

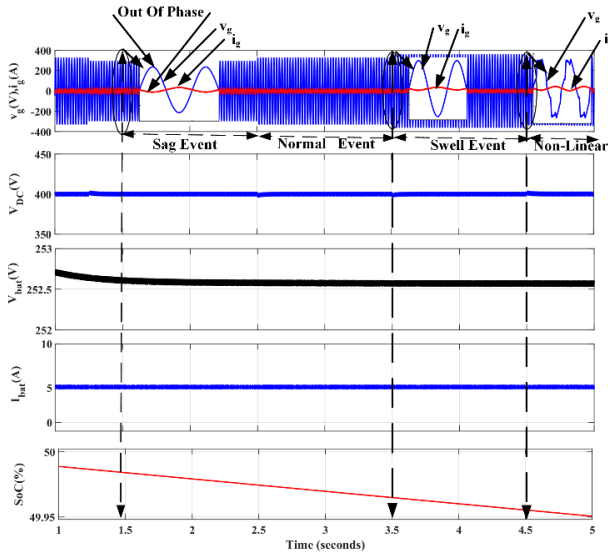


**Fig.6.17 Nonideal Source operating condition under discharging state.**

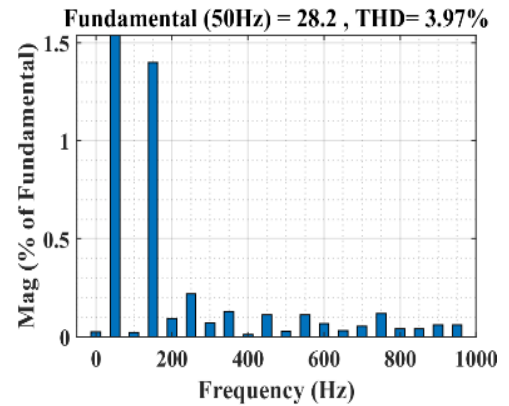


**Fig.6.18 THD under nonideal discharging operating conditions.**

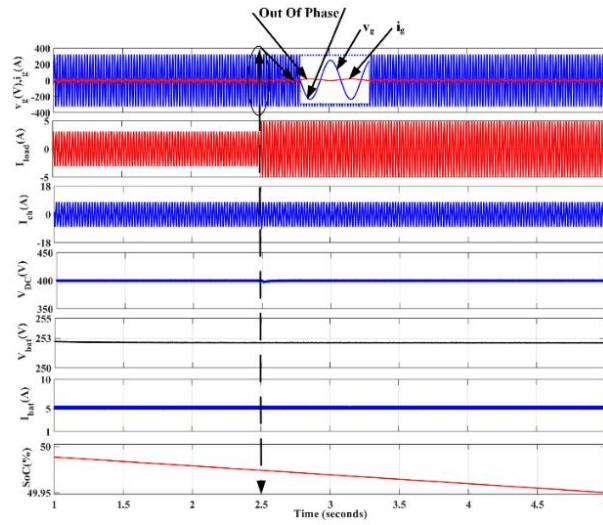


**Fig.6.19 Load change operating condition under discharging state.**

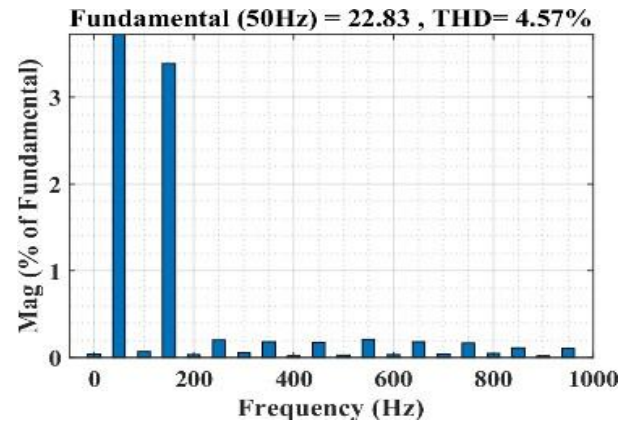


**Fig.6.20 THD under Load change discharging operating conditions.**

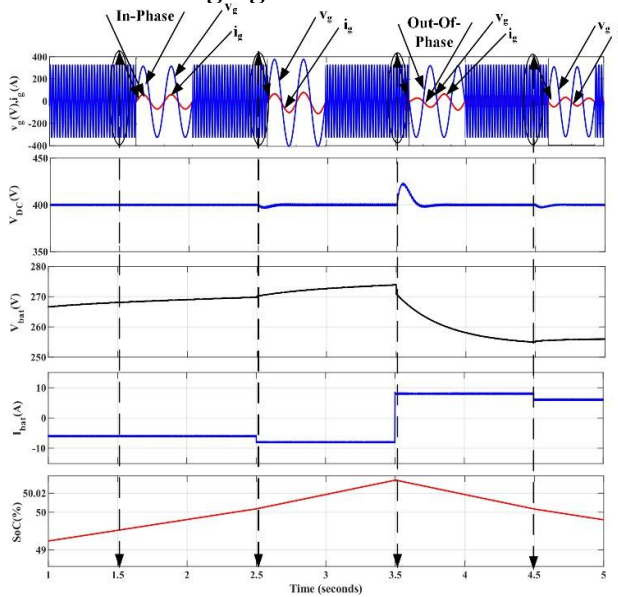


**Fig.6.21 Reference change operating condition showing both charging and discharging.**

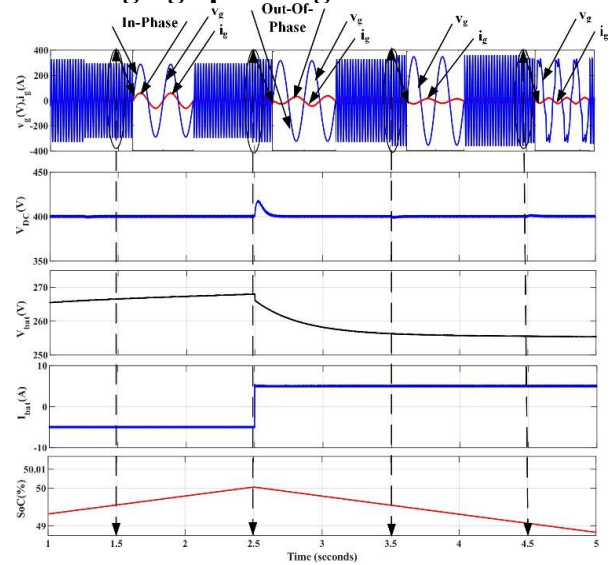


**Fig.6.22 Nonideal Source operating condition under charging state and discharging state.**

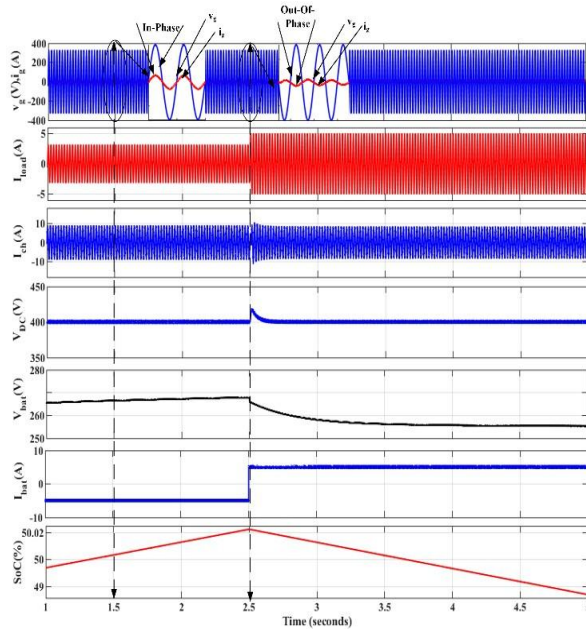


**Fig.6.23 Load change operating condition under charging state and discharging state.**

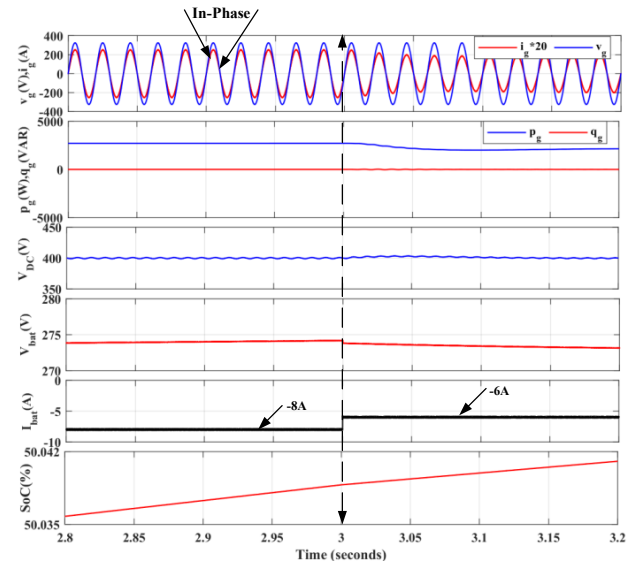


**Fig.6.24 Reference change operating condition showing both charging and discharging.**

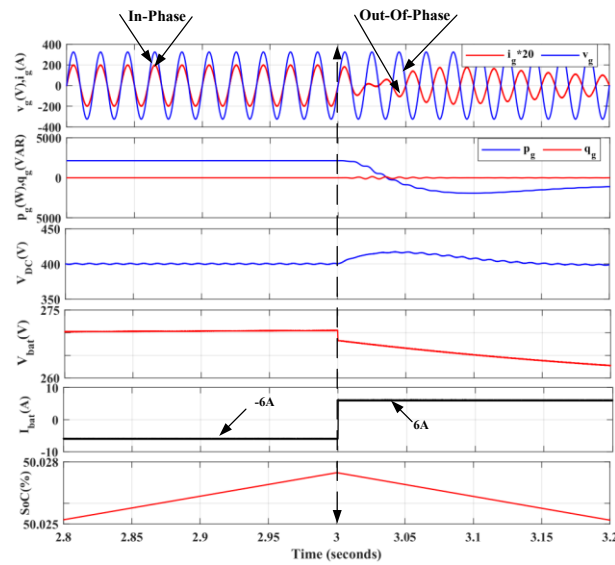


**Fig.6.25 Step change in  $I_{bat}$  during charging condition.**

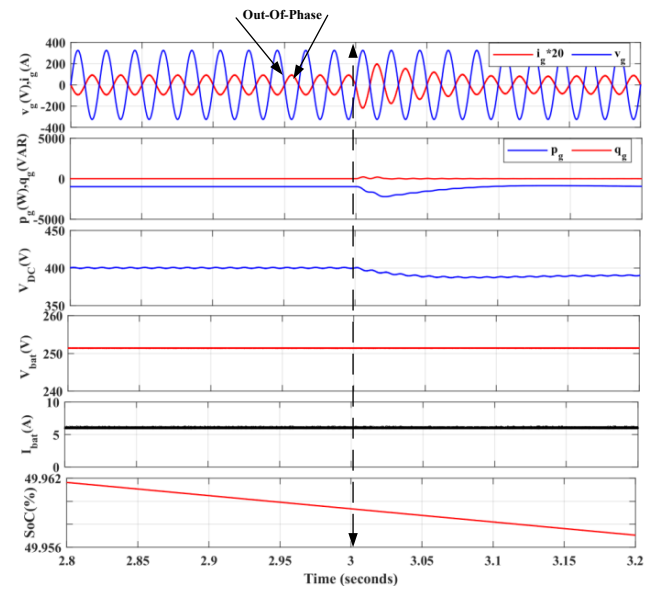


**Fig.6.26 Step change in  $I_{bat}$  during discharging condition.**

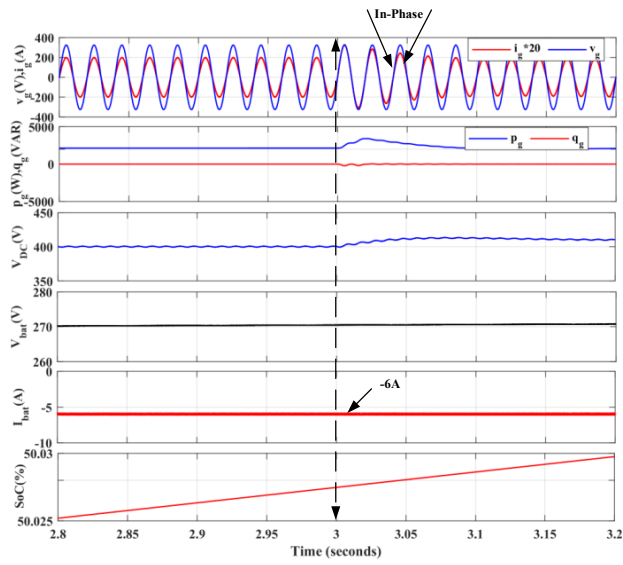


**Fig.6.27 Step change in  $V_{DC}$  during charging condition.**

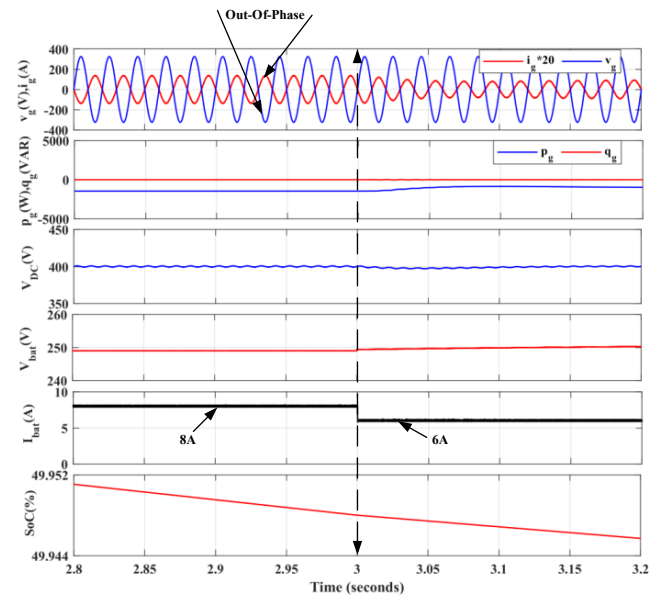


**Fig.6.28 Step change in  $V_{DC}$  during discharging condition.**

## 6.5 Experimental Results:

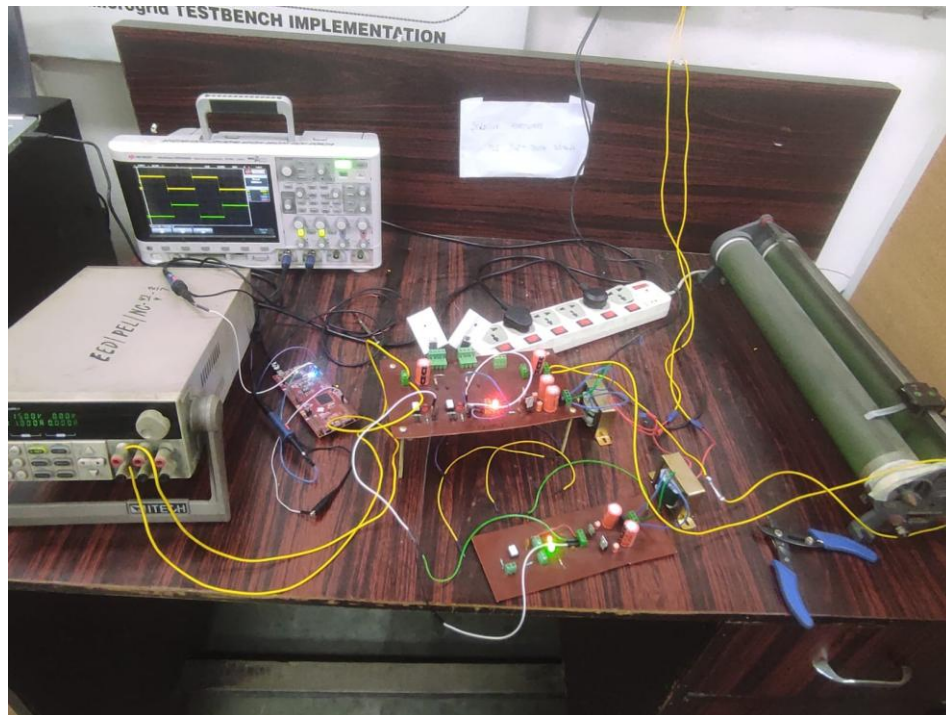


**Fig.6.29 Bidirectional DC-DC converter.**

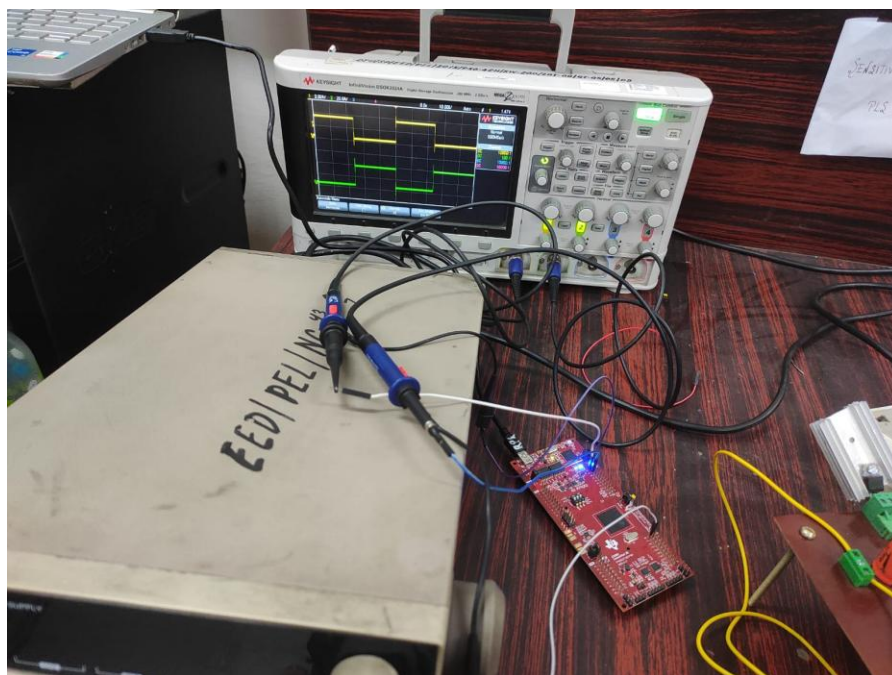


**Fig.6.30 Microcontroller Launchpad**



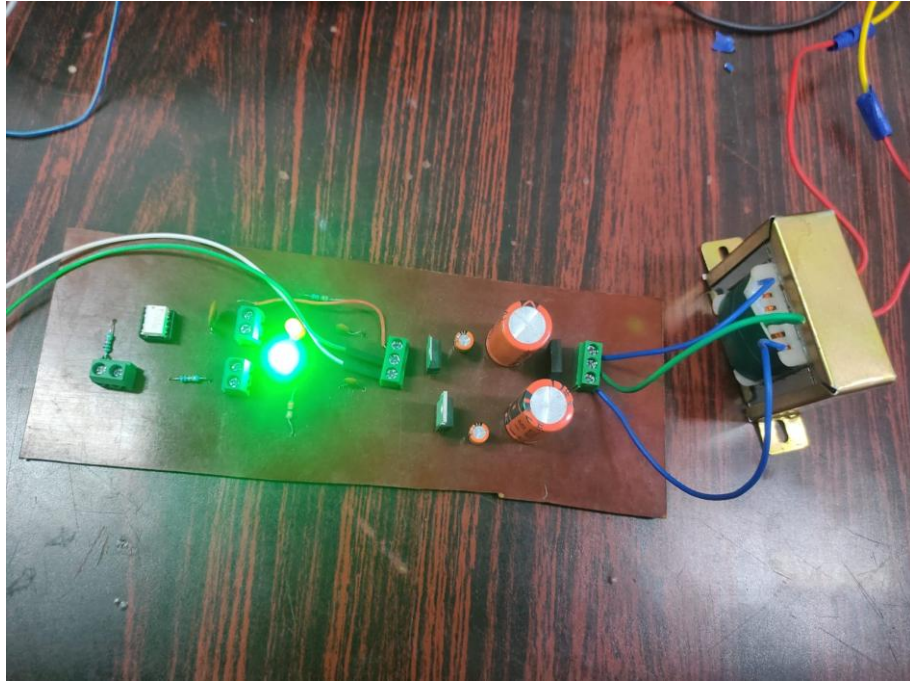


**Fig.6.31 Gate driver circuit.**

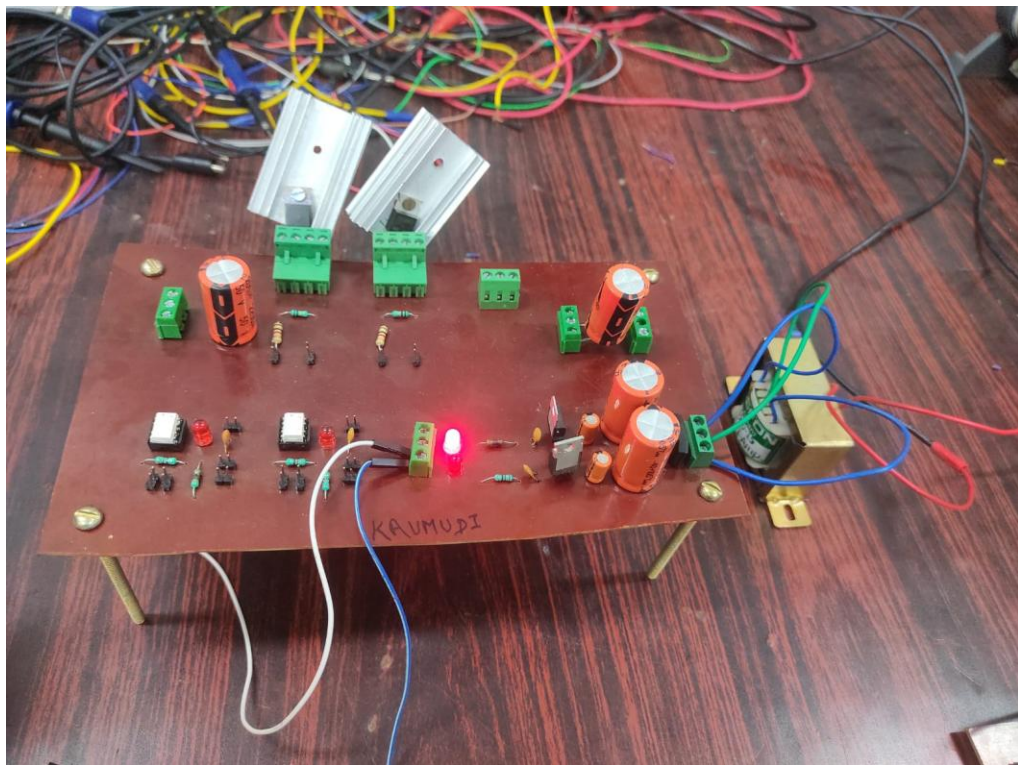


**Fig.6.32 Bidirectional Converter with gate driver circuit.**

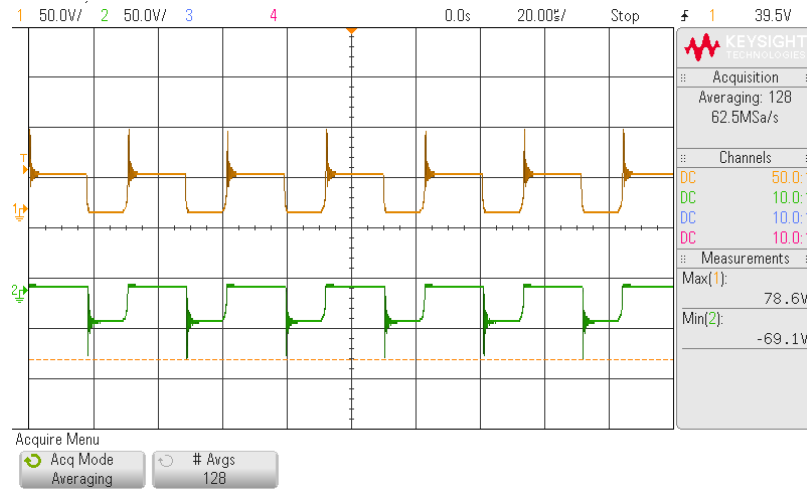


**Fig.6.33 Switch Stress**

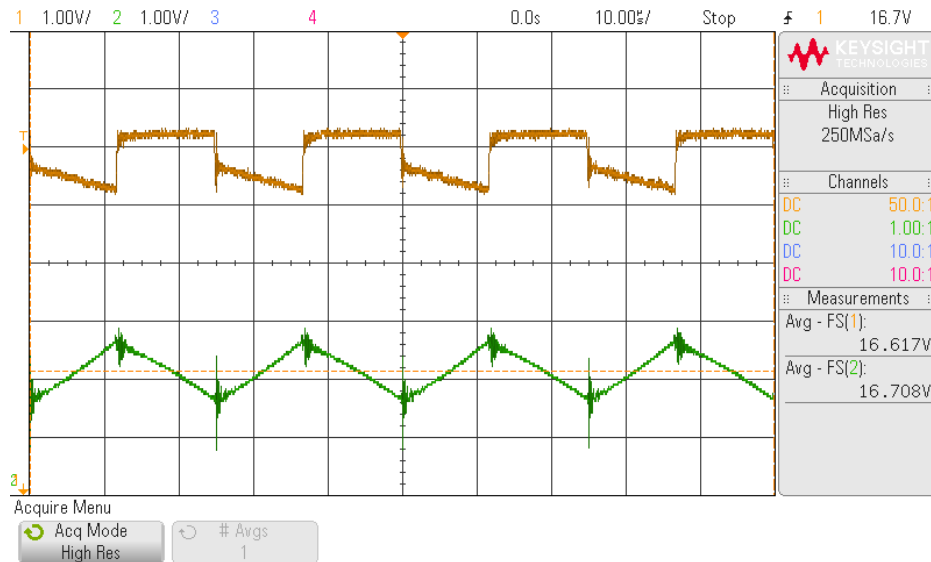


**Fig.6.34 Capacitor Voltage**

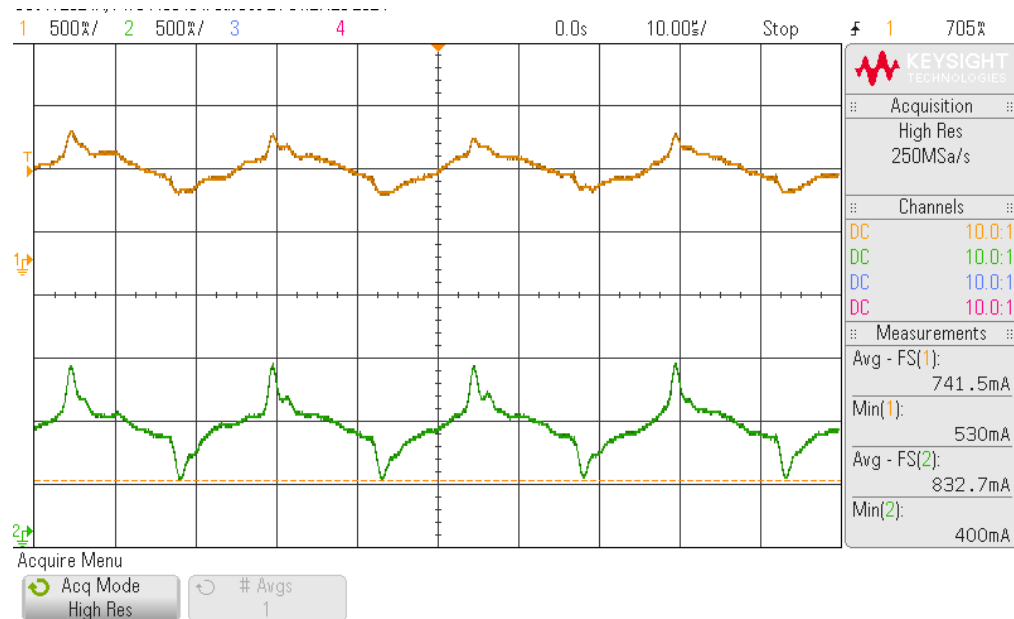


**Fig.6.35 Inductor current**

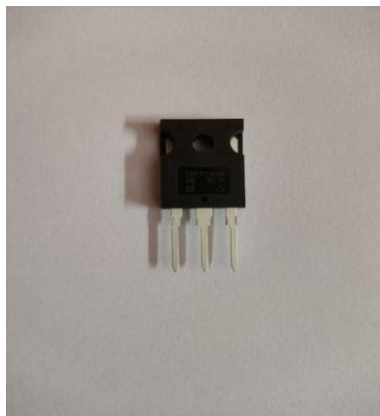


**Fig.6.36 8 IRFP260N MOSFET**



**Fig.6.37 9 MUR 860 Diode**

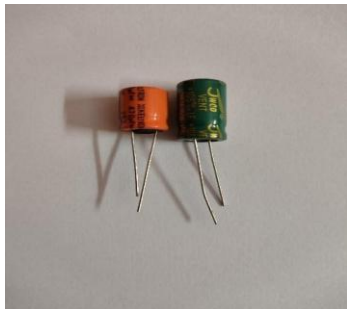


**Fig.6.38 ELECTROLYTIC CAPACITORS**

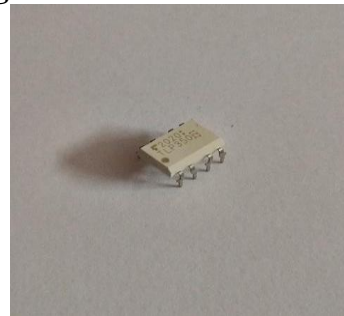


**Fig.6.39 TLP 350**





**Fig.6.40 Hi-Link**

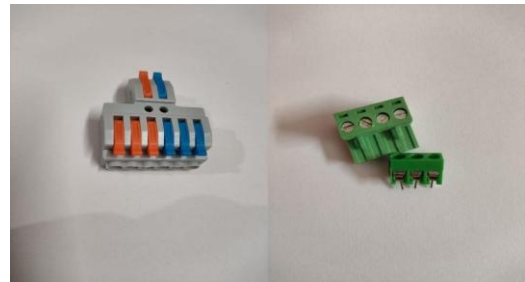


**Fig.6.41 Terminal Connectors**



**Fig.6.42 Ferrite Core Inductor**

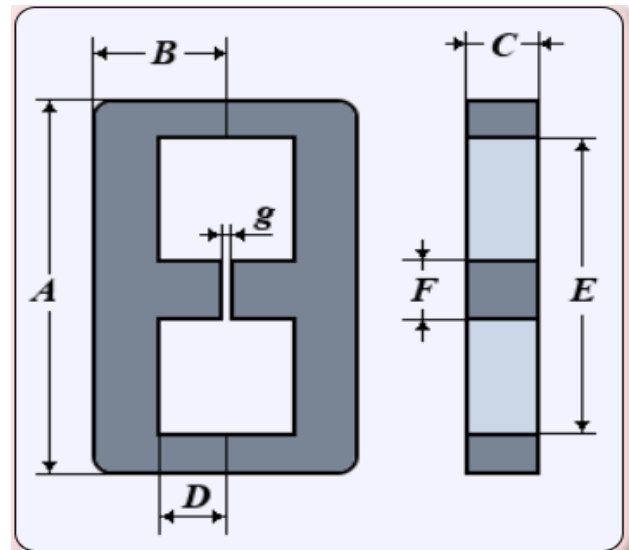


**Fig.6.43 Dimension of Core**



**Fig.6.44 Voltage Sensor**



**Fig.6.45 Power Supply for Sensor**

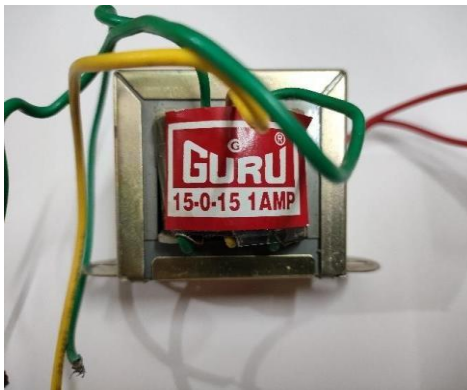


**Fig.6.46 Step Down transformer**

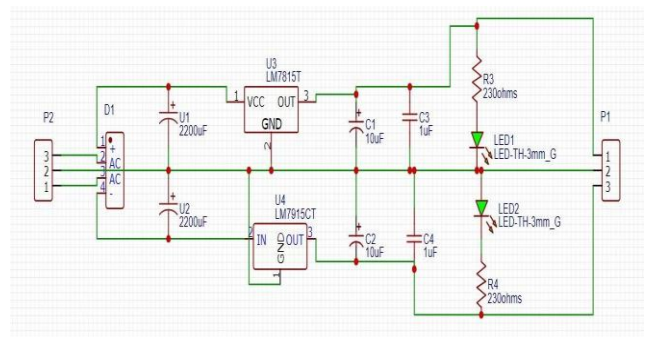


**Fig.6.47 Schematic of power supply**

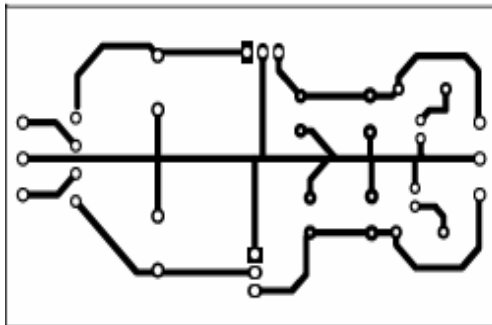


**Fig.6.48 PCB Design of power supply**

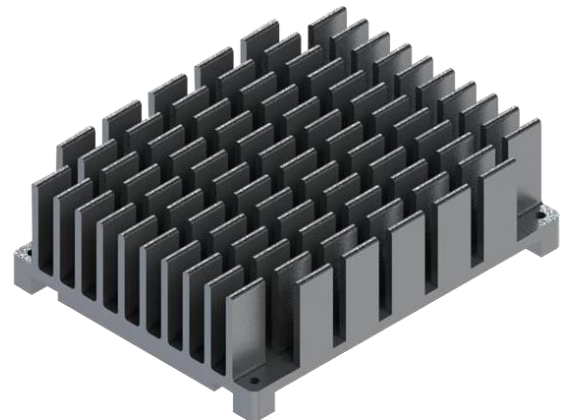


**Fig.6.49 Heat Sink**



**Fig.6.50 DC Fan for cooling**

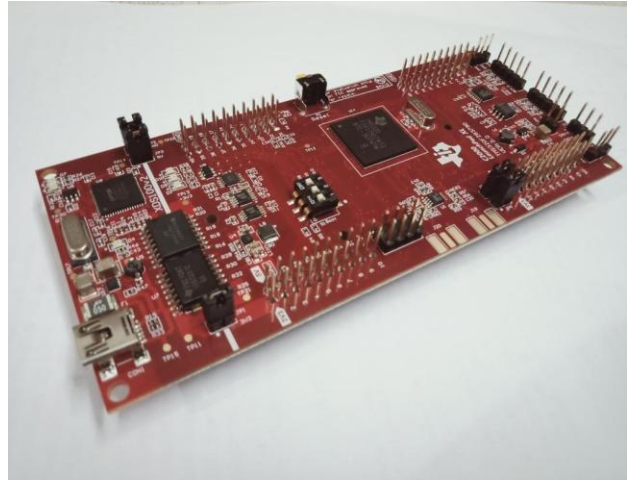


**Fig.6.51 Launchpad F28379D**

A MOSFET (IRF1407), a Texas Instruments F28379D LaunchPad for digital control implementation, a transformer for voltage isolation and level shifting, and inductors and capacitors for energy storage and filtering are some of the power electronic components I used in the experiment. Every component was chosen according to how well it fit the design specifications and performed within the allotted ratings. In order to verify the simulation results of a bidirectional DC-DC converter with MPC-based control for battery charging and discharging applications, the experimental setup was created and put into place

### **Hardware Configuration and Components:**

In order to implement and validate the intended converter system, the following elements were used in the experimental setup:

**MOSFET (IRF1407):** Because of its low on-resistance and high current handling, this device is used as the primary switching device.

**Texas Instruments F28379D LaunchPad :** It is used as a digital controller to implement control algorithms like MPC and generate PWM signals.

**Power transformers:** They are used for isolation and voltage level modification when there is any AC-side interface.

**Inductor and Capacitor:** Energy storage and filtering are accomplished by inductors and capacitors, which keep voltage and current waveforms within predetermined bounds. Design analysis and simulation were used to choose values.

**DC Fan:** A DC fan is used to actively cool power components and regulate heat.

**Heat Sink:** Used to efficiently dissipate heat from power semiconductor devices such as MOSFETs.

**Custom PCB:** EasyEDA was used to design the gate driver circuits and  $\pm 15\text{V}$  DC power supply.

**TLP350 :** The TLP350 Opto-Isolated Gate Driver IC provides electrical isolation while safely driving the MOSFET gate from the LaunchPad PWM outputs.

**Voltage sensor and Current Sensor:** Closed-loop control is made possible by the implementation of voltage and current sensors, which monitor input and output electrical parameters in real time.

**Power Supply Circuit:** Designed on Zero PCB to provide dependable power to the driver and control circuitry.

Every component was chosen with the system's voltage, current, and frequency needs in mind. During experimental testing, the configuration guarantees precise control, safe operation, and efficient heat management.

## **CHAPTER-7**

### **CONCLUSION AND FUTURE SCOPE**

#### **7.1 Conclusion:**

This work focuses on developing different controllers for electric vehicle (EV) charging. The EV charger has two conversion stages: the first is AC-DC, and the second is DC-DC. An EV charger's primary components are these two converters. In addition to charging and discharging the battery pack, the EV charger is made to adjust for reactive power. Both converters are built with bidirectional capability for this purpose. With an anti-parallel diode, IGBT switches are used in the design of the converters. Both charging the battery pack and transferring battery power back to the grid or a local load are capabilities of the EV charger.

On-board and off-board EV chargers, along with associated controllers, have been created in this effort. Two independent controls are needed for the AC-DC and DC-DC conversion stages of the two-stage EV charger. Here, three EV charger controllers for on-board EV chargers and two for off-board EV chargers have been built. This work's primary goal is to create control algorithms for the initial stage of an AC-DC converter in order to address a number of EV charging issues. All EV charger controllers, however, employ the generalized control method for the second stage DC-DC converter. Every EV charger controller is made to be able to obey any active or reactive power command that falls within the charger's rating.

Five different quantities active/reactive power, grid side current, DC link voltage, and battery current are all controlled by the EV charger controller. Active/reactive power and grid side current are the three variables that the proposed controller regulates using an AC-DC converter. The remaining two values, namely battery current and DC link voltage, are controlled by the DC-DC converter. Three references are provided in this instance, and the remaining two are their creations. The two loops that make up the AC-DC converter's control are the inner and outer loops. The inner control loop uses the reference created by the outer loop. The active/reactive power is monitored in the outer loop, which also provides the grid current reference for the inner current control loop. As a result, the inner and outer control loops each need their own regulator. Likewise, DC-DC converter control has a two-control loop architecture. In this case, the battery current reference is generated by tracking the DC link voltage in the outer loop, which is then tracked in the inner current control loop.

The first chapter of the six-chapter thesis covered the fundamental overview, types, and standards of EV chargers. The experimental setup development and operating modes of

the EV charger were detailed in the second chapter. For this, dSPACE The 1104 controller is used to verify the EV charger controller's functioning in real time. A bidirectional EV charger was mathematically modeled in the third chapter. Two EV charger control algorithms for an off-board EV charger have been devised in the fourth chapter. The first control approach uses two proportional integral (PI) regulators for the second stage of the DC-DC converter and four for the first stage of the AC-DC converter.

Two PI regulators are needed for grid current control in the inner loop in the dq frame and two for tracking active/reactive power in the outer loop for AC-DC converter control. It has been discovered that tuning four PI regulators at once for a single controller can occasionally be quite challenging, particularly for inner loops. Furthermore, various frame conversions are needed for this kind of EV charging controller. A unified adaptive neuro-fuzzy inference system (ANFIS) control is employed in the outer loop of the second control strategy to track active/reactive power and generate reference grid current. A hysteresis control is used in the inner loop to track the grid current in a periodic manner. It is discovered that the hysteresis control outperforms the PI regulator in the inner loop.

## **7.2 Future Scope:**

In order to operate an EV charger in a variety of G2V and V2G modes while keeping the amount of ripple content on the DC side within an acceptable range, the primary goal of the proposed study is to build a reliable control system. If the grid needs active power, the EV charger can provide it. If a battery charges more slowly, it can also compensate reactive power (capacitive or inductive). The remaining charger rating is then used to compensate for the reactive power in order to maximize the charger's rating. In addition, if the battery is not connected to the charger Future research can look into the following four areas:

Certain techniques can be used to change the variable switching frequency into a fixed switching frequency in the case of hysteresis control. Certain control strategies that lower THD and ripple can be applied to single stage, single phase on-board EV chargers; as a result, they can also be applied to battery packs with a 5% permitted ripple. It is possible to consider disturbance in the case of a periodic reference controller. Due to the enormous number of EVs linked to the grid, grid parameters may be disturbed. Frequency adaptation can be incorporated into the inner current control loop since periodic controllers are sensitive to changes in frequency.

## **List of Publication:**

**[1]** K. Kumari and M. Singh, "Optimal Design and Performance Analysis of Model Predictive Control for EV Charging Application," **2024 IEEE International Conference on Power Electronics, Drives and Energy Systems (PEDES)**, Mangalore, India, 2024, pp. 1-6, doi: 10.1109/PEDES61459.2024.10961689.

Pedes:<https://ieeexplore-ieee-org.dtlibrary.remotexs.in/document/10961689>.

**[2]** K. Kumari and M. Singh, "Implementation of Robust Control for Smart Home EV Charger through FC -MPC," **2025 IEEE International Conference on Sustainable Energy and Future Electric Transportation (IEEE SeFet 2025)**, India, (Accepted)

**[3]** K. Kumari and M. Singh, "Design and Development of Advanced Model Predictive Control Strategy for Electric Vehicle Application," **2025 IEEE International Conference on Sustainable Energy and Future Electric Transportation (IEEE SeFet 2025)**, India, (Accepted).

**[4]** K. Kumari and M. Singh, " Real-Time Model Predictive Control for Bidirectional EV Charging and Discharging," **2025 IEEE International Conference on Energy, Power and Environment (IEEE ICEPE 2025)**, India, (Accepted).

## References:

- [1] K. Kumari and M. Singh, "Optimal Design and Performance Analysis of Model Predictive Control for EV Charging Application," 2024 IEEE International Conference on Power Electronics, Drives and Energy Systems (PEDES), Mangalore, India, 2024, pp. 1-6, doi: 10.1109/PEDES61459.2024.10961689.
- [2]. G. Yadav and M. Singh, "Robust Control Design for Grid-Tied EV System with SOGI-Based Architecture in Wide Voltage Range Scenarios," 2023 International Conference on Electrical, Electronics, Communication and Computers (ELEXCOM), Roorkee, India, 2023, pp. 1-6, doi: 10.1109/ELEXCOM58812.2023.10370088.
- [3]. T. He, J. Zhu, D. D. -C. Lu and L. Zheng, "Modified Model Predictive Control for Bidirectional Four-Quadrant EV Chargers With Extended Set of Voltage Vectors," in IEEE Journal of Emerging and Selected Topics in Power Electronics, vol. 7, no. 1, pp. 274-281, March 2019, doi: 10.1109/JESTPE.2018.2870481.
- [4] Yadav, G., Singh, M. Real-time investigation of grid-interactive EV charger with two-stage bidirectional converter under wide voltage range scenarios. Electr Eng (2024). <https://doi.org/10.1007/s00202-024-02609>.
- [5] M. Ansari, G. Yadav and M. Singh, "A 3.3kW Modified LLC Resonant Converter for Grid-Tied EV System Under Wide Voltage Range," 2023 3rd International Conference on Intelligent Technologies (CONIT), Hubli, India, 2023, pp. 1-6, doi: 10.1109/CONIT59222.2023.10205690.
- [6] T. C. Cano, A. Rodriguez, I. Castro and D. G. Lamar, "Distributed Input Multiport MMC Based Power Converter for AC and DC Loads," in IEEE Transactions on Power Electronics, vol. 38, no. 7, pp. 7971- 7975, July 2023, doi: 10.1109/TPEL.2023.3260719.
- [7] Lin, C.-H.; Farooqui, S.A.; Liu, H.-D.; Huang, J.-J.; Fahad, M. Finite Control Set Model Predictive Control (FCS-MPC) for Enhancing the Performance of a Single-Phase Inverter in a Renewable Energy System (RES). Mathematics 2023, 11,4553.<https://doi.org/10.3390/math11214553>.
- [8] A. Singh, G. Yadav and M. Singh, "Performance Analysis of 3-Phase Active Front End PWM Rectifier for Air-Core Two-Coil WPT System Configuration," 2023 9th IEEE India International Conference on Power Electronics (IICPE), SONIPAT, India, 2023, pp. 1-6, doi: 10.1109/IICPE60303.2023.10474683.
- [9] B. Sakhdari and N. L. Azad, "Adaptive Tube-Based Nonlinear MPC for Economic Autonomous Cruise Control of Plug-In Hybrid Electric Vehicles," in IEEE Transactions



on *Vehicular Technology*, vol. 67, no. 12, pp. 11390-11401, Dec. 2018, doi: 10.1109/TVT.2018.2872654.

[10] Akshay, G. Yadav and M. Singh, "Validation of a Parameter Design methodology for Air-core two-coil WPT system with multi-resonant LC compensation," 2023 IEEE International Conference on Power Electronics, Smart Grid, and Renewable Energy (PESGRE), Trivandrum, India, 2023, pp. 1-6, doi: 10.1109/PESGRE58662.2023.10404443.

[11] G. Yadav and M. Singh, "Unveiling the Superiority: Comparative Analysis of ANFIS, FOPID, and PI Controllers in Grid-Connected EV Systems for G2V/V2G Applications," 2023 International Conference on Electrical, Electronics, Communication and Computers (ELEXCOM), Roorkee, India, 2023, 10.1109/ELEXCOM58812.2023.10370196.

[12]. H. Kawai, J. Cordier, R. Kennel and S. Doki, "Application of Finite Control Set-Model Predictive Control for Servo Brake Motion in PMSM Drives," in IEEE Canadian Journal of Electrical and Computer Engineering, vol. 46, no. 2, pp. 117-129, Spring 2023, doi: 10.1109/ICJECE.2022.3233029.

[13]. H. Pandey, K. K. Singh, S. Sakalkar, G. Yadav and M. Singh, "Enhancing Wireless Charging for Electric Vehicles: A Comparative Study of Coil Designs and Their Impact on Power Transfer Efficiency," 2024 IEEE Third International Conference on Power Electronics, Intelligent Control and Energy Systems (ICPEICES), Delhi, India, 2024, pp. 1207-1212, doi: 10.1109/ICPEICES62430.2024.10719184.

[14]. M. Ansari, G. Yadav and M. Singh, "A 3.3kW Modified LLC Resonant Converter for Grid-Tied EV System Under Wide Voltage Range," 2023 3rd International Conference on Intelligent Technologies (CONIT), Hubli, India, 2023, pp. 1-6, doi: 10.1109/CONIT59222.2023.10205690.

[15]. G. Garg, D. Talan, Himanshu, G. Yadav and M. Singh, "Implementing ML and DL Based Controllers for Improving Efficiency in EV Charging Application," 2024 IEEE Third International Conference on Power Electronics, Intelligent Control and Energy Systems (ICPEICES), Delhi, India, 2024, pp. 235-240, doi: 10.1109/ICPEICES62430.2024.10719347.

[16]. G. Dangi, H. Chhabra, I. Gandhi, G. Yadav and M. Singh, "Design of Buck Converters and Integration of Electrical with Software Subsystem for Interplanetary Rovers," 2024 IEEE Third International Conference on Power Electronics, Intelligent Control and Energy Systems (ICPEICES), Delhi, India, 2024, pp. 211-216, doi: 10.1109/ICPEICES62430.2024.10719256.

[17]. Akshay, G. Yadav and M. Singh, "Validation of a Parameter Design methodology for Air-core two-coil WPT system with multi-resonant LC compensation," 2023 IEEE

*International Conference on Power Electronics, Smart Grid, and Renewable Energy (PESGRE), Trivandrum, India, 2023, pp. 1-6, doi: 10.1109/PESGRE58662.2023.10404443.*

[18]. G. Yadav and M. Singh, "CNISOGI and LLMF Based Controller Design for Grid-Interactive EV Chargers in Wide Voltage Range Scenarios," 2024 IEEE 4th International Conference on Sustainable Energy and Future Electric Transportation (SEFET), Hyderabad, India, 2024, pp. 1-6, doi: 10.1109/SEFET61574.2024.10718162.

[19]. V. Khadkikar, M. Singh, A. Chandra and B. Singh, "Implementation of single-phase synchronous d-q reference frame controller for shunt active filter under distorted voltage condition," 2010 Joint International Conference on Power Electronics, Drives and Energy Systems & 2010 Power India, New Delhi, India, 2010, pp. 1-6, doi: 10.1109/PEDES.2010.5712526.

[20]. M. Singh, A. Chandra and B. Singh, "Sensorless Power Maximization of PMSG Based Isolated Wind-Battery Hybrid System Using Adaptive Neuro-Fuzzy Controller," 2010 IEEE Industry Applications Society Annual Meeting, Houston, TX, USA, 2010, pp. 1-6, doi: 10.1109/IAS.2010.5615370.

[21]. S. Gandhar, J. Ohri and M. Singh, "Application of SSSC for compensation assessment of interconnected Power System," 2014 IEEE 6th India International Conference on Power Electronics (IICPE), Kurukshetra, India, 2014, pp. 1-5, doi: 10.1109/IICPE.2014.7115750.

[22]. T. Gupta, A. Gupta, D. Joshi and M. A. Mallick, "Stability Analysis and Optimization of a Parasitic Buck Converter Using Leverrier's Algorithm and PI Controller," 2023 9th IEEE India International Conference on Power Electronics (IICPE), SONIPAT, India, 2023, pp. 1-6, doi: 10.1109/IICPE60303.2023.10474949.

[23] A. K. Seth and M. Singh, "Resonant controller of single-stage off-board EV charger in G2V and V2G modes," *IET Power Electronics*, vol. 13, no. 5, pp. 1086-1092, 2020.

[24] T. Gupta, A. Gupta and D. Joshi, "Stability Analysis and Control of Non-Ideal SEPIC Converters Using Leverrier's Algorithm and PI Controller Considering Parasitic Elements," 2023 3rd International Conference on Emerging Frontiers in Electrical and Electronic Technologies (ICEFEET), Patna, India, 2023, pp. 1-6, doi: 10.1109/ICEFEET59656.2023.10452208.

[25] V. Khadkikar, M. Singh, A. Chandra and B. Singh, "Implementation of single-phase synchronous d-q reference frame controller for shunt active filter under distorted voltage condition," 2010 Joint International Conference on Power Electronics, Drives and Energy Systems & 2010 Power India, New Delhi, India, 2010, pp. 1-6, doi: 10.1109/PEDES.2010.5712526.

- [26]. B. T. Vankayalapati, R. Singh and V. K. Bussa, "Two stage integrated on-board charger for EVs," in *IEEE International Conference on Industrial Technology (ICIT)*, Lyon, 2018.
- [27] Z. Huang, S. Wong and C. K. Tse, "An Inductive-Power-Transfer Converter With High Efficiency Throughout Battery-Charging Process," *IEEE Transactions on Power Electronics*, vol. 34, no. 10, pp. 10245-10255, 2019.
- [28] S.S. Williamson and B. Peschiera, "Review and comparison of inductive charging power electronic converter topologies for electric and plug-in hybrid electric vehicles," in *IEEE Transportation Electrification Conference and Expo (ITEC)*, Detroit, MI, 2013.
- [29] M. Forouzes, Y. P. Siwakoti, S. A. Gorji, F. Blaabjerg and B. Lehman, "Step-Up DC DC Converters: A Comprehensive Review of Voltage-Boosting Techniques, Topologies, and Applications," *IEEE Transactions on Power Electronics*, vol. 32, no. 12, pp. 9143-9178, 2017.
- [30]. Szczepanek, C. Botsford and A., "Fast charging vs. slow charging: Pros and cons for the new age of electric vehicles," in *24th Electric Vehicle Symposium*, Stavanger, Norway, 2009.
- [31]. T. Anegawa, "Development of quick charging system for electric vehicle," in *Proc. World Energy Congress*, 2010.
- [32]. Jingshan Li; Shiyu Zhou; Yehui Han, "A BAYESIAN APPROACH TO BATTERY PROGNOSTICS AND HEALTH MANAGEMENT," in *Advances in Battery Manufacturing, Service, and Management Systems*, IEEE, 2017, pp. 151-174.
- [33]. F. Xia, H. Chen, L. Chen and X. Qin, "A Hierarchical Navigation Strategy of EV Fast Charging Based on Dynamic Scene," *IEEE Access*, vol. 7, pp. 29173-29184, 2019.
- [34]. M. T. Lawder et al., "Battery Energy Storage System (BESS) and Battery Management System (BMS) for Grid-Scale Applications," in *Proceedings of the IEEE*, 2014.
- [35]. Ronald Jurgen, *EV Batteries*, in *Electric and Hybrid-Electric Vehicles: Batteries*, SAE, 2011.
- [36]. Gregory Plett, *Battery Management Systems, Volume I: Battery Modeling*, Artech, 2015.

- [37]. M. A. Hannan, M. M. Hoque, S. E. Peng and M. N. Uddin, "Lithium-Ion Battery Charge Equalization Algorithm for Electric Vehicle Applications," *IEEE Transactions on Industry Applications*, vol. 53, no. 3, pp. 2541-2549, 2017.
- [38]. S. R. Ovshinsky et al., "Advanced materials for next generation NiMH portable, HEV and EV batteries," *IEEE Aerospace and Electronic Systems Magazine*, vol. 14, no. 5, pp. 17-23, 1999.
- [39]. X. Wei, X. Zhao and Y. Yuan, "Study of Equivalent Circuit Model for Lead-Acid Batteries in Electric Vehicle," in *International Conference on Measuring Technology and Mechatronics Automation*, Zhangjiajie, Hunan, 2009.
- [40]. Kisacikoglu, Mithat Can, *Vehicle-to-grid (V2G) Reactive Power Operation Analysis of the EV/PHEV Bidirectional Battery Charger*, PhD diss., University of Tennessee, 2013.
- [41]. J. Saikrishna Goud, Kalpana R., Kiran R., Bhim Singh, "Low Frequency Ripple Charging of LiIon Battery using Bidirectional Zeta DC-DC Converter to Improve Charge Transfer Efficiency," in *IEEE 7th International Conference on Power and Energy (PECon)*, 2018.
- [42]. M. C. Falvo, D. Sbordon, I. S. Bayram and M. Devetsikiotis, "'EV charging stations and modes: International standards," in *International Symposium on Power Electronics, Electrical Drives Automation and Motion*, Ischia, 2014.
- [43]. T. Bohn and H. Chaudhry, "'Overview of SAE standards for plug-in electric vehicle," in *IEEE PES Innovative Smart Grid Technologies (ISGT)*, Washington, DC, 2012.
- [44]. A. Zahedmanesh, D. Sutanto and K. M. Muttaqi, "Analyzing the impacts of charging plug-in electric vehicles in low voltage distribution networks: A case study of utilization of droop charging control system based on the SAE J1772 Standard," in *Australasian Universities Power Engineering Conference (AUPEC)*, Melbourne, 2017.
- [45]. S. Habib, M. M. Khan, F. Abbas, L. Sang, M. U. Shahid and H. Tang, "A Comprehensive Study of Implemented International Standards, Technical Challenges, Impacts and Prospects for Electric Vehicles," *IEEE Access*, vol. 6, pp. 13866-13890, 2018.
- [46]. SAE Electric Vehicle and Plug-in Hybrid Electric Vehicle Conductive Charge Coupler, "SAE Standard J1772," Jan, 2010.
- [47]. "IEEE Draft Standard Technical Specifications of a DC Quick Charger for Use with Electric Vehicles," *IEEE P2030.1.1/D2.0*, 2015.

- [48]. S. Nair, N. Rao, S. Mishra and A. Patil, "India's charging infrastructure biggest single point impediment in EV adaptation in India," in *IEEE Transportation Electrification Conference (ITEC-India)*, Pune, 2017.
- [49]. O. C. Onar, J. Kobayashi and A. Khaligh, "A Fully Directional Universal Power Electronic Interface for EV, HEV, and PHEV Applications," *IEEE Transactions on Power Electronics*, vol. 28, no. 12, pp. 5489-5498, 2013.
- [50]. G. Buja, M. Bertoluzzo and C. Fontana, "Reactive Power Compensation Capabilities of V2G-Enabled Electric Vehicles," *IEEE Transactions on Power Electronics*, vol. 32, no. 12, pp. 9447-9459, 2017.
- [51]. M. Y. Metwly, M. S. Abdel-Majeed, A. S. Abdel-Khalik, R. A. Hamdy, M. S. Hamad and S. Ahmed, "A Review of Integrated On-Board EV Battery Chargers: Advanced Topologies, Recent Developments and Optimal Selection of FSCW Slot/Pole Combination," *IEEE Access*, vol. 8, pp. 85216-85242, 2020.
- [52]. A. Narula and V. Verma, "Bi directional trans Z source boost converter for G2V/V2G applications," in *IEEE Transportation Electrification Conference (ITEC-India)*, Pune, 2017.
- [53]. M. Singh, V. Khadkikar, A. Chandra and R. K. Varma, "Grid Interconnection of Renewable Energy Sources at the Distribution Level With Power-Qual Improvement Features," *IEEE Transactions on Power Delivery*, vol. 26, no. 1, pp. 307-315, 2011.
- [54]. S. Kulkarni, A. R. Thorat and I. Korachagaon, "Bidirectional converter for vehicle to grid (V2G) reactive power operation," in *International Conference on Circuit, Power and Computing Technologies (ICCPCT)*, 2017.
- [55]. K. Sinjari and J. Mitra, "Electric Vehicle Charging with Reactive Power Compensation to Distribution Systems," in *IEEE Industry Applications Society Annual Meeting*, 2020.
- [56]. W. Choi, W. Lee and B. Sarlioglu, "Reactive power compensation of grid-connected inverter in vehicle-to-grid application to mitigate balanced grid voltage sag," in *IEEE Power and Energy Society General Meeting (PESGM)*, 2016.
- [57]. D. B. W. Abeywardana, P. Acuna, B. Hredzak, R. P. Aguilera,, "Single-phase boost inverter-based electric vehicle charger with integrated vehicle to grid reactive power compensation," *IEEE Trans. Power Electron.*, vol. 33, no. 4, pp. 3462-3471, 2018.
- [58]. B. Singh, A. Chandra, K. Al-haddad, *Power Quality: Problem and Mitigation Techniques*, UK: John Wiley and Sons, 2015.

- [59]. F. Chishti, S. Murshid and B. Singh, "Development of Wind and Solar Based AC Microgrid With Power Quality Improvement for Local Nonlinear Load Using MLMS," *IEEE Transactions on Industry Applications*, vol. 55, no. 6, pp. 7134- 7145, 2019.
- [60]. D. W. Hart, *Power Electronics*, Mc Graw Hill, 2010.
- [61]. M. Narimani and G. Moschopoulos, "Modeling and control of a single-stage three-level power factor correction AC-DC converter," in *24th Canadian Conference on Electrical and Computer Engineering(CCECE)*, 2011.
- [62]. Tasi-Fu Wu and Yu-Kai Chen, "Modeling PWM DC/DC converters out of basic converter units," *IEEE Transactions on Power Electronics*, vol. 13, no. 5, pp. 870-881, 1998.
- [63]. M. Kesler, M. C. Kisacikoglu and L. M. Tolbert, "Vehicle-to-Grid Reactive Power Operation Using Plug-In Electric Vehicle Bidirectional Offboard Charger," *IEEE Transactions on Industrial Electronics*, vol. 61, no. 12, pp. 6778-6784, 2014.
- [64]. A. K. Seth and M. Singh, "Control of Two-Stage OFF-Board Electric Vehicle Charger," in *1st International Conference on Power Electronics and Energy (ICPEE)*, India, 2021.
- [65]. Amirnaser Yazdani and Reza Iravani, *Voltage-Sourced Converters in Power Systems: Modeling Control and Applications*, Wiley-IEEE Press, 2010.
- [66]. H. Akagi, E. H. Watanabe and M. Aredes, *Instantaneous Power Theory and Applications to Power Conditioning*, USA: John Wiley and Sons, 2007.
- [67]. M. Singh, "Adaptive Network-Based Fuzzy Inference System for Sensorless Control of PMSG Based Wind Turbine with Power Quality Improvement Features," *Ecole De Technologie Superieure*, Montreal, 2010.
- [68]. A.H.R. Rosa, L.M.F. Morais, G.O. Fortes, S.I. Seleme Júnior., "Practical considerations of nonlinear control techniques applied to static power converters: A survey and comparative study," *International Journal of Electrical Power & Energy Systems*, vol. 127, 2021.
- [69]. J.-S. R. Jang., "ANFIS: Adaptive-network-based fuzzy inference system," *IEEE Trans. Syst. Man, Cybern.*, vol. 23, no. 3, pp. 665-685, 1993.
- [70]. M. Singh and A. Chandra., "Application of Adaptive Network-Based Fuzzy Inference System for Sensorless Control of PMSG-Based Wind Turbine With Nonlinear-Load-Compensation Capabilities," *IEEE Transactions on Power Electronics*, vol. 26, no. 1, pp. 165-175, 2011.

- [71]. Nitin Kumar Saxena, Ashwani Kumar. , "Reactive power control in decentralized hybrid power system with STATCOM using GA, ANN and ANFIS methods," *International Journal of Electrical Power & Energy Systems*, vol. 83, pp. 175- 187, 2016.
- [72]. P.K. Gayen, A. Jana. , "An ANFIS based improved control action for single phase utility or micro-grid connected battery energy storage system," *Journal of Cleaner Production*, vol. 164, pp. 1034-1049, 2017.
- [73]. Mossad Mohamed I, Salem Fawzan. , "LFC based adaptive PID controller using ANN and ANFIS techniques," *J Electr Syst Inform Technol*, vol. 1, 2014.
- [74]. J. Saroha, M. Singh and D. K. Jain. , "ANFIS-Based Add-On Controller for Unbalance Voltage Compensation in a Low-Voltage Microgrid," *IEEE Transactions on Industrial Informatics*, vol. 14, no. 12, pp. 5338-5345, 2018.
- [75]. N. Mohan, T.M. Undeland and W.P. Robbins, *Power Electronics Converters, Applications and Design*, John Wiley & Sons, 2003.
- [76]. A.K. Seth and M. Singh, "Unified adaptive neuro-fuzzy inference system control for OFF board electric vehicle charger," *International Journal of Electrical Power and Energy Systems* , vol. 130, 2021.
- [77]. H. Saxena, A. Singh and J. N. Rai, "Application of Time Delay Recurrent Neural Network for Shunt Active Power Filter in 3-Phase Grid-tied PV System," in *National Power Electronics Conference (NPEC)*, Tiruchirappalli, 2019.
- [78]. K. P. Chou, M. Prasad, Y. Y. Lin, S. Joshi, C. T. Lin and J. Y. Chang. , "Takagi-Sugeno-Kang type collaborative fuzzy rule based system," in *IEEE Symposium on Computational Intelligence and Data Mining (CIDM)*, Orlando, FL, 2014.
- [79]. Shun-ichi Amari., "Backpropagation and stochastic gradient descent method," *Neurocomputing*, vol. 5, no. 4-5, pp. 185-196, 1993.
- [80]. Rumelhart, David E. et al., "Learning internal representations by error propagation," *Computer Science, Mathematics*, 1986.





**IEEE PEDES 2024**  
POWER ELECTRONICS, DRIVES AND ENERGY SYSTEMS



## CERTIFICATE OF APPRECIATION

This is to certify that the paper entitled "OPTIMAL DESIGN AND PERFORMANCE ANALYSIS OF MODEL PREDICTIVE CONTROL FOR EV CHARGING APPLICATION" authored by Kaumudi Kumari; Mukhtiar Singh has been presented in the 11<sup>th</sup> IEEE International Conference on Power Electronics, Drives and Energy Systems (PEDES 2024), organized by the Department of Electrical and Electronics Engineering at National Institute of Technology Karnataka, Surathkal, India from 18<sup>th</sup> to 21<sup>st</sup> December 2024.

*R. Kalpana*

**Dr. R Kalpana**

General Chair, PEDES

*Banubhai*

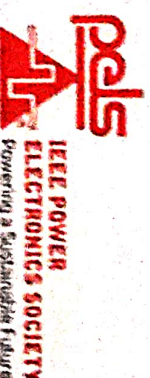
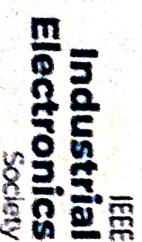
**Dr. A. K. Rathore**

Plenary Chair, PEDES

*Brij N Singh*

**Dr. Brij N Singh**

General Co-Chair, PEDES







**7th International Conference on Energy, Power and Environment (ICEPE 2025)**  
**May 9 – 11 2025**



# CERTIFICATE

THIS IS TO CERTIFY THAT

**Kaumudi Kumari and Mukhtiar Singh**

have successfully presented a paper entitled

**Real Time Model Predictive Control for Bidirectional EV Charging and  
Discharging**

in the 7th International Conference on Energy, Power and Environment (ICEPE 2025)  
on May 9 – 11 2025, Sohra, Meghalaya

**Organizing Chair**

**General Chair**



KAUMUDI KUMARI &lt;kaumudi94@gmail.com&gt;

## Provisional Acceptance of Paper id 454– IEEE SeFet 2025 during 9-12 July 2025 at MNIT Jaipur

1 message

Microsoft CMT <email@msr-cmt.org>  
To: KAUMUDI KUMARI <kaumudi94@gmail.com>

Tue, Apr 8, 2025 at 3:54 PM

Dear Authors,  
Congratulations!

We are pleased to inform you that your paper titled "Design and Development of Advanced Model Predictive Control Strategy for Electric Vehicle Application" (Paper ID: "454") has been provisionally accepted for presentation at the IEEE SeFet 2025 conference, scheduled to take place from July 9-12, 2025, at MNIT Jaipur, Rajasthan, India.

Important Notes:

1. The acceptance is subject to the final plagiarism and quality check and satisfactory incorporation of reviewer comments (available on the Microsoft CMT Portal) and plagiarism limit.
2. The manuscript must strictly adhere to the IEEE format.
3. Papers up to six (6) pages are included in the standard registration fee.
4. A maximum of two (2) additional pages may be allowed, subject to an extra charge as specified on the conference website.

Please ensure the following steps are completed for submitting the camera-ready paper and completing the registration.

### Step-1(Camera-ready file upload)

The authors will have to submit a camera-ready version as per the following guidelines on or before 15th May 2025.

1. The similarity index of your paper must be less than 30%, including references. If the plagiarism exceeds 30%, your paper will not be forwarded for publication in IEEE Xplore.
2. Paper must be revised as per Reviewers comments available on the Microsoft CMT Portal.
3. Paper must be as per the IEEE template (<https://www.ieee.org/conferences/publishing/templates.html>).
4. Proofread your manuscript thoroughly to confirm that it will require no revision.
5. Please include the copyright notice on the left of the footer section of the first page (not all pages) of your manuscript as mentioned below.
  - For papers in which all authors are employed by the US government, the copyright notice is: U.S. Government work not protected by U.S. copyright
  - For papers in which all authors are employed by a Crown government (UK, Canada, and Australia), the copyright notice is: 979-8-3315-3544-5/25/\$31.00 ©2025 Crown
  - For papers in which all authors are employed by the European Union, the copyright notice is: 979-8-3315-3544-5/25/\$31.00 ©2025 European Union
  - For all other papers the copyright notice is: 979-8-3315-3544-5/25/\$31.00 ©2025 IEEE
6. After implementing all corrections and putting copyright number in the first page of your manuscript, follow the following process to prepare Camera Ready submission through IEEE pdf-express:
  - Log in to the IEEE PDF eXpress TM site (<https://ieee-pdf-express.org/account/Login>)
  - First-time users should do the following:
    - i. Click on "Create account".
    - ii. Enter the following:
      - iii. 65155X for the Conference ID
      - iv. your email address
      - v. a password
    - Click on "SUBMIT" Button: (An email helpdesk-ieee will be sent to your email)
    - Account Activation: Go to your email and please click on URL "Click for account activation". (Email Addressed will be verified)
    - Login to your New IEEE PDF Express Account using login credentials
    - Fill the IEEE PDF eXpress User profile: Personal information and Submit; Click ok
    - Go to the "Dashboard" and click on "CREATE NEW TITLE" and continue to enter information as prompted.
    - If Error in converting file, then please correct the paper according to the IEEE Conference paper template and resubmit for the PDF eXpress until "File has been converted successfully" without error.
    - After "File has been converted successfully", download the Pdf from the "Action" Tab in the Dashboard.
7. Download the pdf file of your paper from PDF eXpressPlus website and upload it via the CMT Portal for Camera Ready Paper Submission of SeFeT-2025 at <https://cmt3.research.microsoft.com/SEFET2025>.

**Step-2 (Supplementary File Upload)**

Prepare a response sheet detailing how each of the reviewers' comments has been addressed. Additionally, generate a plagiarism report for your manuscript using a standard plagiarism detection tool such as Turnitin or iThenticate. Create a ZIP folder named after your Paper ID (e.g. PID402) and include both the compliance report to reviewers' comments and the plagiarism report in that folder. Finally, upload this ZIP file under the Supplementary File Upload section. The last date for uploading the camera-ready paper and supplementary file is May 15th, 2025.

**Step-3 (Registration)**

To ensure your paper's inclusion in the conference proceedings, at least one author of each accepted paper must register. Please complete your registration by visiting the following link:

<https://sefet.in/registration.html>. Kindly pay your registration fee to the specified account according to your category listed on the website. The early bird registration deadline is May 15th, 2025. After paying the registration fee, please finalize your registration by filling out the Google form available at: <https://forms.gle/zMnM3kDVHdasDZ2M8>

**Step-4 (Electronic Copyright form submission)**

Procedure for IEEE Copyright Form eCF submission:

To enable your paper to appear in IEEE eXplorer, it is mandatory to transfer the Copyright to IEEE. The corresponding/submitting author of each paper must transfer IEEE eCF. The steps to transfer the Copyright to IEEE are also given below:

1. Login to your CMT Paper Submission Portal and Click on the IEEE copyright link. You will be redirected to IEEE Copyright Form Submission page.
2. Click on "Click here to redirect to the IEEE copyright website" to transfer eCF and you will be redirected to IEEE copyright portal.
3. Follow the steps (Step 1 to Step 5) and provided instructions to complete the IEEE Copyright Transfer process.
4. At the end of Step 5, download the completed Copyright Form and save it as .pdf (Make sure to download a copy of the completed form.)
5. Login to your CMT Paper Submission Portal and upload this pdf file of Copyright Transfer Form

It completes the Copyright Transfer of your paper to IEEE. Please note that separate copyright transfer is required for each paper.

For more details you are requested to visit: <https://sefet.in/camera-ready-paper-submission.html>

Thanks and Regards,  
Team 5th IEEE SeFeT-2025  
Centre for Energy & Environment  
MNIT Jaipur, India-302017

To stop receiving conference emails, you can check the 'Do not send me conference email' box from your User Profile.

Microsoft respects your privacy. To learn more, please read our [Privacy Statement](#).

Microsoft Corporation  
One [Microsoft Way](#)  
[Redmond, WA 98052](#)



KAUMUDI KUMARI &lt;kaumudi94@gmail.com&gt;

## Provisional Acceptance of Paper id 337– IEEE SeFet 2025 during 9-12 July 2025 at MNIT Jaipur

1 message

Microsoft CMT <email@msr-cmt.org>  
To: KAUMUDI KUMARI <kaumudi94@gmail.com>

Tue, Apr 8, 2025 at 3:54 PM

Dear Authors,  
Congratulations!

We are pleased to inform you that your paper titled "Implementation of Robust Control for Smart Home EV Charger through FC -MPC" (Paper ID: "337") has been provisionally accepted for presentation at the IEEE SeFet 2025 conference, scheduled to take place from July 9–12, 2025, at MNIT Jaipur, Rajasthan, India.

Important Notes:

1. The acceptance is subject to the final plagiarism and quality check and satisfactory incorporation of reviewer comments (available on the Microsoft CMT Portal) and plagiarism limit.
2. The manuscript must strictly adhere to the IEEE format.
3. Papers up to six (6) pages are included in the standard registration fee.
4. A maximum of two (2) additional pages may be allowed, subject to an extra charge as specified on the conference website.

Please ensure the following steps are completed for submitting the camera-ready paper and completing the registration.

### Step-1(Camera-ready file upload)

The authors will have to submit a camera-ready version as per the following guidelines on or before 15th May 2025.

1. The similarity index of your paper must be less than 30%, including references. If the plagiarism exceeds 30%, your paper will not be forwarded for publication in IEEE Xplore.
2. Paper must be revised as per Reviewers comments available on the Microsoft CMT Portal.
3. Paper must be as per the IEEE template (<https://www.ieee.org/conferences/publishing/templates.html>).
4. Proofread your manuscript thoroughly to confirm that it will require no revision.
5. Please include the copyright notice on the left of the footer section of the first page (not all pages) of your manuscript as mentioned below.
  - For papers in which all authors are employed by the US government, the copyright notice is: U.S. Government work not protected by U.S. copyright
  - For papers in which all authors are employed by a Crown government (UK, Canada, and Australia), the copyright notice is: 979-8-3315-3544-5/25/\$31.00 ©2025 Crown
  - For papers in which all authors are employed by the European Union, the copyright notice is: 979-8-3315-3544-5/25/\$31.00 ©2025 European Union
  - For all other papers the copyright notice is: 979-8-3315-3544-5/25/\$31.00 ©2025 IEEE
6. After implementing all corrections and putting copyright number in the first page of your manuscript, follow the following process to prepare Camera Ready submission through IEEE pdf-express:
  - Log in to the IEEE PDF eXpress TM site (<https://ieee-pdf-express.org/account/Login>)
  - First-time users should do the following:
    - i. Click on "Create account".
    - ii. Enter the following:
      - iii. 65155X for the Conference ID
      - iv. your email address
      - v. a password
    - Click on "SUBMIT" Button: (An email helpdesk-ieee will be sent to your email)
    - Account Activation: Go to your email and please click on URL "Click for account activation". (Email Addressed will be verified)
    - Login to your New IEEE PDF Express Account using login credentials
    - Fill the IEEE PDF eXpress User profile: Personal information and Submit; Click ok
    - Go to the "Dashboard" and click on "CREATE NEW TITLE" and continue to enter information as prompted.
    - If Error in converting file, then please correct the paper according to the IEEE Conference paper template and resubmit for the PDF eXpress until "File has been converted successfully" without error.
    - After "File has been converted successfully", download the Pdf from the "Action" Tab in the Dashboard.
7. Download the pdf file of your paper from PDF eXpressPlus website and upload it via the CMT Portal for Camera Ready Paper Submission of SeFeT-2025 at <https://cmt3.research.microsoft.com/SEFET2025>.

**Step-2 (Supplementary File Upload)**

Prepare a response sheet detailing how each of the reviewers' comments has been addressed. Additionally, generate a plagiarism report for your manuscript using a standard plagiarism detection tool such as Turnitin or iThenticate. Create a ZIP folder named after your Paper ID (e.g. PID402) and include both the compliance report to reviewers' comments and the plagiarism report in that folder. Finally, upload this ZIP file under the Supplementary File Upload section. The last date for uploading the camera-ready paper and supplementary file is May 15th, 2025.

**Step-3 (Registration)**

To ensure your paper's inclusion in the conference proceedings, at least one author of each accepted paper must register. Please complete your registration by visiting the following link:

<https://sefet.in/registration.html>. Kindly pay your registration fee to the specified account according to your category listed on the website. The early bird registration deadline is May 15th, 2025. After paying the registration fee, please finalize your registration by filling out the Google form available at: <https://forms.gle/zMnM3kDVHdasDZ2M8>

**Step-4 (Electronic Copyright form submission)**

Procedure for IEEE Copyright Form eCF submission:

To enable your paper to appear in IEEE eXplorer, it is mandatory to transfer the Copyright to IEEE. The corresponding/submitting author of each paper must transfer IEEE eCF. The steps to transfer the Copyright to IEEE are also given below:

1. Login to your CMT Paper Submission Portal and Click on the IEEE copyright link. You will be redirected to IEEE Copyright Form Submission page.
2. Click on "Click here to redirect to the IEEE copyright website" to transfer eCF and you will be redirected to IEEE copyright portal.
3. Follow the steps (Step 1 to Step 5) and provided instructions to complete the IEEE Copyright Transfer process.
4. At the end of Step 5, download the completed Copyright Form and save it as .pdf (Make sure to download a copy of the completed form.)
5. Login to your CMT Paper Submission Portal and upload this pdf file of Copyright Transfer Form

It completes the Copyright Transfer of your paper to IEEE. Please note that separate copyright transfer is required for each paper.

For more details you are requested to visit: <https://sefet.in/camera-ready-paper-submission.html>

Thanks and Regards,  
Team 5th IEEE SeFeT-2025  
Centre for Energy & Environment  
MNIT Jaipur, India-302017

To stop receiving conference emails, you can check the 'Do not send me conference email' box from your User Profile.

Microsoft respects your privacy. To learn more, please read our [Privacy Statement](#).

Microsoft Corporation  
One [Microsoft Way](#)  
[Redmond, WA 98052](#)

# 9% Overall Similarity

The combined total of all matches, including overlapping sources, for each database.





## Filtered from the Report

- Bibliography
- Small Matches (less than 10 words)




## Exclusions

- 41 Excluded Matches

## Match Groups


-  **134 Not Cited or Quoted 9%**  
Matches with neither in-text citation nor quotation marks
-  **2 Missing Quotations 0%**  
Matches that are still very similar to source material
-  **0 Missing Citation 0%**  
Matches that have quotation marks, but no in-text citation
-  **0 Cited and Quoted 0%**  
Matches with in-text citation present, but no quotation marks

## Top Sources

- 6%**  Internet sources
- 4%**  Publications
- 3%**  Submitted works (Student Papers)

## Integrity Flags

### 1 Integrity Flag for Review

-  **Hidden Text**  
158 suspect characters on 2 pages  
Text is altered to blend into the white background of the document.

Our system's algorithms look deeply at a document for any inconsistencies that would set it apart from a normal submission. If we notice something strange, we flag it for you to review.

A Flag is not necessarily an indicator of a problem. However, we'd recommend you focus your attention there for further review.



**IEEE PEDES 2024**  
POWER ELECTRONICS, DRIVES AND ENERGY SYSTEMS



**11<sup>th</sup> IEEE International Conference on Power Electronics, Drives and  
Energy Systems 2024 (PEDES 2024)  
18-21 December 2024  
National Institute of Technology Karnataka**

**NITK SURATHKAL**  
GST No.: 29AAATN4896K1ZT

**IEEE PEDES 2024**

**RECEIPT**

**No. PEDES/404**

**Date: 11.09.2024**

Received with thanks from **Kaumudi Kumari** an amount of **15162.53 INR**(Fifteen thousand one hundred sixty-two rupees and fifty-three paise) by online transfer/cheque/cash towards the Registration Fee for the **2024 IEEE International Conference on Power Electronics, Drives and Energy Systems (PEDES 2024)** organized by **Electrical and Electronics Department, NITK Surathkal** during 18-21 December 2024 at NITK Surathkal, Mangalore, India.

**R Kalpana**

General Chair-IEEE PEDES 2024  
Associate Professor  
Dept. of E and E Engg.,  
NITK Surathkal, INDIA



7<sup>TH</sup> International Conference on Energy, Power & Environment 2025

(ICEPE 2025)

May 9<sup>th</sup> – 11<sup>th</sup>, 2025

Organised by

**Department of Electrical Engineering**  
**NATIONAL INSTITUTE OF TECHNOLOGY MEGHALAYA**

7P4R+PGJ, Saitsohpen, Sohra, -793108, Meghalaya, India

**Payment Receipt**

Receipt No. NITMGH/EE/ICEPE2025/PR- 212

Date: 23/05/2025

Received from: Kaumudi Kumari

Affiliation: Delhi Technological University, Delhi

Amount Received: 7500 (Rupees: Seven Thousand Five Hundred only)

Transaction ID/Cash/DD No./Cheque No: 510076917706

Mode of Payment: UPI

₹ 7500

Cheque /Drafts Subject to realization only.

**ICEPE 2025**  
**Department of Electrical Engineering**  
**National Institute of Technology**  
**Meghalaya, Sohra**

*Piyush*

(Authorized Seal & Signature)